CHALMERS
UNIVERSITY OF TECHNOLOGY

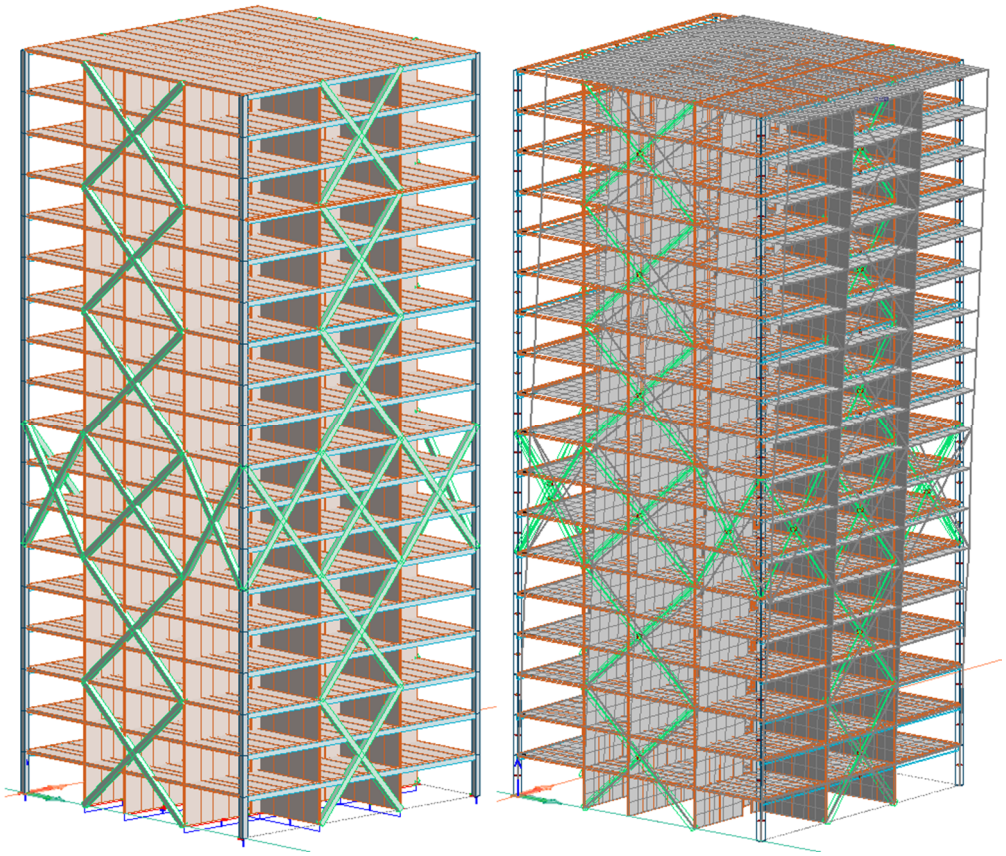

Stability and Dynamic Properties of Tall Timber Structures

A parametric study of the structural response due to wind action

Master's thesis in Structural Engineering and Building Technology

Ahmad Alalwan
Joakim Larsson

Department of Architecture and Civil Engineering
Division of Structural Engineering
Research Group of Lightweight Structures
CHALMERS UNIVERSITY OF TECHNOLOGY
Master's Thesis ACEX30-19-41
Gothenburg, Sweden 2019

MASTER'S THESIS ACEX30-19-41

Stability and Dynamic Behaviour of Tall Timber Structures

A parameter study of the structural response due to wind action

Master's Thesis in the Master's Programme Structural Engineering and Building Technology

Ahmad Alalwan
Joakim Larsson

Department of Architecture and Civil Engineering
Division of Structural Engineering
Research Group of Lightweight Structures
CHALMERS UNIVERSITY OF TECHNOLOGY
Göteborg, Sweden 2019

Stability and Dynamic Properties for Tall Timber Structures

A parametric study of the structural response due to wind action

Master's thesis in the Master's Programme Structural Engineering and Building Technology

Ahmad Alalwan

Joakim Larsson

Examensarbete ACEX30-19-NN
Institutionen för arkitektur och samhällsbyggnadsteknik
Chalmers tekniska högskola, 2019

Department of Architecture and Civil Engineering
Division of Structural Engineering and Building Technology
Research Group Lightweight Structures
Chalmers University of Technology
SE-412 96 Göteborg
Sweden
Telephone: + 46 (0)31-772 1000

Cover:
Structure before and after exposure to dynamic wind-action.
Department of Architecture and Civil Engineering
Göteborg, Sweden, 2019

Stability and Dynamic Properties of Tall Timber Structures

A parametric study of the structural response due to wind action

Master's thesis in the Master's Programme Structural Engineering and Building Technology

Ahmad Alalwan

Joakim Larsson

Department of Architecture and Civil Engineering
Division of Structural Engineering
Research Group of Lightweight Structures
Chalmers University of Technology

ABSTRACT

The interest in building taller structures in timber is increasing in the building sector. However, the high strength-to-weight ratio of timber leads to a relatively light structure which is often associated with vibrations. The dynamic properties are essential in the design of tall timber structures, where wind-induced vibrations of the building in service state is addressed. The dynamic response is influenced by mass, stiffness and damping. These parameters influence the acceleration of the building which can be perceived as a discomfort for human occupancy.

The aim is to find a structural concept that makes a taller structure than the usual today feasible. The objective is to make a parametric study and investigate how a multi-storey residential building of timber can be optimized with respect to dynamic wind loading. With a combination of numerical and analytical methods, accelerations are calculated and evaluated against the criteria for human comfort according to *ISO 10137* and *ISO 6897*. An analytical calculation sheet is set up according to *SS-EN-1991-1-4* and *EKS 10* to define wind-induced acceleration.

Starting from a beam-column structure with a central core, the effect of adding inner walls and exterior bracing is studied to see what limits the number of storeys for an open plan building. Analysis of the dynamic response due to wind shows the fundamental mode shape in torsion before exterior bracing is added. Results have shown that the structure can reach 5-storeys with inner walls of cross-laminated timber and 4-storeys with no walls. Moreover, it's found that diagonal bracing in the facades improves the torsional stiffness significantly and the fundamental mode becomes a transversal mode.

An outrigger bracing system has been found to be the most efficient, leading to a structure of 12-storeys. The parameters mass and stiffness are modified by adding concrete floors and assigning larger sections to the structure. Results show that the building can achieve 15-storeys with pure timber and 21-storeys when concrete floors are added. Secondary parametric action i.e. adding another outrigger generates a gain of one-storey and modifying the truss-work to steel gives a structure of 23-storeys.

Key words: Acceleration, dynamic response, human occupancy, mode shape, parametric study, tall timber structure, wind-induced vibrations.

Stabilitet och dynamiska egenskaper för höga träkonstruktioner

En parameterstudie av den strukturella responsen inducerat av vindlaster

Examensarbete inom masterprogrammet Konstruktionsteknik och Byggnadsteknologi

Ahmad Alalwan

Joakim Larsson

Institutionen för arkitektur och samhällsbyggnadsteknik
Avdelningen för Konstruktionsteknik och byggnadsteknologi
Forskargrupp Lättviktskonstruktioner
Chalmers Tekniska Högskola

SAMMANFATTNING

Intresset för att bygga högre hus i trä ökar i byggsektorn. Träets höga bärförmåga i förhållande till sin vikt leder däremot till en lättviktstruktur som ofta är förknippad med vibrationer. De dynamiska egenskaperna är essentiella vid utformandet av höga trähus i bemärkelsen av vind-inducerade vibrationer. Den dynamiska responsen är beroende av massa, styvhet och dämpning. Dessa parametrar påverkar byggnadens acceleration på grund av vind och kan upplevas som obehag för personvistelse i huset.

Målet är att hitta ett strukturellt koncept som möjliggör en högre byggnad än vad som är möjligt idag. Delmålet är att göra en parameterstudie och undersöka hur ett flerbostadshus kan optimeras med avseende på dynamiska vindlaster. Med en kombination av numeriska och analytiska metoder kan accelerationer räknas fram och utvärderas mot komfort-kriteriet enligt *ISO 10137* och *ISO 6897*. Ett beräkningsark är definierat för att räkna fram accelerationer enligt *SS-EN-1991-1-4* och *EKS 10*.

Med start från ett pelare-balksystem med en centralt belägen kärna studeras effekten av att lägga till bärande innerväggar samt diagonaler i fasaden samt att se vad som begränsar antalet tillåtna våningar för ett koncept med öppen plan. Analys av den dynamiska responsen visar att den första vibrationsmoden är i vridning innan stabiliserande element existerar i fasaden. Resultat visar att byggnaden kan nå 5 våningar med korslaminerade innerväggar och 4 våningar utan. Dessutom har det framkommit att stabiliserande diagonaler i fasaden ger betydande vridstyvhet och att den första vridmoden skiftar till en transversell mod.

Ett ’outrigger bracing’ system har visat sig vara det mest effektiva och leder till att byggnaden kan nå 12 våningar. Parametrarna massa och styvhet modifieras via addering av betongbjälklag samt att ange större tvärsnitt till de strukturella elementen. Resultaten visar att byggnaden kan nå 15 våningar med endast trä-element och 21 våningar när betongbjälklag är implementerade. Sekundära parametriska åtgärder såsom att lägga till en andra outrigger genererar en ökning på en våning och att modifiera diagonalerna till stål ger en byggnad av 23 våningar.

Nyckelord: Acceleration, dynamisk respons, höga träbyggnader, mod, parameterstudie, vind-inducerade vibrationer.

Contents

Preface

This report is the final part of the Master's programme *Structural Engneering and Building Technology* at Chalmers University of Technology in Göteborg, Sweden. The initiative for this thesis-topic came from Thomas Hallgren, structural engineer at COWI AB, and it is a collaboration with the division of Architecture and Structural Engineering. The thesis is guided by the research group of Lightweight Structures at Chalmers, where professor Mohammad Al-Emrani is the examiner.

The work has been carried out at COWI's Göteborg office during the spring of 2019 where the workspace and required software are provided. We would like to raise a special acknowledgement to our supervisor, Thomas Hallgren who has shared his expertise and knowledge within the field of structural dynamics and given us lots of good feedback during the whole working process. In addition, thanks to our colleagues at the office for the good tips and tricks when using the numerical software, FEM-Design 17. We also want to thank our supervisor at Chalmers, Robert Jockwer for the good conversations regarding everything from report-formatting to strategic choices for the development of the study.

Göteborg, June 2019

Joakim Larsson
Ahmad Alalwan

Notations

Roman upper-case letters

A	Cross-sectional area
A_i	Area of individual wall
A_{ref}	Reference area of structure
B^2	Background response factor
D_s	Dynamic magnification factor
E	Young's modulus
F	Non-dimensional frequency
G	Shear modulus
G_k	Total dead weight
H_i	Pure translational component of transversal force
$H_{i,C}$	Torsional component of transverse force
I_v	Turbulence intensity
P	Point load
Q_k	Total imposed load
R^2	Resonance response factor
S_{bi}	Bending stiffness of individual wall
S_{si}	Shear stiffness of individual wall
S_T	Global torsional stiffness
T	Global torsional moment
T_{600}	Reference time for basic mean velocity
T_a	Time with a number of years
T_n	Natural time-period
$\ddot{X}_{max}$	Peak acceleration

Roman lower-case letters

b	Width of the structure
c	Damping coefficient
c_0	Topography factor
c_{cr}	Critical damping coefficient
c_e	Exposure factor
c_f	Force coefficient in the wind direction
c_r	Roughness factor
c_{pe}	Pressure coefficient for the external pressure
$c_s c_d$	Structural factor
d	Depth of the structure
f_n	Eigenfrequency for mode shape n
f_0	First eigenfrequency
g	Constant of gravity
h_{ref}	Reference height
k	Stiffness
k_b	Bending coefficient
k_l	Turbulence factor
k_p	Peak factor
k_r	Terrain factor

k_s	Shear coefficient
l	Height or span of the structure or structural element
l_i	Height of individual wall
m	Structural mass
$m(s)$	Mass per unit length
m_e	Equivalent mass per unit length
n_1	First eigenfrequency (expressed in *SS-EN 1991-1-4* and *EKS 10*)
q	Distributed load
q_m	Mean velocity wind pressure
$q_p(z_e)$	Peak wind pressure
r	Frequency ratio
u	Displacement
v	Up-crossing frequency
v_b	Basic wind speed with return period of 50 years
v_{b,T_a}	Basic wind speed with return period of T_a years
v_{CG}	Onset wind velocity
v_{crit}	Critical wind velocity
v_m	Mean wind velocity
w_e	Wind pressure
x_t	x-coordinate for rotational centre
y_C	Non-dimensional wind energy spectrum
y_t	y-coordinate for rotational centre
z	Height of the structure
z_0	Roughness length
z_e	Reference height for external pressure

Greek upper-case letters

Φ	Fundamenal flexural mode shape
Ω	Forced frequency

Greek lower-case letters

β_w	Timoshenko shear coefficient for a distributed load-case
δ	Logarithmic decrement of damping
δ_s	Logarithmic decrement of structural damping
δ_a	Logarithmic decrement of aerodynamic damping
δ_d	Logarithmic decrement of damping due to special devices
ζ	Mode shape factor
κ	Timoshenko shear coefficient for a concentrated load-case
ξ	Damping factor
ρ	Density of air
$\sigma_{\ddot{X}}$	Standard deviation of acceleration
ϕ_b	Size factor with respect to width
ϕ_h	Size factor with respect to height
ψ_2	Load case factor
ω_n	Angular eigenfrequency

1 Introduction

The introductory chapter is subdivided into background, problem description, aim and objective, chosen methods to solve the problem and the limitations of the study.

1.1 Background

The interest in building taller structures with timber is increasing in the building sector. Structural systems for high-rise buildings have traditionally consisted of steel and concrete. Production of these materials is intensively energy consuming and emission releasing. Furthermore, it accounts for a great portion of total greenhouse gas emissions of materials production in the building sector. The sector has a big responsibility for limiting the climate change as construction and operation of today's buildings stands for 39% of the greenhouse gas emissions (WGBC, 2017).

Timber is a material with obvious advantages since it is renewable and often referred as 'carbon neutral' (Harte, 2009). A study points out the environmental benefit of implementing timber into multi-storey buildings from 3-21 storeys by a comparative life cycle assessment. Results shows that a timber structure would cause 34% up to 84% lower climate change impact than a concrete structure, depending on height of the building and applied production technology (Bohne, Lohne, & Skullestad, 2016).

However, timber buildings bring some structural challenges when the number of storeys is increased. The high strength-to-weight ratio of timber leads to a relatively light structure which is often associated with vibrations. A limitation in design is wind-induced effects. The mutual objective for the two tallest timber buildings is to limit vibrations for achieving acceptable comfort for human occupancy. The highest timber building is Mjöstornet, a mixed-use building of 18-storeys. It's been possible to build by combinations of engineered wooden products (EWP) and using concrete floors to increase the structural mass (Abrahamsen, 2017). Same material combination has been used in the design of Treet, the 2nd tallest timber structure which is a 14-storey residential building (Bjertnaes & Malo, 2014).

What characterizes tallness is subjective and dependent on the context of the building. In historical terms, a timber building that was higher than previous buildings of the same type or particular material might be said to be tall. An essential aspect is the height relative to context, which relates the building to its surroundings. The proportion of a building in the context of its own geometry and massing may indicate tallness if it has a slender appearance.

What defines a single material building according to the Council On Tall Buildings and Urban Habitat (CTBUH) is that the main vertical and lateral structural elements are constructed from a single material. An additional demand under proposition by CTBUH is that the material should occupy at least 85% of the building height or floor area (Foster, Ramage, & Reynolds, 2017).

1.2 Problem description

A limitation to tall timber structures is its sensitivity to wind loads. The high strength-to-weight ratio of timber leads to a relatively light structure. The dynamic properties are essential in design, where wind-induced vibrations of the building in service state is addressed. The dynamic response is influenced by mass, stiffness and damping. These parameters influence the acceleration of the building which can be perceived as a discomfort for human occupancy (Reynolds, et al., 2015).

1.3 Aim and objective

The aim is to find a structural concept that makes a taller structure than the usual today feasible. The objective is to make a parametric study and investigate how a multi-storey residential building of timber can be optimized with respect to dynamic motion induced by wind. Part of the work is to find out what effects different elements have and to find a concept that leads to the final goal, which is a higher structure with acceptable static and dynamic properties.

1.4 Methodology

The study starts with a literature study of standards accounting for wind effects, material properties of timber, structural systems and how they are applied in high-rise timber buildings. Wind standards is from Eurocode *SS-EN 1994-1-4*, international standards *ISO 10137* and *ISO 6897* along with the national annex *EKS 10*. Research within the topic is analyzed to localize problems that arise in other projects. The literature study serves as a knowledge base and intends to give a widened picture of the topic.

The analysis can be initiated after the base FE-model is established in the software *FEM-Design*. Building geometry, site conditions along with imposed and wind loading are assigned. The building will be a residential building of 22x22 meters with a central core in CLT. The remaining structure will be part of the parametric study. The location/placement and number of stabilizing walls are modified so the structure obtains varying horizontal stiffness. Some timber floors can be replaced with concrete to increase the equivalent mass to acquire better dynamic performance.

Verification of the FE-model is carried out to assure valid output and to get deeper understanding of the structural behavior. Internal and external forces in FEM-Design are compared to hand calculations. A convergence study is carried out to have efficient computational time throughout the parametric study.

The structural behavior is partly obtained from FE simulations where the numerical outputs, in terms of equivalent mass and eigenfrequencies, are a prerequisite for analytical post-processing. Eurocode and EKS standards are used to define the acceleration of the building in service state.

The structural response, described in terms of accelerations, is evaluated to *ISO 10137* and/or *ISO 6897* depending on the eigenfrequency of the building. *ISO 10137* is used for a wind-return period of 1-year and *ISO 6897* is for a 5-year wind-return period and in a low-frequency range (0.063 up to 1 Hertz).

The parametric study is performed in an iterative process in the following phases:

1. FE-simulation.
2. Post-processing of numerical results
3. Parametric action
    a. Modifying stiffness
    b. Modifying mass

1.5 Limitations

The focus in this study is to analyse the performance in service state, hence the ultimate state is roughly checked in the numerical software. One reference building of 22x22m with a central core is analysed. The building is situated in Gothenburg and adopted to Swedish conditions.

The structural behaviour is analysed with corresponding wind standards and does not go deep into theory of dynamics. Consequently, the limitations in the standards also applies for this study. The influence of damping in the study is restricted to structural damping, as damping devices tends to give rise to questions regarding costs and detailing.

2 Theoretical framework

The theoretical framework describes literature study which covers the theoretical background. An introduction to material properties of timber is given along with the general wind loading on structures and background of structural dynamics. Some structural applications in the context of tall buildings are studied.

2.1 Timber as construction material

Timber is a traditional construction material that's been used for many centuries. It's a natural organic material with several advantages. It has a high strength to weight ratio and can be manufactured in different in a wide range of shapes and sizes. It can be combined with other construction materials and is the only material that doesn't contribute to greenhouse emissions.

Since timber is natural organic, some complexities come with the usage. Its properties are highly variable and are sensitive to environmental and loading conditions. It is orthotropic due to its high strength and stiffness parallel to the grain i.e. longitudinal direction but low strength properties perpendicular to the grain, which refers to the radial and tangential direction. The material also has stiffness deviations and different shrinkage/swelling characteristics exists in all three orthogonal directions. The orthotropic directions can be seen in Figure 1 (Harte, 2009).

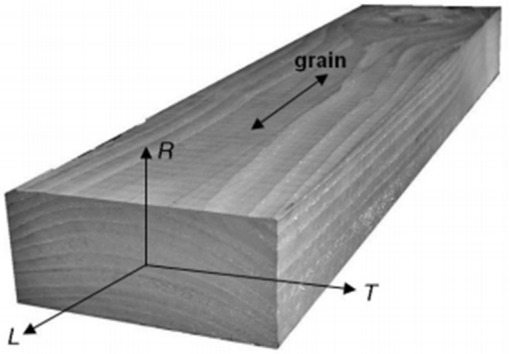

Figure 1: Orthotropic directions for wood (Harte, 2009).

Wood is a hygroscopic material that is capable of exchanging moisture with its surroundings. Its properties vary significantly with the moisture content, which is defined as the ratio of the mass of water that can be removed from the wood to the mass of the dry wood. The moisture content must be chosen carefully, not only due to strength and swelling/shrinkage differences, but also because wood is susceptible to attack by a variety of organisms. Preservative treatment can be used if the moisture content cannot be controlled in an exposed environment.

Measurements of mechanical properties are normally performed on timber specimens with approximately 12% moisture content. The mechanical properties origins from testing and grading where the material is classified to satisfy different end user requirements and ensure product reliability. When designing structural elements, one must account for the presence of defects. Defects such as knots makes it difficult to determine the actual strength of the specimen. It's analytically described by assuming defects to smeared out over the volume and consequently dependent of the element size (Harte, 2009).

2.1.1 Engineered wooden products

Engineered wooden products (EWP) was developed to overcome the size limitation of sawn timber. Sawn timber can only be found to certain dimensions due to the size of the trees and the industrial process. The maximum size of sawn timber in Sweden has a depth of 245 mm and a length of less than 5,5 meters. Larger dimensions are possible to form out of sawn timber boards, veneers, particles or fibers by using adhesives to hold the components together. The EWP in forms of beams and panels are chronologically shown in Figure 2.

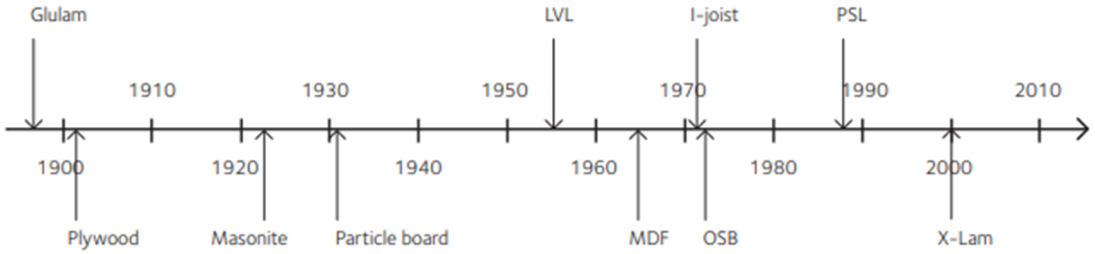

Figure 2: Development of EWP over the 20th century (Swedish Wood, 2015).

Majority of the EWP was developed in North America during the 1900's due to lack of material from old growth timber. It led to an increased use of material from smaller diameter trees, lower quality logs and new tree species. Consequently, it was found that new value-added products with good structural properties can be developed by having a controlled production process (Swedish Wood, 2015).

2.1.2 Glulam

Glulam is the first EWP and is made from four or more laminations that's bonded together with adhesives. The boards/lamellas are oriented in the same fiber direction, which also is in the axial direction of the glulam beam. Normal glulam laminations in Sweden is 45 mm thick with a width of up to 215 mm. Wider elements can be produced by gluing two or more glulam beams together. Glulam can either be homogeneous with lamellas of same quality or made to match stresses by having high strength lamellas in outer layers. The last type is denoted as combined glulam.

Mechanical properties for a homogenous cross section are indicated for example as GL32h whereas different lamellas of different strength are GL32c. Tests of load carrying capacities have shown the average glulam to be stronger and have lower variability in strength compared to a solid section as seen in Figure 3. That is due to low-strength defects, which is smeared-out when solid wood is cut into smaller pieces and randomly glued together. The defects in glulam tends to be more uniformly distributed, leading to less variability in strength.

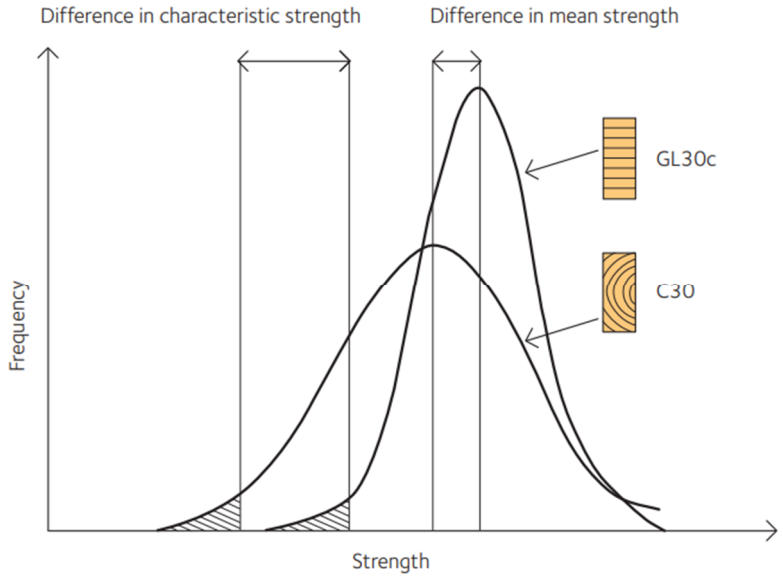

Figure 3: Distribution function for the strength of glulam beam and structural timber (Swedish Wood, 2015).

Apart from the strength gain, the material can take many shapes and forms, such as curved beams, pitched beams, portals and arches. This allows for a creative design and it plays an importance role for hyping the material. Glulam implementations for tall buildings can be used as trusses and columns, providing much stiffness to a structure (Swedish Wood, 2015).

2.1.3 Cross-laminated timber

Cross-laminated timber (CLT) is the newest EWP and was developed in central Europe in the 90s. It consists of three or more layers of sawn timber. The sawn timber boards in each layer are placed and glued perpendicularly to the layer above/below as seen in Figure 4. Cross-sections is usually built with boards having the same strength class as in the main bearing direction (Swedish Wood, 2017).

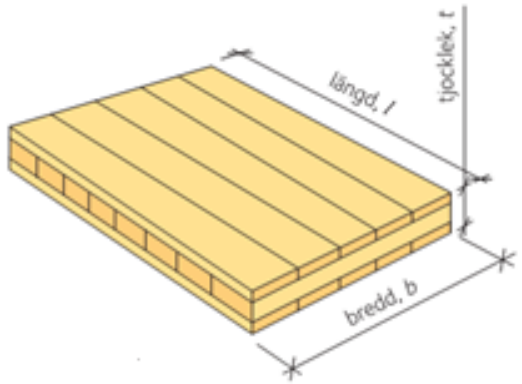

Figure 4: Layout of a 3-layered CLT panel (Swedish Wood, 2017).

The size of CLT panels depends on the manufacturer, but are generally from 60 mm thick, up to 500 mm thick, 3000 mm wide and with a length of up to 24 m. The strength parameters for CLT are mainly set for each manufacturer after testing of the material by an independent third party (Swedish Wood, 2015).

The layout of the panels enables both lateral and vertical force transfer. Diaphragm action is achieved and is used for shear walls, roof and floor elements. Two types of diaphragm action are distinguished for roof and floor elements, denoted as semi-rigid or flexible. The horizontal load distribution depends on the rigidity of the floor/roof and supporting elements. Whether the diaphragm is flexible or rigid, the principle of distributing horizontal forces can be seen in Figure 5. Loads are transferred to the slabs from exterior walls which is transferred to shear walls (Swedish Wood, 2017).

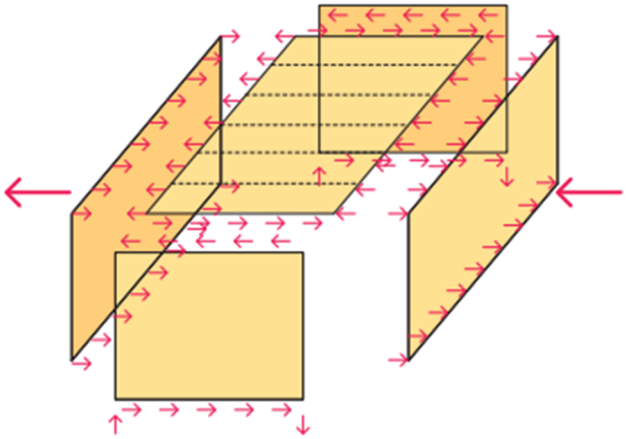

Figure 5: Horizontal load transfer by diaphragm action (Swedish Wood, 2017).

CLT panels is efficient to work with in production, where the elements often arrive to the building site ready for assembly. Customization of the elements can be made at the factory with the help of advanced machines. Holes for doors and windows as well as grooves for electrical fittings is already prepared for example (Swedish Wood, 2015).

The cross section can be designed freely by the number of boards and take curved shapes. It makes CLT applicable for projects such as sports arenas, bridges, industrial buildings. It is gradually becoming an alternative to conventional materials in multi-storey buildings and commercial construction, due to its high strength and stiffness properties. The research and manufacturing development have been getting lots of attention in the industry. Both clients and entrepreneurs over the world starts to realize the advantages of building in timber. The manufactured volume of CLT in Europe can be seen in Figure 6 (Swedish Wood, 2017).

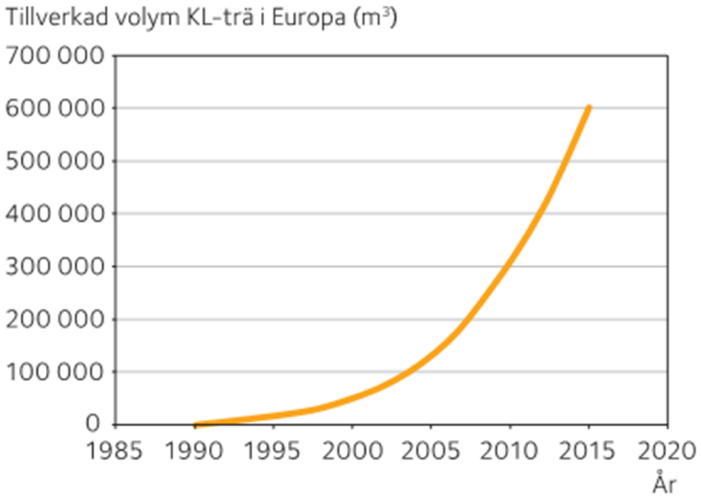

Figure 6: Manufactured volume of CLT in Europe over time (Swedish Wood, 2017).

2.2 Background of structural dynamics

2.2.1 Eigenfrequency

Eigenfrequencies are the frequencies at which the structure will tend to vibrate when subjected to external forces. Frequency is an oscillation per time, denoted in Hertz, and describes the motion in terms of cycles per second. A simple model to describe natural frequencies is by an undamped mass-spring system with a single degree of freedom, shown in Figure 7. The influencing parameters is mass (m) and stiffness (k) (Craig & Kurdila, 2006).

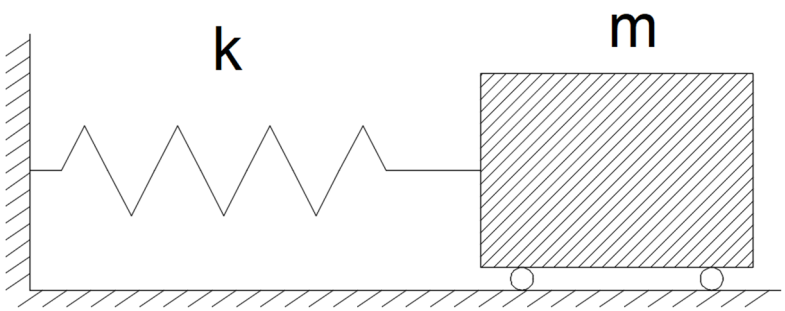

Figure 7: Mass-spring system of an undamped single degrees of freedom system

$$\omega_n = \sqrt{\frac{k}{m}} \quad \text{where } \omega_n \text{ is the angular frequency in [rad/s]} \tag{2.1}$$

$$f_n = \frac{\omega_n}{2\pi} \quad \text{where } f_n \text{ is the eigenfrequency in [cycle/s]} \tag{2.2}$$

$$T_n = \frac{1}{f_n} \quad \text{where } T_n \text{ is the natural time period [s]} \tag{2.3}$$

The eigenfrequency, or so-called natural frequency, is dependent on mass and stiffness of the oscillating system. The relation between natural frequency and time-period is shown in Figure 8

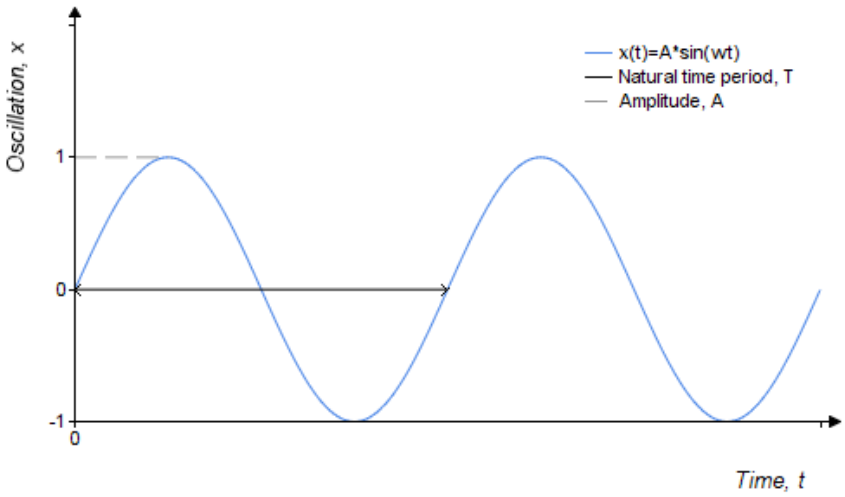

Figure 8: Oscillation over time for an undamped SDOF system

2.2.2 *Acceleration*

The equation of motion for the SDOF oscillating system can be described by Newton's second law where the total force is defined as the product of acceleration and mass. Subsequently accelerations can be decreased by an increased mass. Moreover, acceleration is defined from the derivative of the velocity which in turn is the derivative of the displacements as shown in Figure 9 (Craig & Kurdila, 2006).

The eigenfrequency of a specific mode shape for a specific oscillating system is constant and cannot be changed without changing the properties of the system like boundary conditions, stiffness, mass or damping. Larger applied force results in larger oscillation amplitude which leads to increased acceleration for the same oscillating frequency.

Decreasing the acceleration can be achieved either by an increased mass and/or stiffness, but at the same time decrease the oscillating amplitude. Furthermore, an increasing damping could also be used to slow the oscillating motion, as described in upcoming section, leading to a decrease of the acceleration.

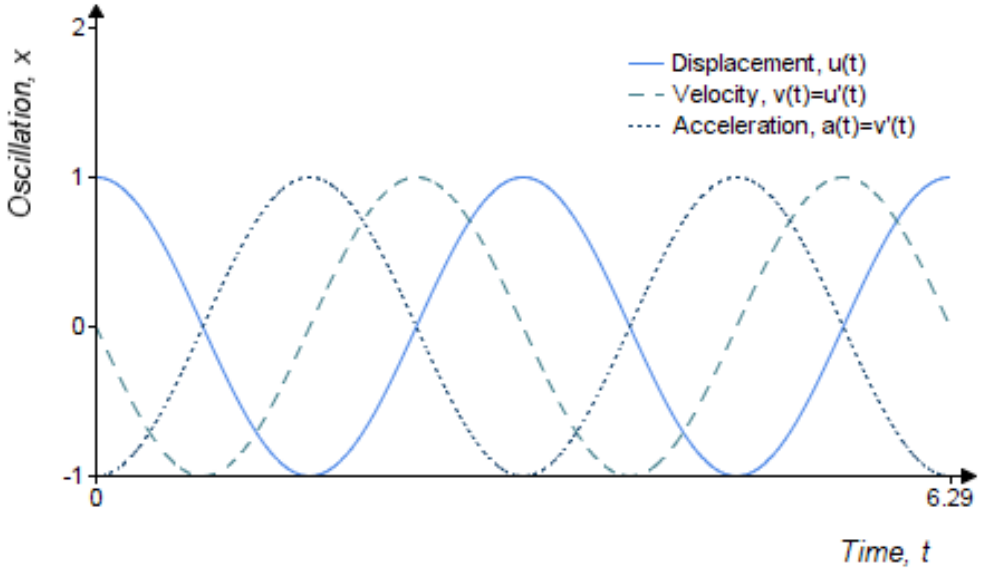

Figure 9: Accelerations expressed from the second derivative of the displacements.

2.2.3 Mode shape

The mass-spring system in Figure 7 is a single degree of freedom system, meaning that it has only one eigenfrequency and one mode shape. The mode shape describes the deformed shape of the oscillating system. Physical objects have multiple degrees of freedom with several mode shapes. Every eigenfrequency have a mode shape of its own.

The study of mode shapes for buildings is usually limited to a few critical shapes with transversal or torsional shapes. Translational modes in x and y-direction are most commonly analyzed in the design for wind action. Different mode shapes of a tall timber building subjected to wind load are illustrated in Figure 10.

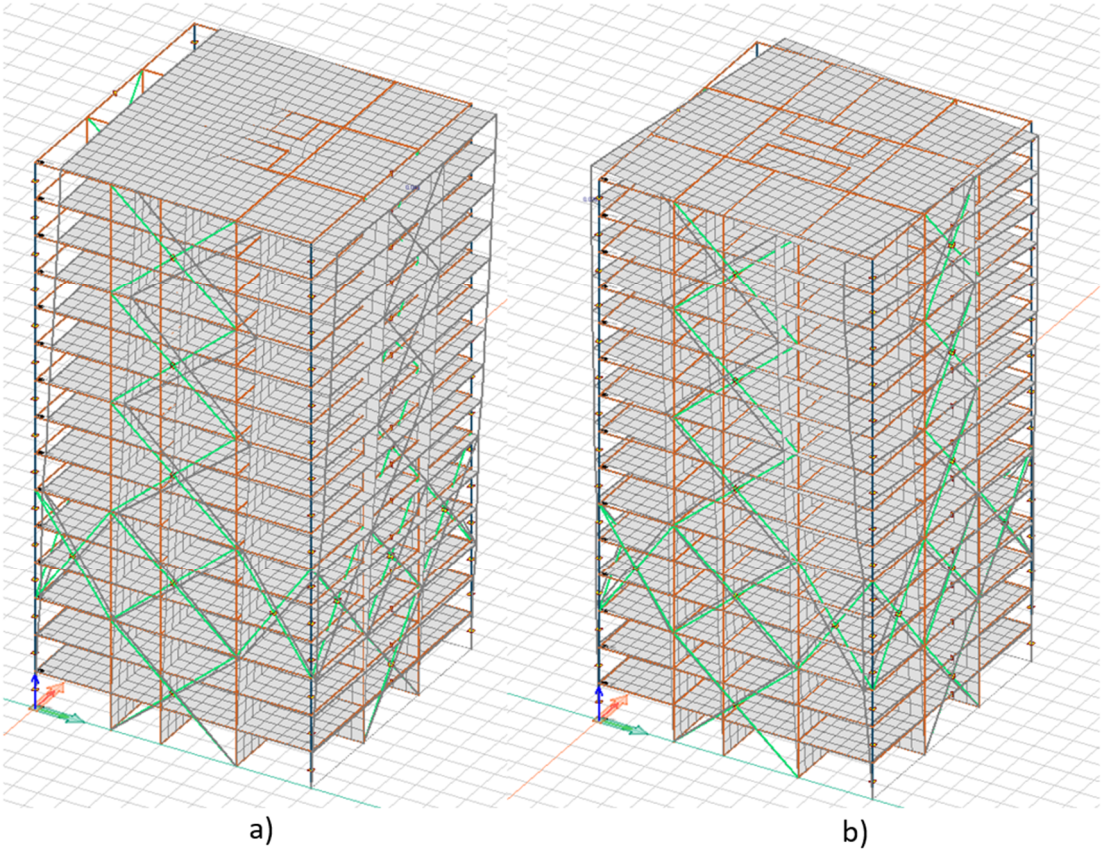

Figure 10: Mode shapes of timber building subjected to wind load. a) Translational; b) Rotational.

2.2.4 Damping

Real objects always have self-damping which origins from frictional forces. The frictional forces come from the relative motion between different elements that provide damping. In addition, internal losses also occur on a microscopic level in the material, known as material damping (Mokeretla, 2011).

Damping is naturally causing dissipation of energy until the oscillations stop. The magnitude of damping is characterized by a damping factor, ξ expressed as the ratio between the damping coefficient and the critical damping coefficient.

$$\xi = \frac{c}{c_{cr}} \quad \text{where } c \text{ is the damping coefficient} \tag{2.4}$$

$$c_{cr} = 2m\omega_n \quad \text{where } c_{cr} \text{ is the critical damping coefficient} \tag{2.5}$$

The exact damping factor of a structure is difficult to define in the design process and is usually approximated. Linear viscous damping is the simplest way to consider damping. The damping force in linear viscous damping is directly proportional to the velocity of the oscillating system. Three cases of linear viscous damping exist: an underdamped ($\xi < 1$), critically damped ($\xi = 1$) and overdamped ($\xi > 1$).

The most important case is the underdamped system, which has oscillations with decreasing amplitude. An overdamped system has no oscillation, where the amplitude slowly decays. The critically damped case responds similar to the overdamped, but the amplitude decreases more rapidly, as seen in Figure 11 (Craig & Kurdila, 2006).

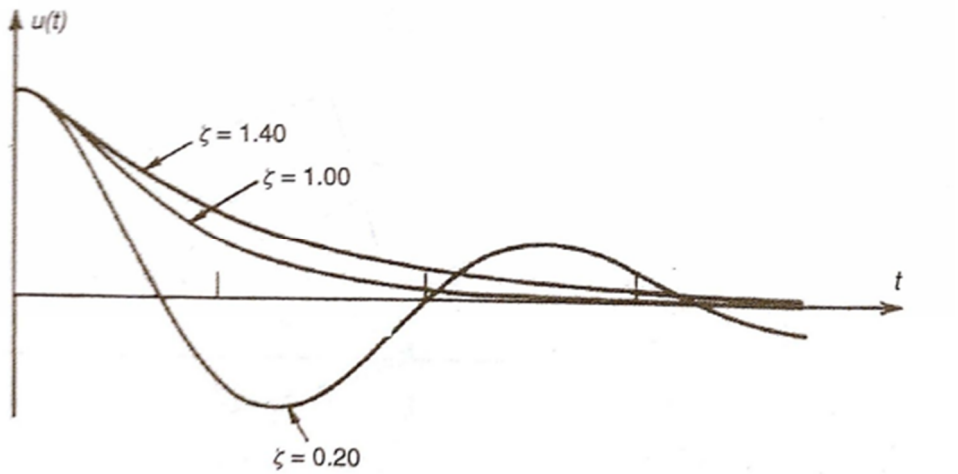

Figure 11: Response of a viscous damped SDOF system (Craig & Kurdila, 2006).

Damping in SS-EN-1991-1-4 is expressed in terms of logarithmic decrement of damping and is suitable for approximating the damping factor. The damping factor can be computed by finding the logarithmic value of the oscillation amplitude in the beginning of a cycle u_P in relation with the amplitude at the end of the same cycle, u_Q (Craig & Kurdila, 2006).

The principle is shown in Figure 12, expressed as:

$\delta = ln\frac{u_P}{u_Q} = \xi\omega_n T_d$ where δ is the logarithmic decrement of damping (2.6)

$\delta = 2\pi\xi$ where δ is approximated for underdamped systems (2.7)

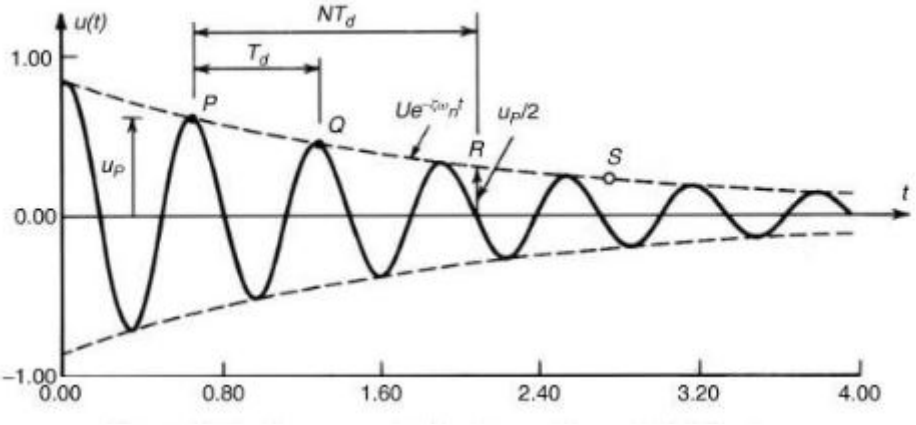

Figure 12: Amplitude decrease of a damped system (Craig & Kurdila, 2006).

2.2.5 Resonance

Resonance is a phenomenon in which a dynamic force drives a structure to vibrate near or at its natural frequency, causing the system to oscillate with higher amplitudes which continues to grow. It can be found when a dynamic load acts as a forced frequency, Ω which's applied near or at the same frequency as the oscillating structure, ω_n. The effect on the amplitude is formulated by the dynamic magnification factor, D_s and is shown in Figure 13 for different levels of damping.

$r = \frac{\Omega}{\omega_n}$ where r is the frequency ratio (2.8)

$D_s = \left|\frac{1}{1-r^2}\right|$ where D_s is the dynamic magnification factor (2.9)

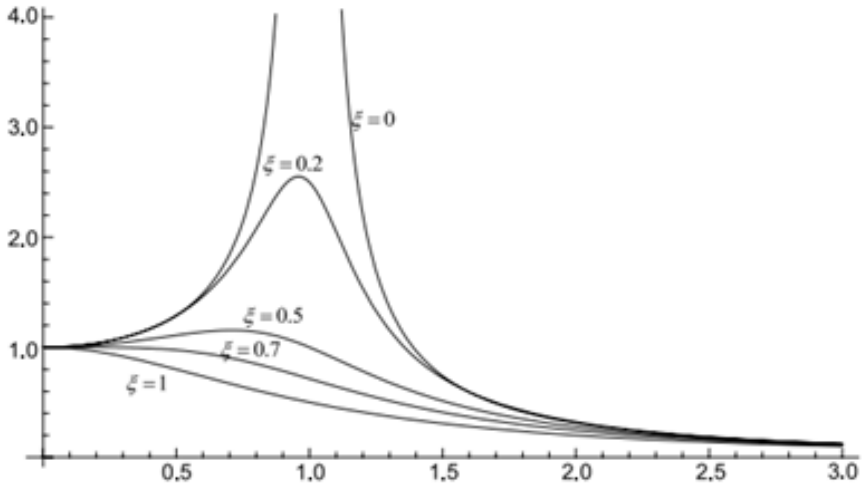

Figure 13: Variation of the steady-state dynamic magnification factor with damping and frequency ratio (Craig & Kurdila, 2006).

2.3 Wind induced effects

2.3.1 Wind loading on structures

Wind is the term used for air in motion and is induced by pressure differences which in turn origins from temperature differences. Wind is composed of a multitude of eddies of varying sizes and rotational characteristics carried along in a general stream of air. The eddies move relative to the earth's surface and gives the wind its gusty/turbulent character. The gustiness of strong winds in the lower levels of the atmosphere largely arises from interaction with surface features. The average wind speed over a time period of ten minutes or more, tends to increase with height, while the gustiness tends to decrease with height. Eddies around a structure can be seen in Figure 14.

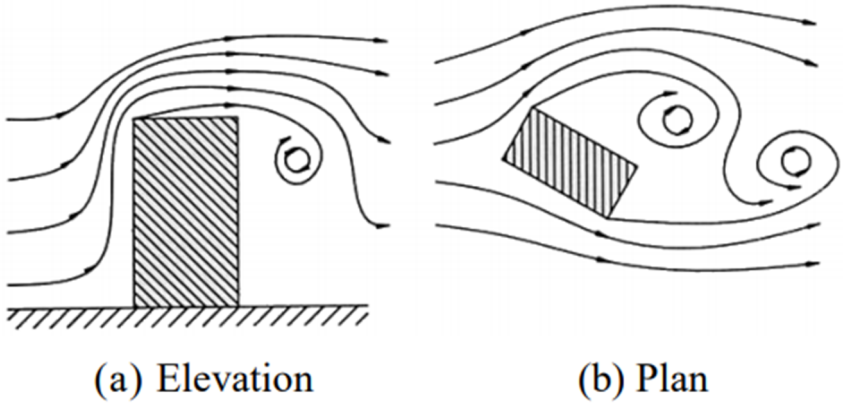

Figure 14: Generation of eddies around a structure (Mendis, et.al., 2007).

The flow pattern generated around a building is complex and influenced by distortions of the mean flow, flow separation, the formation of vortices and development of the wake. Large aerodynamic loads act on the structure in form of intensive localized fluctuating forces. The building tends to vibrate in rectilinear and torsional modes under the influence of the fluctuating forces, seen in Figure 15.

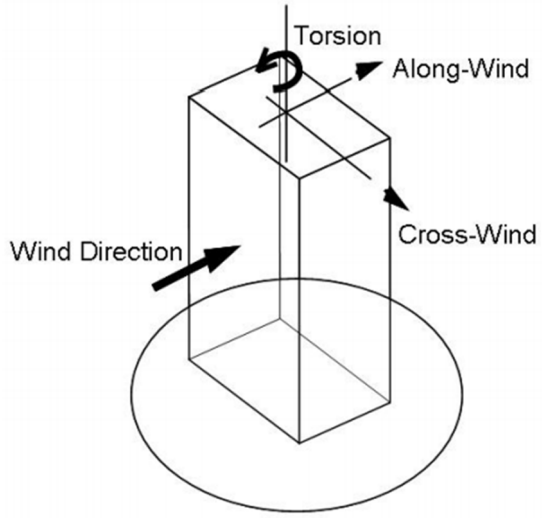

Figure 15: Wind response from fluctuating forces (Mendis, et.al., 2007).

The amplitude of such oscillations is dependent on the aerodynamic forces and the dynamic characteristics of the building. Structures that respond dynamically to wind effects is those who are tall and/or slender. Phenomena's that gives rise to dynamic

response of structures in wind are buffeting, vortex shedding, galloping and flutter. The last two depend on turbulence effects and how it affects the wake development. Flutter and galloping are generally not considered for design of buildings.

Slender structures are likely to be sensitive to dynamic response in line with the wind direction due to turbulence buffeting. Buffeting is assumed to consist of a mean component and a fluctuating component due to wind speed variations from the mean. These serve as a base for the gust factor approach, which is applied in many design codes. The mean wind component is generated from mean wind speed and load coefficients. Fluctuating loads are determined from a method that considers turbulence intensity, size reduction effects and dynamic amplification (Mendis, et.al., 2007). The principal wind loading on a structure with effect of turbulence is shown in Figure 16.

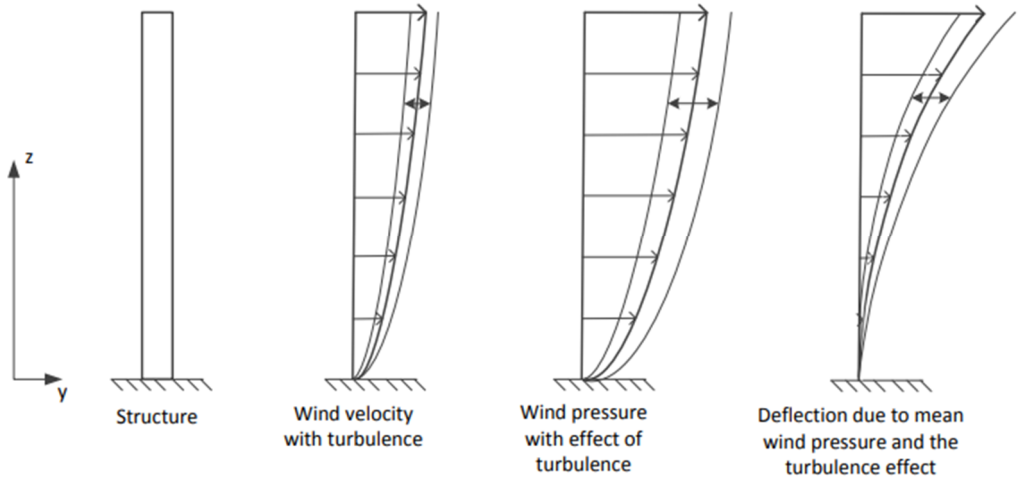

Figure 16: Load pattern on a structure with the effect of turbulence (Reynolds, et al., 2015).

Vortex shedding is the most common form of cross wind action and occurs if the natural frequency of the building coincides with the shedding frequency of the vortices. The structure will experience resonance where large amplitude displacement may occur. Vortex shedding is often referred to as the critical velocity effect. When vortices shed, it creates an asymmetric pressure on the transversal sides of the building.

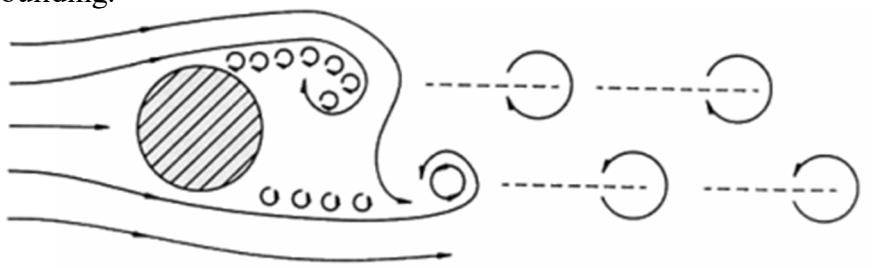

Figure 17: Wind movement under shedding of vortices (Mendis, et.al., 2007).

Wind induced effects is in structural design handled either by a static analysis or a dynamic analysis. The static approach is based on a quasi-steady approximation and assumes that the building is a fixed rigid body in the wind. It approximates peak wind pressures on building surfaces by the product of the mean pressure coefficients and gust dynamic wind pressure. The method has some limitations and is not appropriate for tall and/or slender structures (Mendis, et.al., 2007).

2.3.2 *Human response*

There is no single standard that's internationally accepted as a comfort-criteria in design of tall buildings. Accelerations has become the standard parameter for evaluation of the human response because it is readily measured in practice and can be analytically calculated. It's expressed either as root mean square (r.m.s) or peak acceleration, depending on used standard. The human perception and tolerance of vibrations varies between individuals and depends on factors such as the natural frequency of the building, occupant's gender and age, expectancy and activity, accelerating motions etc. Lots of research has been made in a low frequency range of 0-1 Hz by looking at these parameters. Some guidelines of the human perception can be found in Figure 18.

Thresholds and tolerance levels can be very subjective. Generally, failure of meeting acceleration thresholds in service state is not a catastrophe. It's a matter of evaluating the performance towards its function and communicating with the user or owner. The allowed peak acceleration is generally stricter for residential buildings compared to office buildings. Residential buildings are assumed to be occupied the whole day and it's believed that people are more tolerant at work than at home (Taranath, 2011).

LEVEL	ACCELERATION (m / sec^2)	EFFECT
1	< 0.05	Humans cannot perceive motion
2	0.05 - 0.1	a) Sensitive people can perceive motion; b) hanging objects may move slightly
3	0.1 - 0.25	a) Majority of people will perceive motion; b) level of motion may affect desk work: c) long - term exposure may produce motion sickness
4	0.25 - 0.4	a) Desk work becomes difficult or almost impossible; b) ambulation still possible
5	0.4 - 0.5	a) People strongly perceive motion; b) difficult to walk naturally; c) standing people may lose balance.
6	0.5 - 0.6	Most people cannot tolerate motion and are unable to walk naturally
7	0.6 - 0.7	People cannot walk or tolerate motion.
8	> 0.85	Objects begin to fall and people may be injured

Figure 18: Human perception levels (Coull & Stafford Smith, 1991)

2.3.3 Structural response in 2-D

A tall structure can be expressed as a fixed cantilever beam. The wind load results in a total deformation, consisting of a shear and bending component. The deformed shape for respective component is shown in Figure 19 with a magnitude depending on height of the building, material properties and section dimensions. Two known beam-theories that describe overall deformations are Euler-Bernoulli and Timoshenko beam-theory.

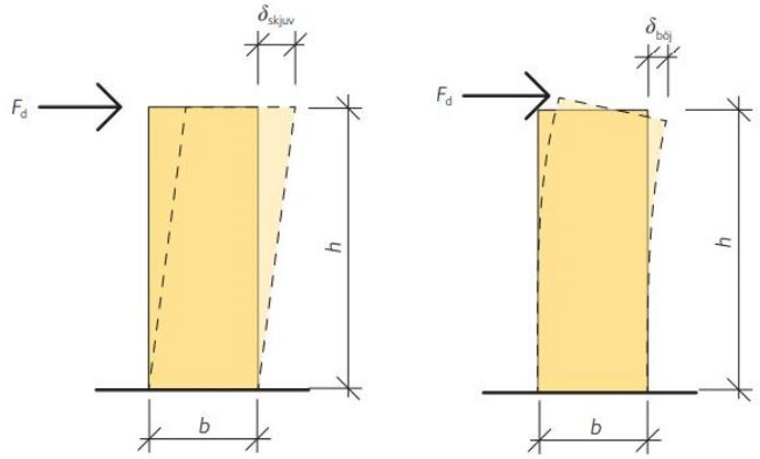

Figure 19: Shear and bending deformation of a structure (Swedish Wood, 2017).

Euler-Bernoulli beam theory, also known as classical beam theory, simplifies the linear-elastic material properties by assuming plane sections to remain plane after deformation and perpendicular to the longitudinal axis after bending. The theory neglects transverse shear effects and assumes that shear strains are small enough to be neglected.

Timoshenko beam theory accounts for transverse shear strains in which plane sections do not remain plane after deformation, seen in Figure 20. A rotation is formed between the cross section and the bending line due to shear deformations. This effect in turn lowers the stiffness of the beam which predicts larger deformations and lower natural frequencies (NPTEL, 2019).

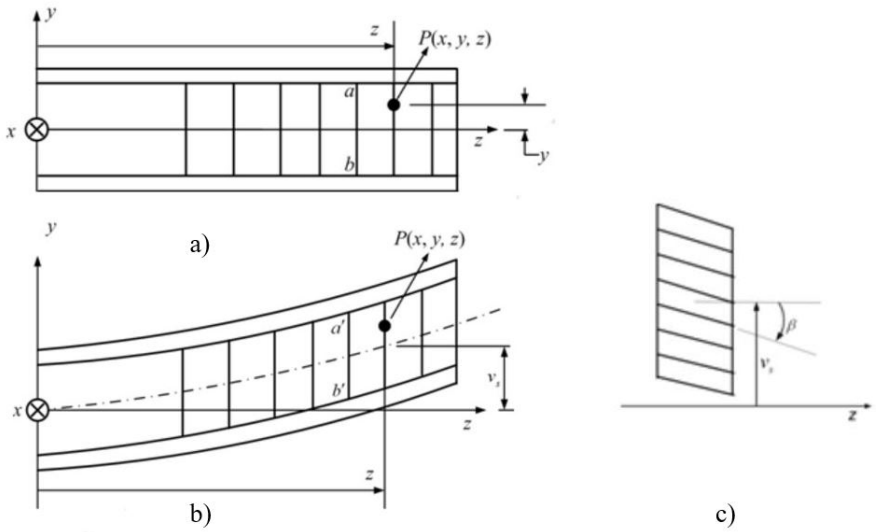

Figure 20: Response of a Timoshenko beam. a) beam before deformation; b) the beam after shear deformation; c) Rotation due to shear (NPTEL, 2019).

2.4 Structural systems

An overview of structural systems that's possible to implement into tall timber buildings is introduced. Three fundamental ways to achieve horizontal stability is illustrated in Figure 21. Rigid joints are not present in timber projects of today as the horizontal resistance is limited. Hence the methods of diagonal bracing and shear wall are described.

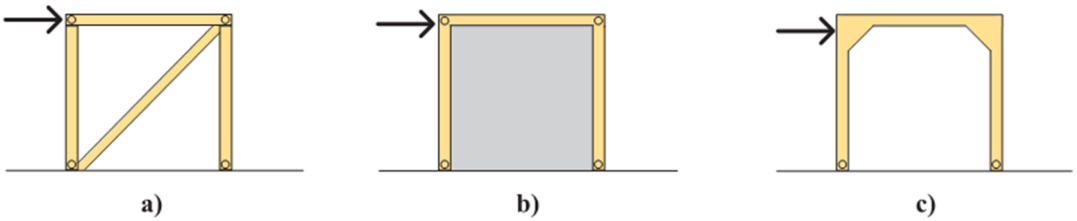

Figure 21: Different ways to stable a structure. a) diagonal bracing; b) shear wall; c) rigid joints (Swedish Wood, 2015).

2.4.1 Braced frame structures

Bracing is an efficient method to resist horizontal forces in a frame structure. Lateral stiffness is provided by diagonal members that acts in axial compression or tension. Diagonals along with beams and columns forms a braced frame and behaves as a vertical cantilever truss under horizontal loading. The diagonals and beams act as the web members of the truss and transfer horizontal shear forces, while the columns act as chords. The chords carry the external moment, with tension in the windward column and compression in the leeward column.

Braced frame systems are considered an efficient solution because it can be applied for any height and uses the full axial capacity of the material. Consequently, bracing provides lots of lateral stiffness for the minimum amount of additional material. The main disadvantage of bracing systems is the conflict with internal planning and it limits the placement of doors and windows (Coull & Stafford Smith, 1991).

Bracing systems are grouped into two categories, concentric and eccentric bracing. Eccentric bracing is not concentric with the main joints which gives less horizontal stiffness compared with concentric bracing. Eccentric bracing is mainly used in seismic design when ductility needs special considerations. Some examples of the two types can be seen in Figure 22.

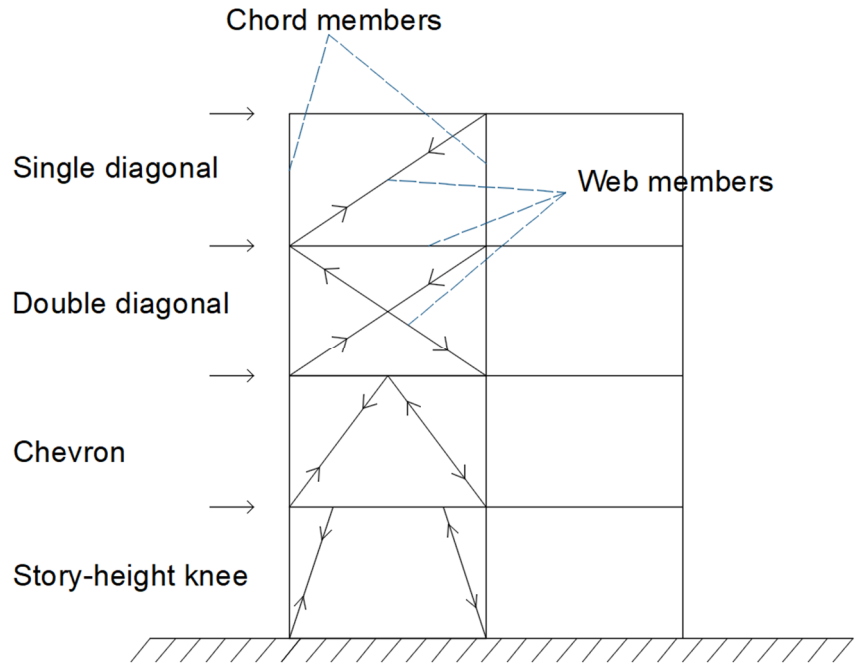

Figure 22: Different types of bracing.

The overall behaviour of a braced frame system can be seen in Figure 23 and it's a combined effect of flexural and shear deformations. Flexural configuration occurs due to axial deformation of the chords when subjected to wind loading, which in turn causes lateral deflections. Shear configuration is caused by shear deformations of the web members. The shear deformations are gradually decreasing with the height (Coull & Stafford Smith, 1991).

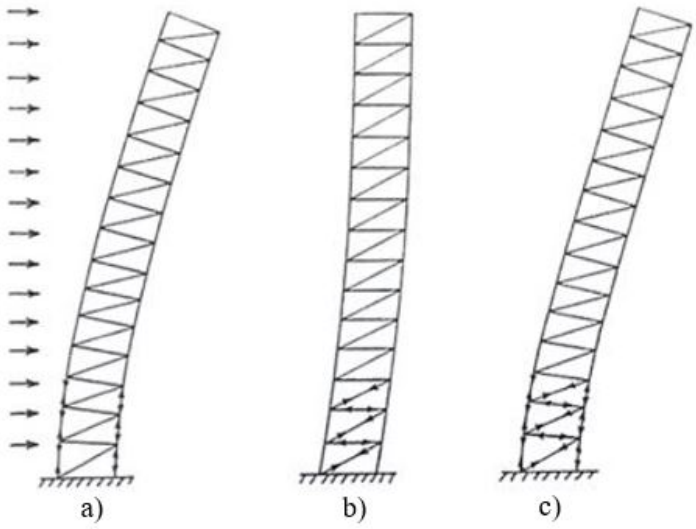

Figure 23: Deformation effects of a braced structure when subjected to wind loading. a) Flexural deformation; b) Shear deformation; c) Combined effect (Coull & Stafford Smith, 1991).

2.4.2 Shear walls

Shear walls are able to carry both vertical and lateral loads. Shear walls are commonly used in residential buildings and hotels where partitions between apartments are needed. Similar floor-by-floor layout allows them to be vertically continuous. They have a high in-plane stiffness and can stabilize the structure individually or in combination with rigid frames or braced frames. They act as vertical cantilevers in form of separate planar walls and/or as non-planar connected walls and cores around elevator or staircase shafts as seen in Figure 24.

An issue with shear walls is that the solid form tends to restrict open-floor planning. Although, this is not the case for central core structures which enables open-plan surfaces, due to its high torsional and flexural stiffness. The wall placement in general should be made so that they attract dead loading that's sufficient enough to suppress max tensile bending stresses in the wall caused by wind loading (Coull & Stafford Smith, 1991).

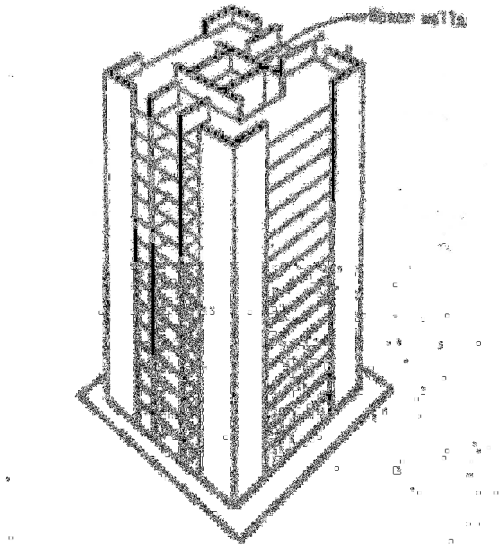

Figure 24: Braced shear wall structure with separate and combined shear walls (Coull & Stafford Smith, 1991).

2.4.3 Outrigger system

An outrigger system is formed by linking a core structure and a perimeter system with braced members. The purpose is to activate perimeter columns to resist lateral forces, overturning and/or torsion. Activating perimeter/corner columns generates more stiffness for a low amount of extra material. A fully activated outrigger system has one or several 'belt trusses' that encircles the building which drive perimeter columns to work against lateral forces. In the event that additional flexural stiffness is required, the great lever arm at outrigger columns makes slightly additional material more effective than in the core.

The number and placement of outriggers is varying based on height. A simplified case of outrigger placement and deflection when subjected to a lateral force on top storey is presented in Figure 25 and Table 1. As for all diagonals the challenge with this type of bracing is additional interference with openings will most likely disrupt the aesthetics of the building (Choi, Joseph, & Mathias, 2012).

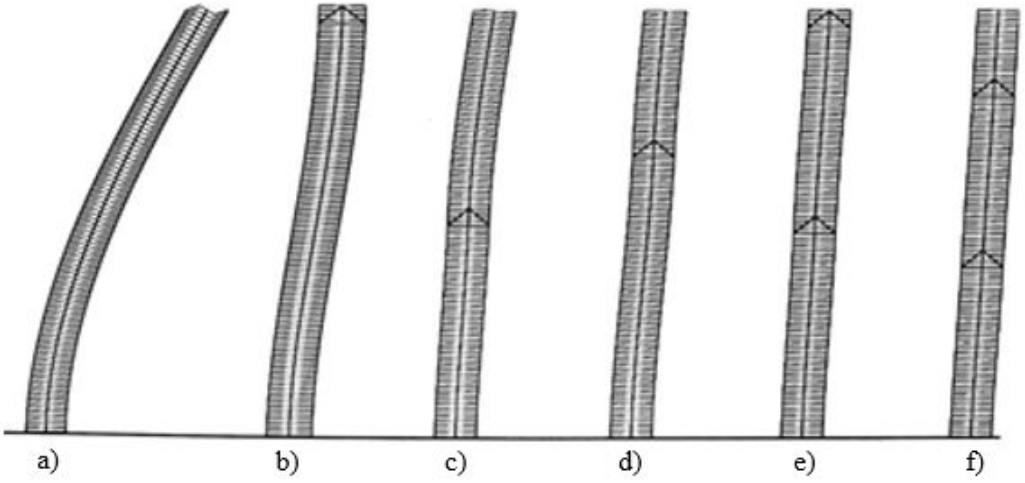

Figure 25: Effect of outrigger locations on building drift from a simplified load case of lateral point load on the roof (Choi, Joseph, & Mathias, 2012).

Table 1: Effect of outrigger location on building drift.

Outrigger placement						
Case	a	b	c	d	e	f
Outrigger height	0	h	h/2	2h/3	h, h/2	4h/5, 2h/5
Drift/Drift (a)	1	1/4	1/6	1/9	1/16	1/25

As indicated from Figure 25 and seen in Table 1, the drift of the building is gradually decreasing when configuration of the system is made. The best location of a single outrigger is in the top third of the building case (d) and case (f) for two outriggers.

2.4.4 Braced tube

Another combined system is the braced tube where large-scale diagonals are placed in facades, spanning over the whole base of one building as seen in Figure 26. This provides lots of stiffness w.r.t flexure, shear and torsion and is referred to as one of the most efficient bracing system. An advantage with this type of bracing is that the spacing between columns can be increased, as the diagonals are very stiff and has fewest possible indifferences regarding inclination, meeting points with other trusses. Stress differences in columns can be more 'evened' by redistribution of axial loads, prohibiting the existence of highly stressed columns. The system correlates to very large sections of diagonal, which has a large impact on the building both from an architectural and structural point of view (Coull & Stafford Smith, 1991).

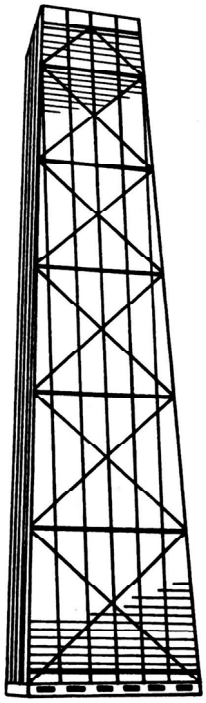

Figure 26: External diagonals used in a braced tube (Coull & Stafford Smith, 1991).

2.4.5 Structural applications in tall timber buildings

Structural systems such as braced frame and shear wall structure are used to build higher in timber and are in their context referred as a Post and beam system. The structural system of the tallest and second tallest timber structure is studied to find what's been essential in the design.

Treet is a 14-storey multi-residential building, located in Bergen. It was built in 2015 and has been the tallest timber structure until Mjöstornet was finished in 2019. The governing factor in the design of Treet is the wind-induced vibrations in service state. Calculation of the dynamic wind is based on a reference wind speed of 26 m/s.

The structural system of Treet, shown in Figure 27, is a trussed beam and column system. The central core is of CLT walls but are only included as vertical bearing for stairs and elevators. Glulam columns and trusses of quality GL30c is implemented to transfer vertical and lateral forces. Concrete slabs are placed on the intermediate storeys and the roof with purpose to add more mass to the structure. The slabs serve as a base for stacking volumetric modules onto each other. Modules are stacked for 4 storeys starting from the foundation, also in concrete. (Bjertnaes & Malo, 2014).

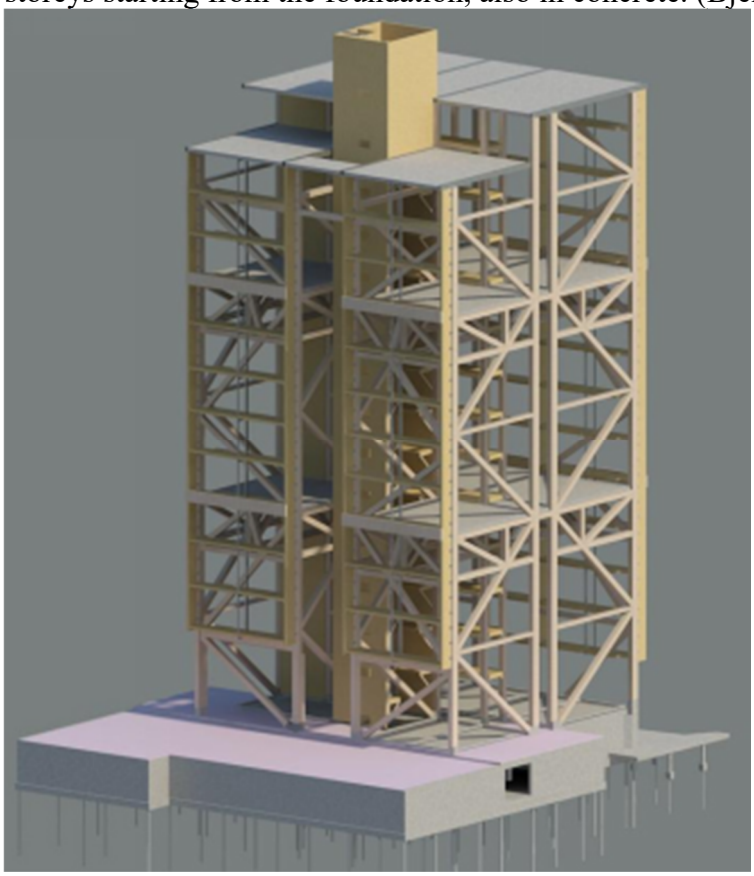

Figure 27: Structural skeleton of Treet (Bjertnaes & Malo, 2014).

Mjöstornet is a mixed-use building of 18-storeys, sited in Brumundal. It has a geometry of 17x31 m^2 and designed for wind-induced vibrations. The dynamic wind is based on a reference wind speed of 22 m/s.

The load bearing elements of Mjöstornet can be seen in Figure 28. Large glulam trusses (GL30c, GL30h) are used for bracing the structure along with internal columns and beams. The biggest cross-sections of diagonals are 625x990 mm and 1485x625 for columns in the corner columns. CLT walls are used for secondary bearing of elevators and staircases and does not contribute to horizontal stability of the building. Concrete floors with a thickness of 300 mm is implemented to increase the structural mass. These are inserted from the 12^{th} storey up to the top (18^{th}) and was mainly needed to limit wind-induced vibrations on the slender side of the building (Abrahamsen, 2017).

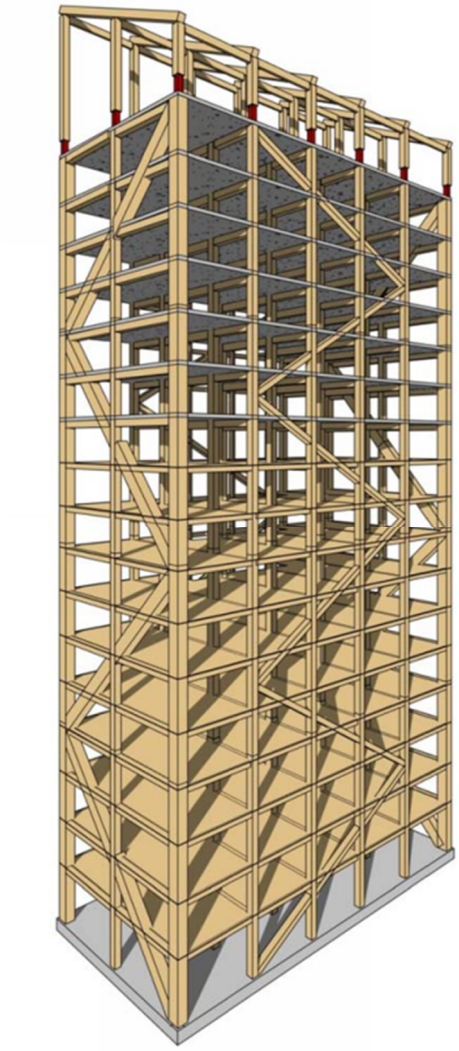

Figure 28: Structural skeleton of Mjöstornet (Abrahamsen, 2017).

3 Standards accounting for wind effects

This chapter introduces the required standards for analyzing the structural behavior due to wind-induced effects. Dynamic effects from wind is treated as a quasi-static load in which the analytical methodology is based upon, *SS-EN-1991-1-4* and *EKS 10*. Evaluation of the structural response is stated in *ISO 10137* and *ISO 6897*.

3.1 SS-EN 1991-1-4

The wind action is represented by a simplified set of pressures whose effects are equivalent to the extreme effects of the turbulent wind. The modelling of wind actions covers dynamic response due to along-wind turbulence which is in resonance with the fundamental mode shape. The standard is restricted to buildings up to 200m high and does not cover torsional vibrations for tall buildings.

3.1.1 Wind forces and pressures

Wind velocity is used as a basis for wind pressure calculation, which is defined as a mean and fluctuating component. The mean velocity depends on the wind climate and the height, variation of wind pressure is determined from the terrain roughness and orography. This is reformulated in terms of peak velocity pressures which is used to define wind pressures.

Wind pressure acting on external surfaces, w_e is defined as:

$$w_e = q_p(z_e) \cdot c_{pe} \tag{3.1}$$

where:

$q_p(z_e)$ is the peak velocity pressure

z_e is the reference height for the external pressure

c_{pe} is the pressure coefficient for the external pressure

The velocity pressure profile is shown in Figure 29 at different heights. For buildings taller than the width of its base, the velocity pressure profile changes.

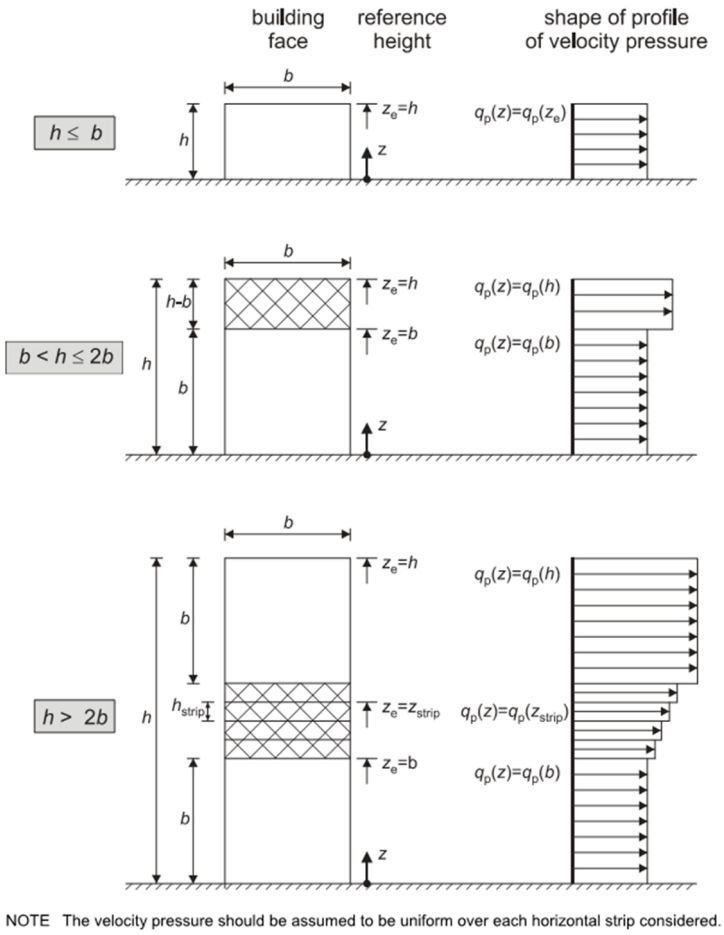

Figure 29: Reference height, z_e, depending on height, base and corresponding velocity pressure profile.

3.1.2 Dynamic characteristics of structures

Dynamic characteristics in Eurocode assumes linear-elastic structure responds and possess classic normal modes. Dynamic structural properties are characterized by:

- Natural frequency
- Modal shapes
- Equivalent mass
- Logarithmic decrements of damping

If the height exceeds 50 meters of a multi storey building, following approximation of the fundamental frequency may be used:

$$n_1 = \frac{46}{h}\,[\text{Hz}] \qquad (3.2)$$

where:

h is the height of the structure

The fundamental mode shape, Φ_1 of buildings, towers and chimneys cantilevered from the ground may be estimated as:

$$\Phi_1(z) = \left(\frac{z}{h}\right)^{\zeta} \quad (3.3)$$

where

$\zeta = 0.6$ for slender frame structures with non load-sharing walling or cladding

$\zeta = 1{,}0$ for building with central core plus peripheral columns or larger columns plus shear bracings

$\zeta = 1{,}5$ for slender cantilever buildings and buildings supported by central reinforced concrete cores

$\zeta = 2{,}0$ for slender cantilever buildings and buildings supported by central reinforced concrete cores

$\zeta = 2{,}5$ for slender cantilever buildings and buildings supported by central reinforced concrete cores

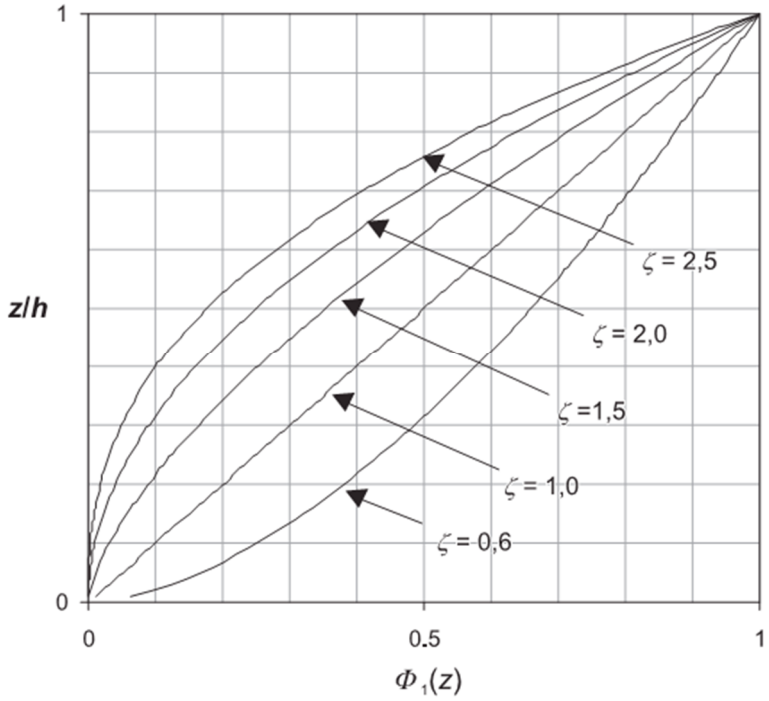

Figure 30: First flexural mode shape for buildings, towers and chimneys cantilevered from the ground.

Equivalent mass per unit length m_e of the fundamental mode is given by:

$$m_e = \frac{\int_0^{\ell} m(s)\cdot\Phi_1^2(s)\,ds}{\int_0^{\ell} \Phi_1^2(s)\,ds} \quad (3.4)$$

where:

$m(s)$ is the mass per unit length

ℓ is the height or span of the structure or structural element

i = 1 is the mode number

Logarithmic decrement of damping δ for fundamental bending mode may be estimated by:

$$\delta = \delta_s + \delta_a + \delta_d \quad (3.5)$$

where:

δ_s is the logarithmic decrement of structural damping

δ_a is the logarithmic decrement of aerodynamic damping for the fundamental mode

δ_d is the logarithmic decrement of damping due to special devices

The logarithmic decrement of aerodynamic damping δ_a, for the fundamental bending mode of along wind vibration may be estimated by:

$$\delta_a = \frac{c_f \cdot \rho \cdot b \cdot v_m(z_s)}{2 \cdot n_1 \cdot m_e} \quad (3.6)$$

where:

c_f is the force coefficient in the wind direction

ρ is the density of air

b is the base of the building

$v_m(z_s)$ is the mean wind velocity

n_1 is the fundamental frequency

m_e is the logarithmic decrement of damping due to special devices

3.1.3 Vortex-shedding and aeroelastic instabilities

Critical wind conditions can be evaluated with regards to vortex-shedding and galloping. The criteria for verifying the risk for the two wind phenomena are given.

First, vortex-shedding occurs when vortices are shed alternately from opposite sides of the structure. This gives rise to a fluctuating load perpendicular to the wind direction. Structural vibrations may occur if the frequency of vortex-shedding is the same as the eigenfrequency of the structure.

The effect of vortex-shedding need not to be investigated when

$$v_{crit,i} > 1.25 v_m \tag{3.7}$$

where:

$v_{crit,i}$ is the critical wind velocity for mode i

v_m is the characteristic 10 minutes mean wind velocity

Second, galloping is a self-induced vibration of a flexible structure in cross wind bending mode. Galloping oscillation starts at a special onset wind velocity and the amplitudes increase rapidly with increasing wind velocity.

The effect of galloping need not to be investigated when

$$v_{CG} > 1.25 v_m \tag{3.8}$$

where:

v_{CG} is the onset wind velocity

v_m is the characteristic 10 minutes mean wind velocity

3.2 EKS 10

EKS, “Boverkets konstruktionsregler” is the Swedish annex which complements the Eurocode. It’s a mandatory ruleset based on Swedish conditions for achieving structural stability and durability. National choices are given in addition to the Eurocodes. and covers data of geology, climate, security level, way of living etc.

3.2.1 Wind characteristics

Measured reference wind speed, v_b in Sweden can be seen in Figure 31 and Figure 32. It’s measured as the mean wind speed over 10 minutes at a height 10 metres above ground with a return period of 50 years. The surrounding area is approximated to have low vegetation and isolated obstacles.

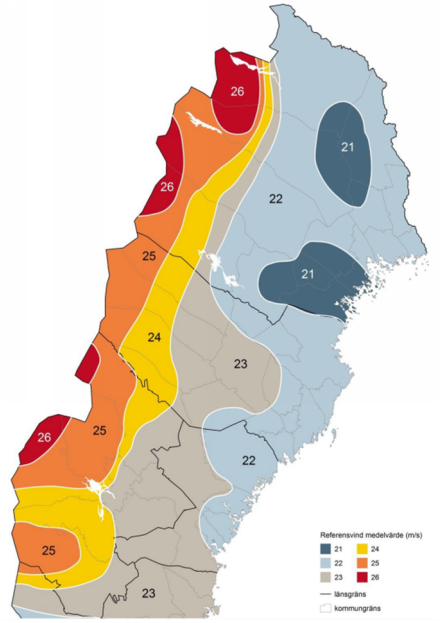

Figure 31: Reference wind speed in northern part of Sweden.

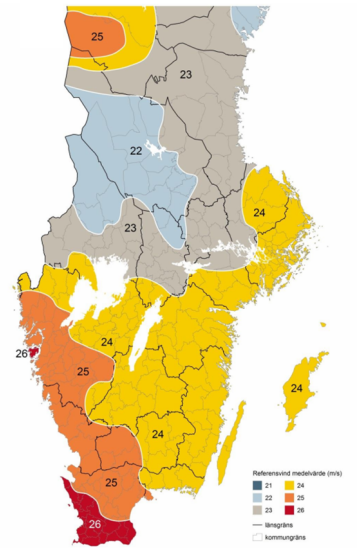

Figure 32: Reference wind speed in southern part of Sweden.

The context of the building is expressed in terms of terrain categories. Surroundings and different ways to classify them can be seen in Table 2.

Table 2: Classification of terrain categories and terrain parameters (SS-EN 1991-1-4, 2005).

Terrain category		z_0 m	z_{min} m
0	Sea or coastal area exposed to the open sea	0,003	1
I	Lakes or flat and horizontal area with negligible vegetation and without obstacles	0,01	1
II	Area with low vegetation such as grass and isolated obstacles (trees, buildings) with separations of at least 20 obstacle heights	0,05	2
III	Area with regular cover of vegetation or buildings or with isolated obstacles with separations of maximum 20 obstacle heights (such as villages, suburban terrain, permanent forest)	0,3	5
IV	Area in which at least 15 % of the surface is covered with buildings and their average height exceeds 15 m	1,0	10
NOTE: The terrain categories are illustrated in A.1.			

The peak velocity, $q_p(z)$ can be defined by the wind reference speed in addition to information of placement/location and height of the building. An exposure factor, $c_e(z)$ is defined from Figure 33. This can be used for cases in Sweden where topography doesn't need to be considered. Peak velocity pressure is formulated as:

$$q_p(z) = c_e(z) \cdot q_b = c_e(z) \cdot \frac{1}{2} \cdot \rho \cdot v_b^2 \tag{3.9}$$

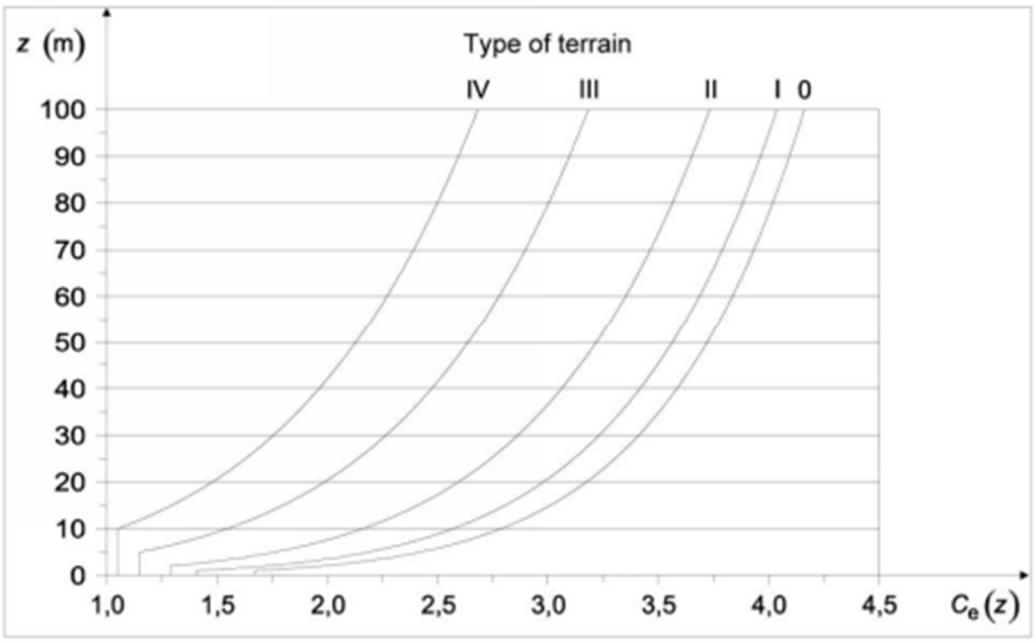

Figure 33: Exposure factor, dependent on the height and terrain category.

If contributions from topography decreases the peak velocity, following expression may be used:

$$q_p(z) = [1 + 6 \cdot I_v(z)] \cdot \left[k_r \cdot \ln\left(\frac{z}{z_0}\right) \cdot c_0(z)\right] \cdot q_b \tag{3.10}$$

$$I_v(z) = \frac{k_l}{c_0(z) \cdot \ln\left(\frac{z}{z_0}\right)} \quad (3.11)$$

where:

$I_v(z)$ is the turbulence intensity at height z

k_l is the turbulence factor

k_r is the terrain factor

z_0 is the roughness length

$c_0(z)$ is a topography factor

3.2.2 Wind-induced accelerations

The following method according to paragraph 6.3.2(1) is used to calculate sways in the first mode of a cantilevered structure with constant mass along the main axis. The maximum/peak accelerations are defined as:

$$\ddot{X}_{max}(z) = k_p \sigma_{\ddot{x}}(z) \quad (3.12)$$

$\sigma_{\ddot{X}}(z)$ is the standard deviation of the acceleration, expressed as:

$$\sigma_{\ddot{X}}(z) = \frac{3 I_v(h) R q_m(h) b c_f \phi_{1,x}(z)}{m_e} \quad (3.13)$$

where:

$\phi_{1,x}(z) = \left(\frac{z}{h}\right)^{1.5}$

$q_m(h)$ is the velocity pressure at height h

Wind speed with a return period of five years is calculated to be compared to comfort requirements in ISO 6897, which considers the human response to horizontal motion for structures in the frequency range 0,063 to 1 Hz.

$$v_{Ta} = 0{,}75 v_{50} \sqrt{1 - 0{,}2 ln\left(-ln\left(1 - \frac{1}{T_a}\right)\right)} \quad (3.14)$$

where

T_a is the time of a number of years

$v_{Ta} = 0{,}855 v_{50} = 0{,}855 v_b$ is the characteristic wind speed over a 5-year period where v_{50} is the characteristic value of the reference wind speed with a return period of 50-years.

General recommendation to define k_p, B and R is accordingly:

$k_p = \max\left(\sqrt{2\ln(vT)} + \frac{0{,}6}{\sqrt{2\ln(vT)}}, 3\right)$ is the peak factor (3.15)

$v = n_{1,x}\frac{R}{\sqrt{B^2+R^2}}$ is the up-crossing frequency (3.16)

$B^2 = exp\left[-0{,}05\left(\frac{h}{h_{ref}}\right) + \left(1-\frac{b}{h}\right)\left(0{,}04 + 0{,}01\left(\frac{h}{h_{ref}}\right)\right)\right]$ (3.17)
is the background response factor

$R^2 = \frac{2\pi F \phi_b \phi_h}{\delta_s+\delta_a}$ is the resonance response factor (3.18)

$F = \frac{4y_C}{(1+70{,}8{y_C}^2)^{5/6}}$ is the non-dimensional frequency (3.19)

$y_C = \frac{150 n_{1,x}}{v_m(h)}$ is the non-dimensional wind energy spectrum (3.20)

$\phi_b = \frac{1}{1+\frac{3{,}2 n_{1,x} b}{v_m(h)}}$ is the size factors with respect to width (3.21)

$\phi_h = \frac{1}{1+\frac{2 n_{1,x} h}{v_m(h)}}$ is the size factor with respect to height (3.22)

3.3 ISO 10137

The international standard has the status of a Swedish standard and intends to give recommendations of how to evaluate vibrations, considering human occupancy, for buildings in serviceability state. For the purposes of the standard, it's assumed that the structure responds linearly to the applied loads.

The criteria for human occupancy are governing the performance in service state. Dynamic wind actions with a one-year return period is considered in terms of peak accelerations to achieve acceptable daily living conditions. Accelerations for a wind with a return period of one-year is defined as 72% of the acceleration magnitude for a wind of five-year return period (ISO 6897, 1984).

The evaluation of habitability can be found via Figure 34 where curve one applies for office buildings and curve two for residential buildings. The evaluation curve for residential use defined as 67% of the curve used for office buildings. In addition, the resultant curve for residence is close to 90% of the perception probability.

$$\ddot{X}_{max}(z) = 0.72 k_p \sigma_{\ddot{X}}(z) \tag{3.23}$$

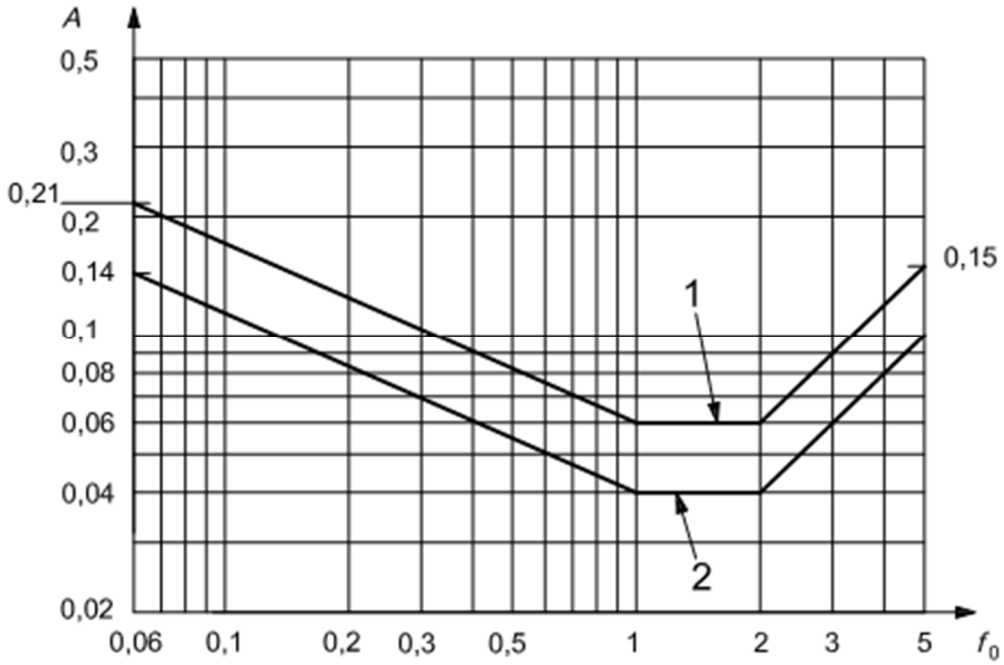

Figure 34: Evaluation curves for wind-induced vibrations.

where:

A is the peak acceleration, m/s^2

f_0 is the first eigenfrequency, Hz

**Hence the general notation of peak acceleration is $\ddot{X}_{max}$ in accordance with EKS 10.*

3.4 ISO 6897

This international standard serves as a guideline to evaluate the response of occupants due to horizontal motion of the structure in a low frequency range from 0,063 to 1 Hz. It applies for offshore structures and high-rise buildings. The horizontal motion is expressed as root mean square (r.m.s) accelerations during the worst 10 minutes of a wind storm with a return period of 5 years. Suggested thresholds of r.m.s accelerations are shown in Figure 35 where curve 1 applies for buildings used for general purposes and curve 2 is for off-shore fixed structures.

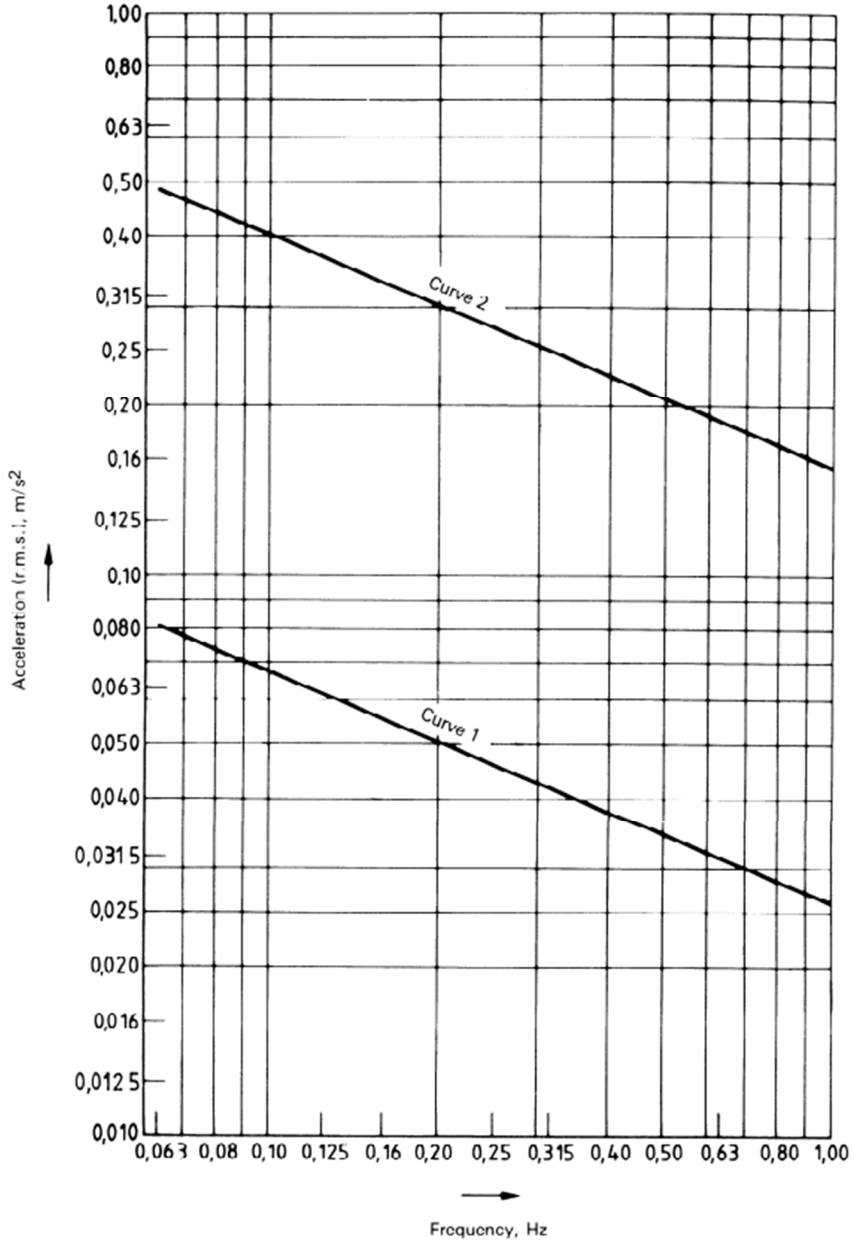

Figure 35: Suggested satisfactory magnitudes of horizontal motion of buildings.

4 Numerical modelling

The FE-software, *FEM-Design 17 3D Structure* is used to numerically solve differential equations. The differential equations in total describes the structural behaviour of the building. This chapter intends to present the numerical modelling and to validate its output.

4.1 Finite element model

The residential building has a footprint of 22x22 metres with one elevator and one staircase shaft located in the centre of the building, forming a central core. The principal plan of the reference consists of six apartments with load-carrying inner walls between compartments, see Figure 36. The foundation is a cast in-situ concrete slab to provide a stiff foundation and limit exposure of the timber to water.

The parametric study is carried out for multiple concepts with the purpose of evaluating what effects different structural elements have. Stabilizing members are gradually added and analysed, starting from just the core up to the principal plan in Figure 36. A 3D representation with door openings is shown in Figure 37. Trusses in the façade are used instead of exterior shear walls in the parametric study.

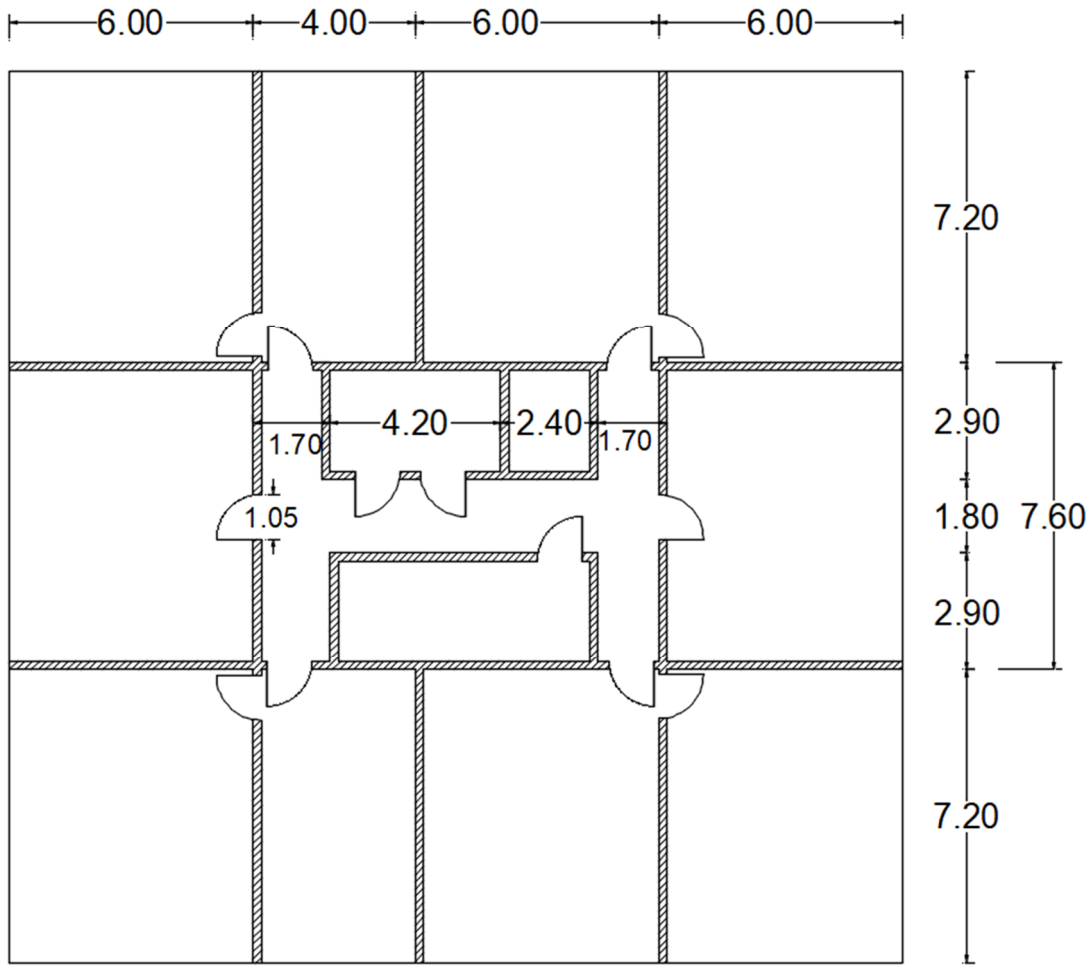

Figure 36: Plan view of the building

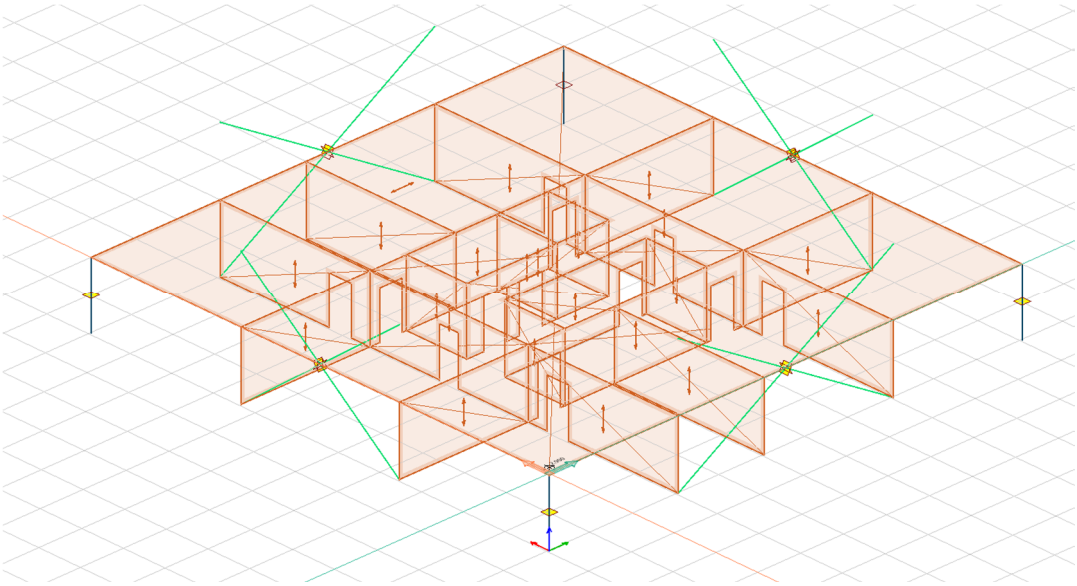

Figure 37: FE-base model with door openings on respective storey.

4.1.1 Material

The structural system in FEM-Design is modelled based on materials on the market. CLT panels of 5 layers are used to form internal walls of 200mm thick and floors of 230mm. Glulam of quality GL32h is assigned to columns, beams and trusses. Corresponding material properties can be seen in Table 3 and Table 4.

Table 3: Material properties of CLT panels

CLT	$E_{m,k}$ [N/mm^2]	$E_{t,k}$ [N/mm^2]	$E_{c,k}$ [N/mm^2]	$G_{v,k}$ [N/mm^2]	$G_{r,k}$ [N/mm^2]	ρ [kg/m^3]
0˚	5861	4440	4440	590	590	400
90˚	978	1880	1880	-	-	-

Table 4: Material properties of GL32h

Gl32h	$E_{0,mean}$ [N/mm^2]	$E_{90,mean}$ [N/mm^2]	$E_{0,05}$ [N/mm^2]	G_{mean} [N/mm^2]	$G_{0,05}$ [N/mm^2]	ρ_{mean} [kg/m^3]
-	14200	300	11800	650	540	490

4.1.2 Boundary conditions

Columns and walls are assigned simply supported boundaries, using a predefined type as in Figure 38. These boundaries are able to transfer vertical and lateral forces but can't transfer moment. Wall boundaries are modelled as 'line supports' in FEM-Design, seen in Figure 39, meanwhile columns are assigned 'point supports'. The structural elements are prefabricated to fully extent, whereas a simply supported boundary condition also applies for wall-slab, slab-slab connections. Vertically continuous walls are by default treated as a one unit, making the building to act as a cantilever beam.

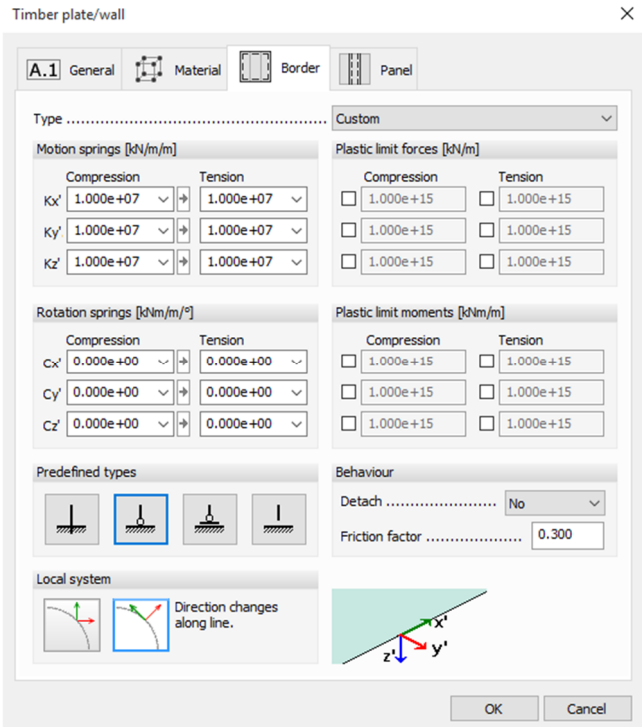

Figure 38: Boundary condition for plate/wall elements.

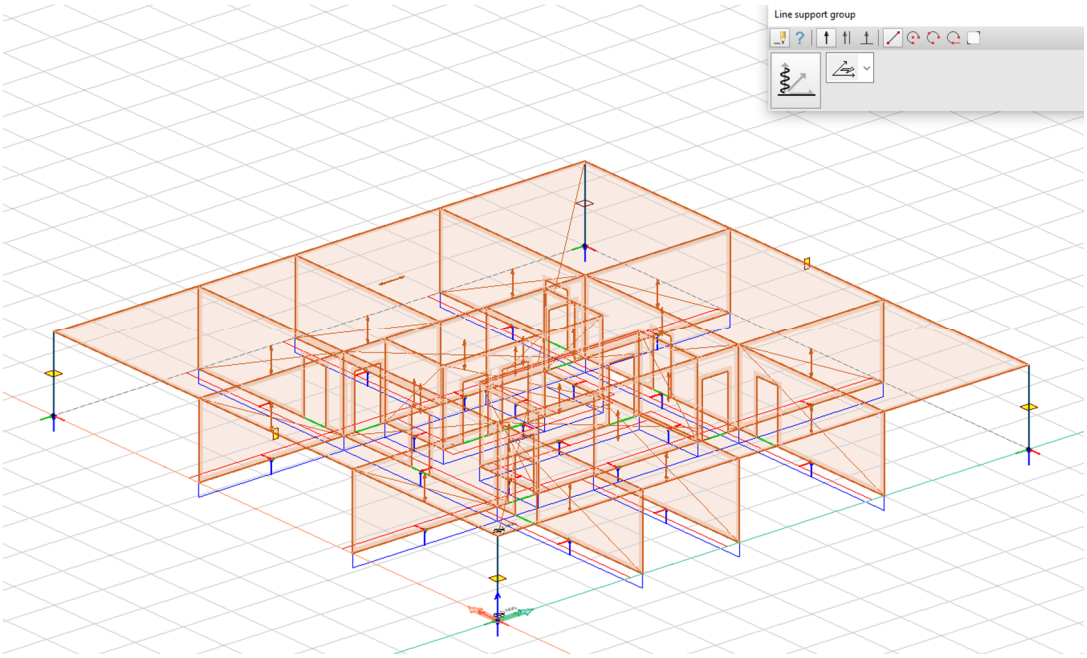

Figure 39: Wall-slab boundary condition from FEM-design.

4.1.3 Loads

The structural loading origins from dead, imposed and wind loads. An imposed load of 2 kN/m^2 is assigned to every floor as stated in *EKS 10* for a residential building. A line load of 3,3 kN/m^2 is applied on the walls of the core to represent the dead loading from the façade cladding with a weight of 50 kg/m^2. The purpose is to consider the dead load so that it's transferred via the walls directly and subsequently not give rise to increased internal forces in the floors.

The wind loads are generated after the reference wind speed and terrain category are defined. A wind speed of 25 m/s is used assuming that the building is located in Gothenburg. Terrain category 3, assuming an urban area. The load is applied as a line load distributed over the floors as in Figure 40. The value of the distributed force can be seen in Table 5. The increasing values from storeys 8 and up are calculated using by the velocity profile which's represented in Figure 29.

Table 5: Wind loads from FEM-Design

Wind loads from FEM-Design

Storey	Level [m]	X+ [kN/m]	Y+ [kN/m]	X- [kN/m]	Y- [kN/m]
Storey 1	2,9	3,09	3,09	3,09	3,09
Storey 2	5,8	3,09	3,09	3,09	3,09
Storey 3	8,7	3,09	3,09	3,09	3,09
Storey 4	11,6	3,09	3,09	3,09	3,09
Storey 5	14,5	3,09	3,09	3,09	3,09
Storey 6	17,4	3,09	3,09	3,09	3,09
Storey 7	20,3	3,09	3,09	3,09	3,09
Storey 8	23,2	3,57	3,57	3,57	3,57
Storey 9	26,1	3,57	3,57	3,57	3,57
Storey 10	29	3,57	3,57	3,57	3,57
Storey 11	31,9	3,57	3,57	3,57	3,57
Storey 12	34,8	1,79	1,79	1,79	1,79

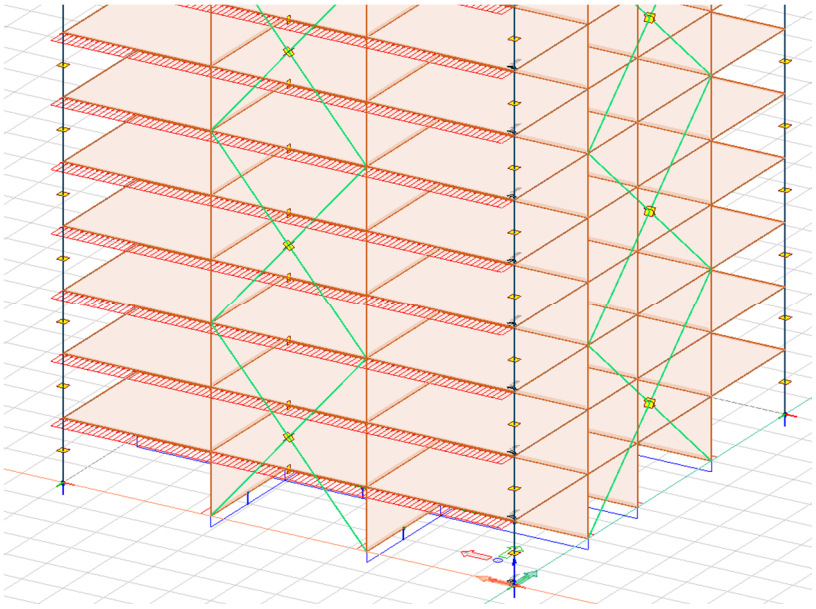

Figure 40: Wind load in x direction expressed as a line load on floor levels.

The software needs to be told what value each load case has as mass conversion factor to actually see it as mass and to be able to analyse the dynamic response of the building. Mass is favourable for this dynamic response so unfavourable values are considered to account for worst case scenario.

Table 6: Dynamic load defined by mass conversion in FEM Design.

Mass conversion	
Factor	Name
1	Self-weight
0,3	Imposed
-	Wind load X+
-	Wind load Y+

4.1.4 Mesh

The numerical finite element model approximates the structural response by dividing the structure into small 'finite' elements. A general rule of thumb when considering mesh size, the finer, the more accurate. Finer mesh means more elements and more equations to be solved. Consequently, the software requires longer computational time. The target mesh size should be chosen fine enough to represent accurate results with an efficient computational time. A convergence study is a well-used method to localize an efficient mesh size. Results from the study can be seen in Figure 41 and Figure 42.

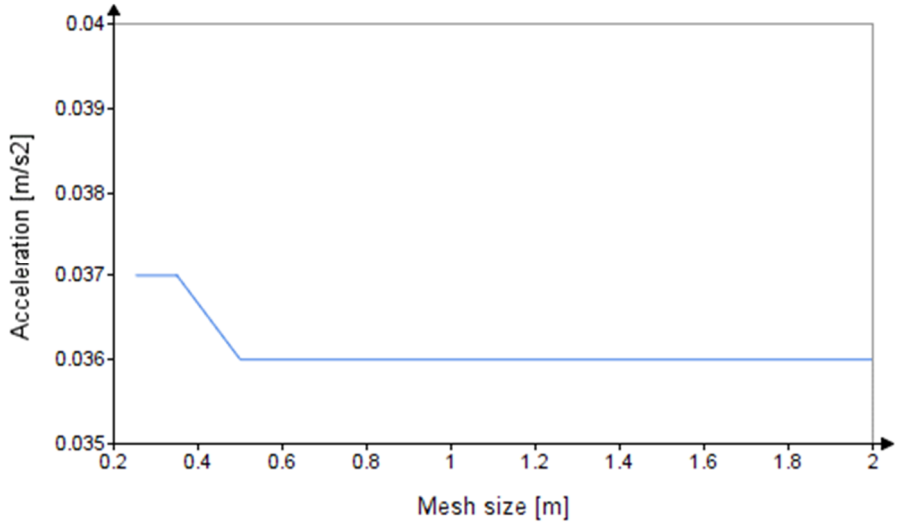

Figure 41: Acceleration depending on mesh size.

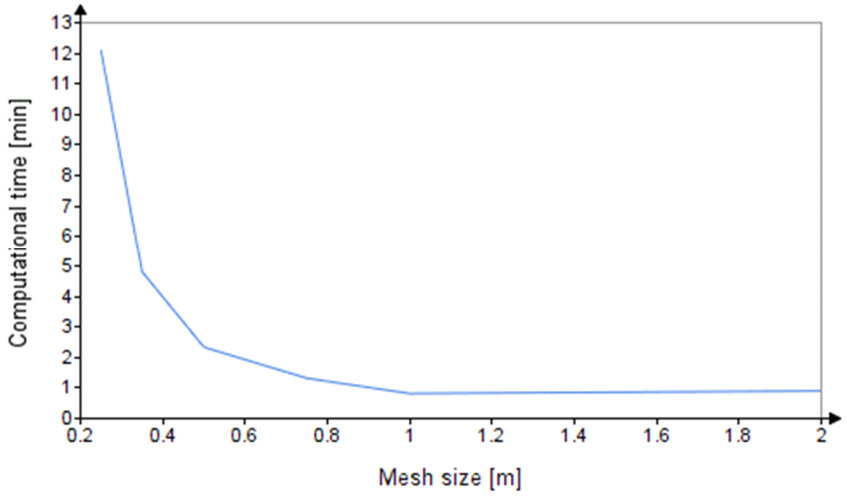

Figure 42: Computational time depending on mesh size

The linear dynamic calculation of eigenfrequencies is based on the mass and stiffness of the subregions. These parameters are not very sensitive by selected mesh size. The convergence study is relating eigenfrequencies to accelerations, depending on mesh size, as can be seen in Figure 41. The curve indicates almost no differences in acceleration, making the selected mesh size dependent on computational time. Elements of 1x1 m is therefore used in the parametric study.

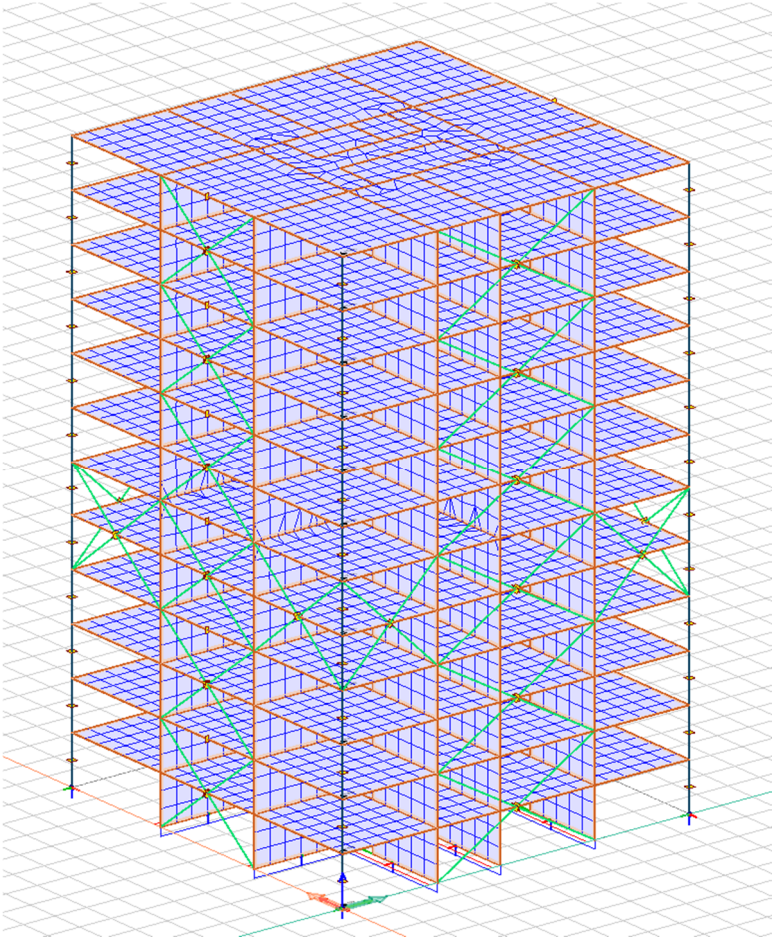

Figure 43: Meshed structural model of 12-storeys.

4.2 Verification of the FE-model

A verification is carried out to understand how the numerical model describes parameters such as load distribution, masses, reactions and overall deformation behaviour. Numerical output is compared to hand calculations, where a simplified FE-model is used to validate the loads and parts of the structural behaviour. Solid walls are implemented as the influence of openings makes it complex to estimate the actual stiffness. The analytical results are expressed in detail in Appendix B.

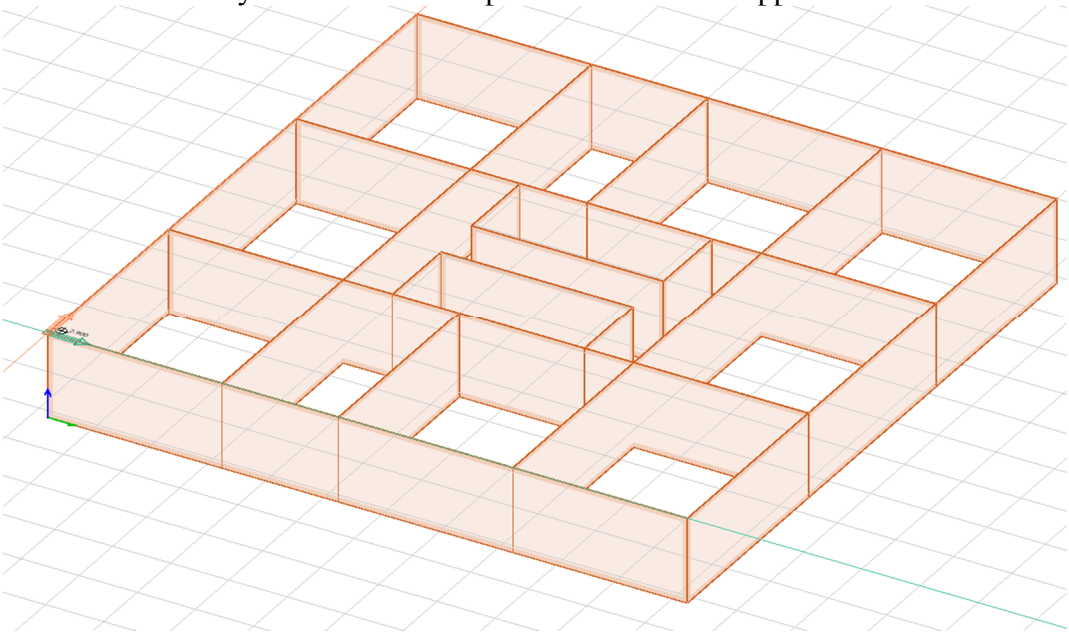

Figure 44: FE-model used for verification

4.2.1 Wind load

Wind load is calculated according to SS-EN-1991-1-4. The loading in both models is expressed as a line load, distributed over the floors. The magnitude of the wind load follows the velocity profile and depends on building height, visualized in Figure 29. The analytical and numerical results are close to identical, as both models describe the same wind.

4.2.2 Moment at the supports

The originated moment from wind loads on respective storey is defined by the total force on each level multiplied by the current height i.e. lever arm and summed up. The total moment is then compared to the sum of moment reaction at the supports for respective wall in x-direction, taken from FEM-Design. The numerical moment is taken from x-direction, see Figure 45. The difference is 4% larger in FEM Design and is originated by the small differences of the wind load at top storeys.

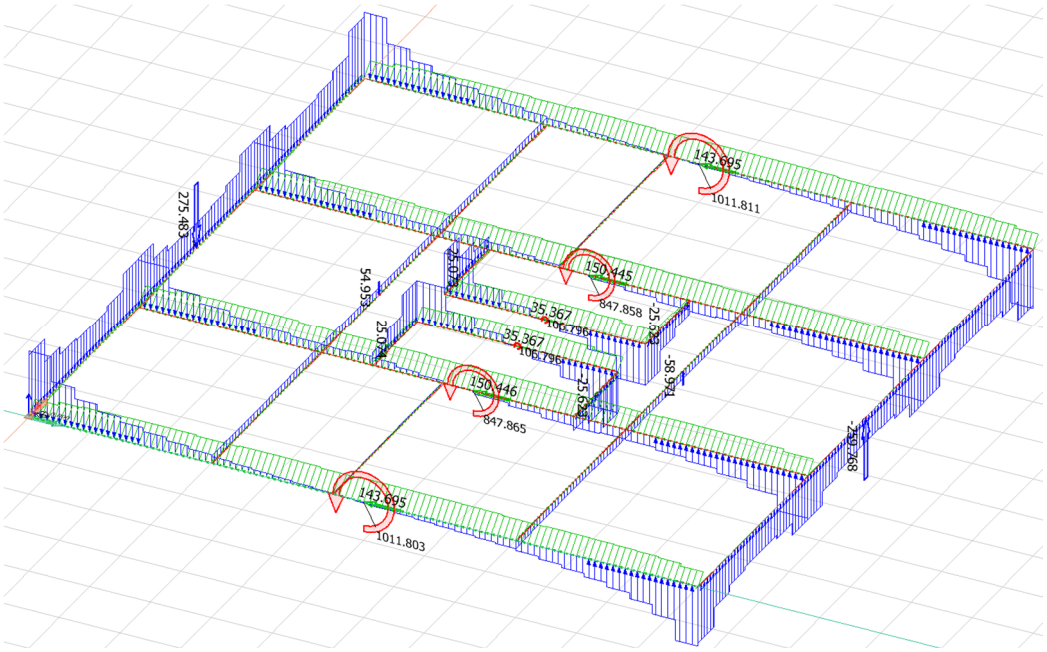

Figure 45: Numerical moments at the supports in respective wall in x-direction.

4.2.3 Mass distribution

The mass distribution of the structure is defined from dead loading i.e. floor and walls together with imposed loading. The FE-model is able to describe mass per storey and total mass of the structure when a dynamic analysis is carried out. Hand calculations is based on the mass conversion, accounting for 30% of imposed load and full effect of the dead load as a mass.

$$G_{storey} = \frac{G_k + \psi_2 Q_k}{g} \tag{4.1}$$

where

G_k is the dead weight from the floor and inner walls in CLT

ψ_2 is the load factor according to EKS 10

Q_k is the total imposed load on the floor

g is the constant of gravity

The analytical mass distribution per storey is kept constant, meanwhile the numerical mass distribution slightly varies. In addition, it should be noted that the numerical model describes the mass at the roof and base with half the height of walls. Summing up the total mass, difference between the two models is 0.2%.

4.2.4 Horizontal force distribution on walls

The structural response due to wind loading is investigated, looking at internal forces of shear walls. An analytical approach for computing lateral reactions in braced members is established and presented according to (Engström, 2017).

When the horizontal loading is submitted on the building, the braced system will deform and create internal forces to resist the loading. Influencing factors on the total deformation are the modulus of elasticity and geometry of the walls i.e. length and thickness in addition to height. The stiffness of the braced member can be defined as the load required to displace the member by one unit.

Two types of stiffness are distinguished, shear stiffness and bending stiffness.
The contribution of each type depends on the material, the height of the element and how the horizontal loading is distributed on the element. The last aspect can be seen in Figure 46, whereas k_s and k_b applies for a unique load- case.

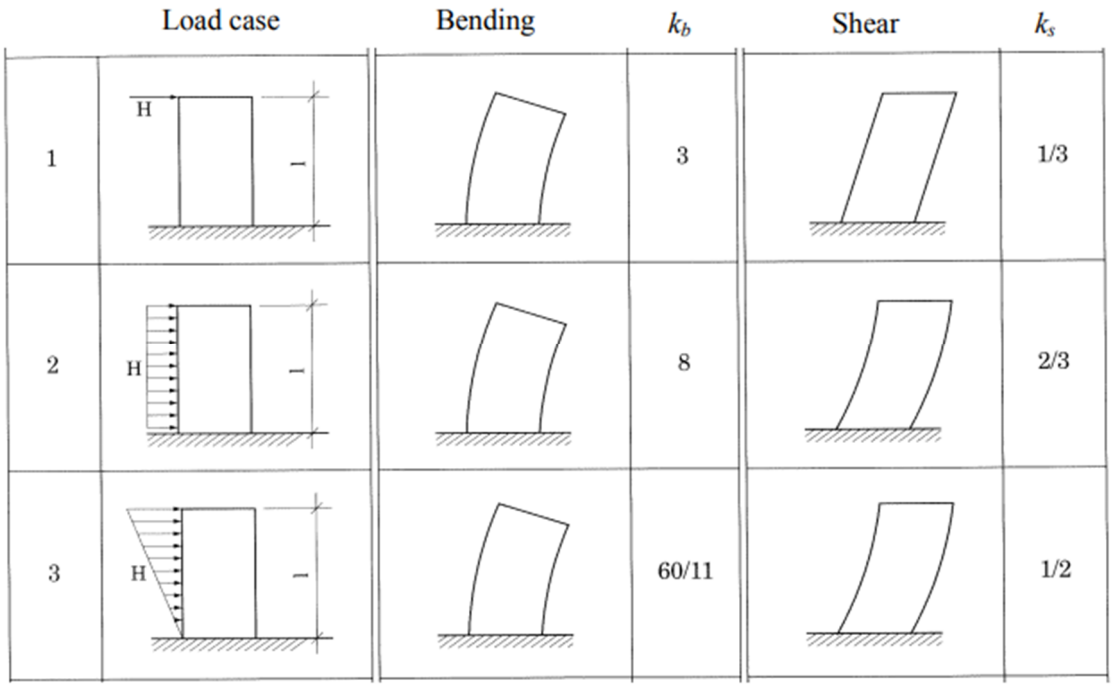

Figure 46: Shape and Contribution of bending stiffness and shear stiffness, depending on load case (Engström, 2017).

The stiffness of the bracing member is defined as:

$$\frac{1}{S} = \frac{1}{S_{si}} + \frac{1}{S_{bi}} \tag{4.2}$$

where S_{si} is the shear stiffness and S_{bi} is the bending stiffness

$$S_{si} = k_s \frac{E_i * A_i}{l_i} \tag{4.3}$$

$$S_{bi} = k_b \frac{E_i * I_i}{{l_i}^3} \tag{4.4}$$

where:

S_{si} is the shear stiffness

S_{bi} is the bending stiffness

A_i is the area of the individual wall

l_i is the height of the individual wall

k_s, k_b are the shear, bending coefficients

The stiffness of timber plates is in most cases governed by shear stiffness and can be approximated, saying that all walls work in shear only i.e. neglected bending stiffness. Shear stiffness is expressed as being directly proportional with the sectional area. If all walls have same thickness, as for this case, the stiffness is directly proportional with the length of the bracing member.

The correctness of this assumption can be validated by plotting the deformed shape and compare the curve to a shape induced by shear/bending. As for this case, the deformed shape in Figure 47 indicate that the shear stiffness governing.

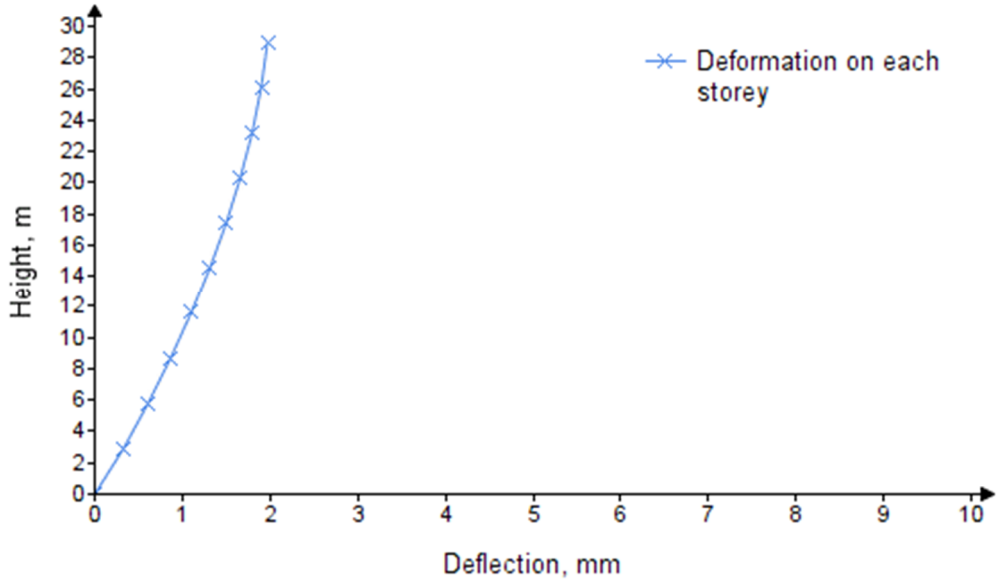

Figure 47: Deformed shape of the building

Furthermore, other factors that influence the horizontal force distribution on the walls is the stiffness of floor diaphragms. If the diaphragm is rigid, there is no deformations of the slab and all walls will deform equally. This results in a force distribution which is dependent on the wall stiffness as in Figure 48.

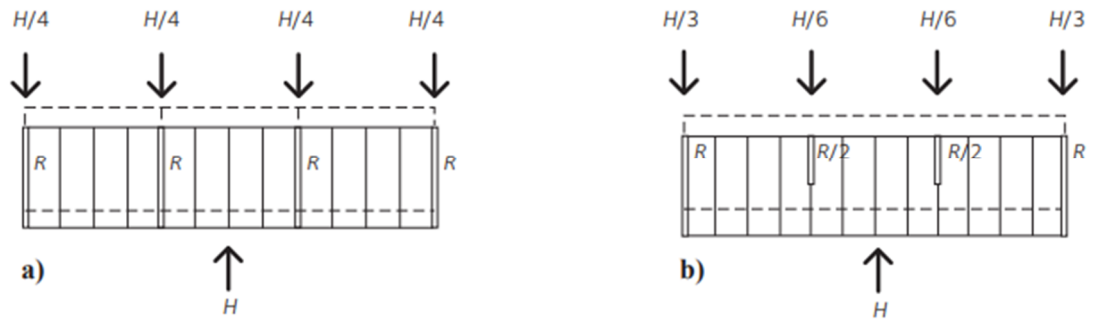

Figure 48 : Horizontal load distribution for a rigid diaphragm. a) walls with equal rigidity; b) walls with different rigidity (Swedish Wood, 2015).

If the diaphragm is flexible, each wall will resist forces according to their tributary area regardless the stiffness of different walls as for case a) in Figure 49. Another alternative is if the diaphragm is semi-rigid as for case b). Semi-rigid diaphragms are highly indeterminant and the force distribution is difficult to estimate (Swedish Wood, 2015).

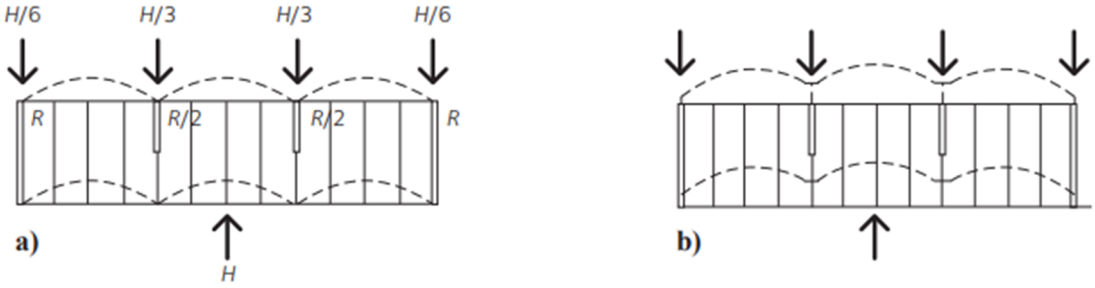

Figure 49: Distribution of horizontal forces for a) flexible roof diaphragm; b) semi-rigid roof diaphragm (Swedish Wood, 2015).

The analytical horizontal force distribution is based upon a rigid diaphragm as for case b) in Figure 48. Moreover, the total horizontal force in each individual wall is dependent on the wall configuration in the plan. If the lateral force resultant acts beyond the rotational center, an eccentricity is existing which give rise to a torsional moment. The moment needs to be treated together with the translational force.

The combined effect of translation and torsion is controlled via superposition of load cases shown in Figure 50. The rotational center of the structural system is defined as:

$$x_t = \frac{\sum(a_i.S_{yi})}{\sum S_{yi}} \quad (4.5)$$

$$y_t = \frac{\sum(b_i.S_{xi})}{\sum S_{xi}} \quad (4.6)$$

where S_{xi} and S_{yi} are the stiffness of bracing members in x and y direction respectively.

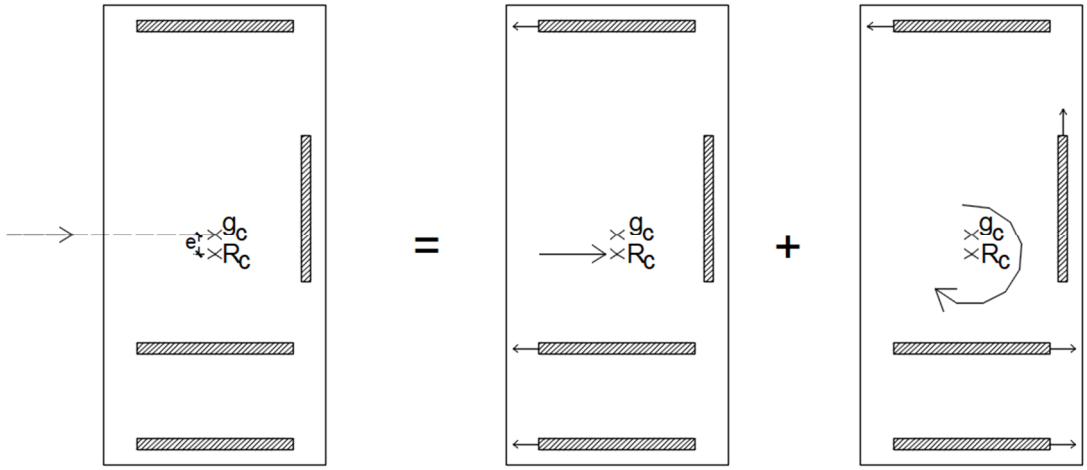

Figure 50: Superposition of load cases in a statically indeterminate system

The contribution of each element corresponding to pure transversal load

$$H_{i,x} = H_{tot,x} \cdot \frac{S_{xi}}{\sum S_{xi}} \qquad \text{for walls in x-direction} \qquad (4.7)$$

$$H_{i,y} = H_{tot,y} \cdot \frac{S_{yi}}{\sum S_{yi}} \qquad \text{for walls in y-direction} \qquad (4.8)$$

and the contribution corresponding to pure rotation

$$H_{i,Cx} = T \cdot \frac{S_{xi} \cdot y_i}{S_T} \qquad \text{for walls in x-direction} \qquad (4.9)$$

$$H_{i,Cy} = T \cdot \frac{S_{yi} \cdot x_i}{S_T} \qquad \text{for walls in y-direction} \qquad (4.10)$$

where S_T is the global torsional stiffness, defined as:

$$S_T = \sum(S_{xi} \cdot {y_i}^2) + \sum(S_{yi} \cdot {x_i}^2) \qquad (4.11)$$

The total horizontal load i.e. the sum of translational and rotational component is calculated for respective shear wall. Identification of each wall is numbered according to Figure 51 in which the comparison is based upon.

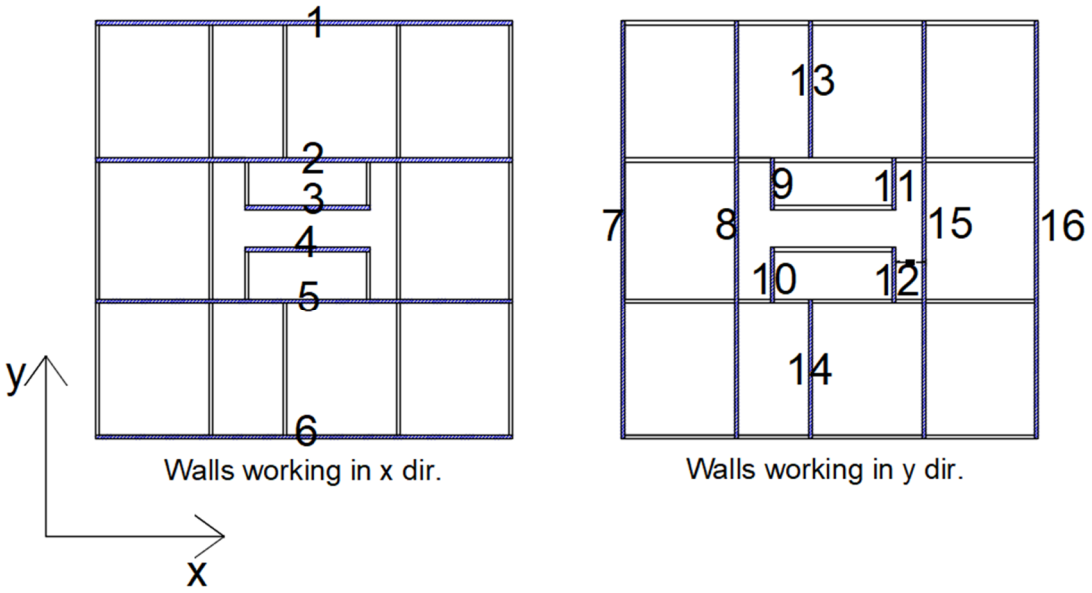

Figure 51: Wall ID in x and y-direction.

Comparison between hand calculation and the FE-analysis is given in Table 7.

Table 7: Comparison between horizontal force distribution.

Horizontal force distribution

Wall ID	H_{xi} [kN]	$H_{xi.FEM}$ [kN]	diff
1	140	145	0,04
2	140	152	0,09
3	42	34	0,19
4	42	34	0,19
5	140	152	0,09
6	140	145	0,04
7	126	124	0,02
8	126	124	0,01
9	17	12	0,25
10	17	13	0,21
11	16	12	0,24
12	16	13	0,19
13	41	36	0,12
14	41	45	0,10
15	125	132	0,06
16	124	127	0,03

The differences between the two methods can be explained by the rigidity of the floor-diaphragm and the neglected bending stiffness in the analytical approach. Moreover, the analytical results are based upon a rigid diaphragm which appears to not reflect the numerical model where the force distribution is more complex.

4.2.5 Deflection check

A simplified version of the numerical model is used to describe shear deformations, as in Figure 20, and bending deformations in service state. Hence, the exterior walls are modelled while inner walls are not. Numerical deformations are compared to a Timoshenko beam for two load cases, the first with a concentrated force and the second with a uniformly distributed load as in Figure 52. The Timoshenko model for respective load case is expressed according to (Avén, 1983).

The difference in deflections using this model is 2.4% for the concentrated load-case and 0.8% for the uniformly distributed.

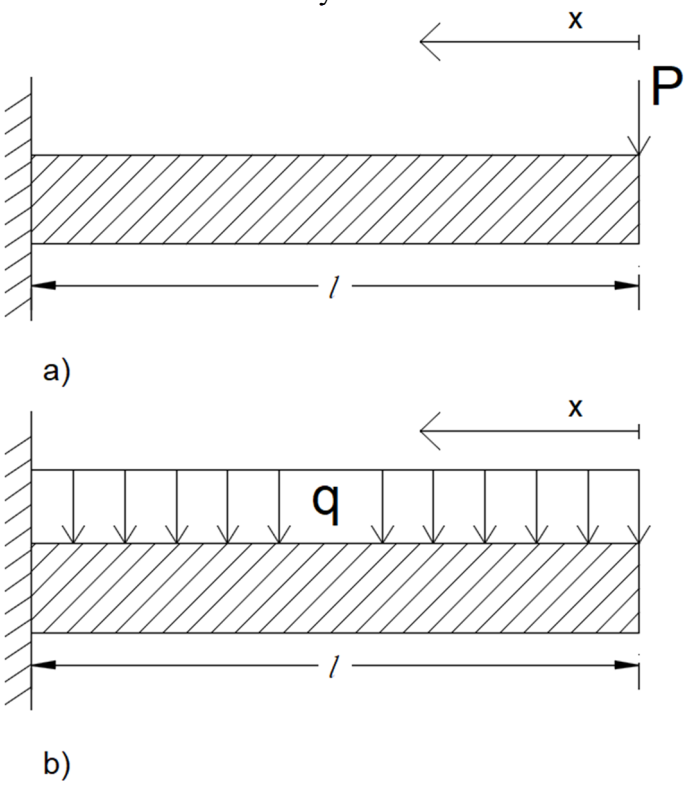

Figure 52: a cantilever Timoshenko beam under a) concentrated load at the free end; b) uniformly distributed load.

The deflection, $u(x)$ for respective load case is defined as:

$$u(x) = \frac{P(l-x)}{\kappa AG} + \frac{Px}{2EI}\left(l^2 - \frac{x^2}{3}\right) + \frac{PL^3}{3EI} \quad (4.12)$$

$$u(x) = \frac{ql^2}{2EA} + \frac{ql^2\beta_w}{2GA} \quad (4.13)$$

where:

x is the distance between the considered point and the free end

κ is the Timoshenko shear coefficient for load case a

β_w is the Timoshenko shear coefficient for load case b

5 Results

The impact of modifying mass and stiffness are evaluated and set in relation to *ISO 10137* and *ISO 6897* to find beneficial and efficient parametric actions. Subsequently, this is applied to the structural analysis where optimization of the building is made to reach highest possible number of storeys.

5.1 Parametric effects

The analysed parameters are mass and stiffness. The effect of modifying one or the other will most likely correlate and creating a combined effect on the acceleration.
The effect of just changing mass or stiffness can theoretically be obtained by changing the material density, modulus of elasticity respectively. Hence the impact is described by the acceleration-frequency relation. Figure 53 shows the impact of a doubled mass, stiffness for a 1-year return wind as the frequency exceeds 1 Hz. Furthermore the effect is shown in a low frequency range where Figure 54 describes the influence on a 1-year wind i.e. *ISO 10137* and Figure 55 for a 5-year wind according to *ISO 6897*.

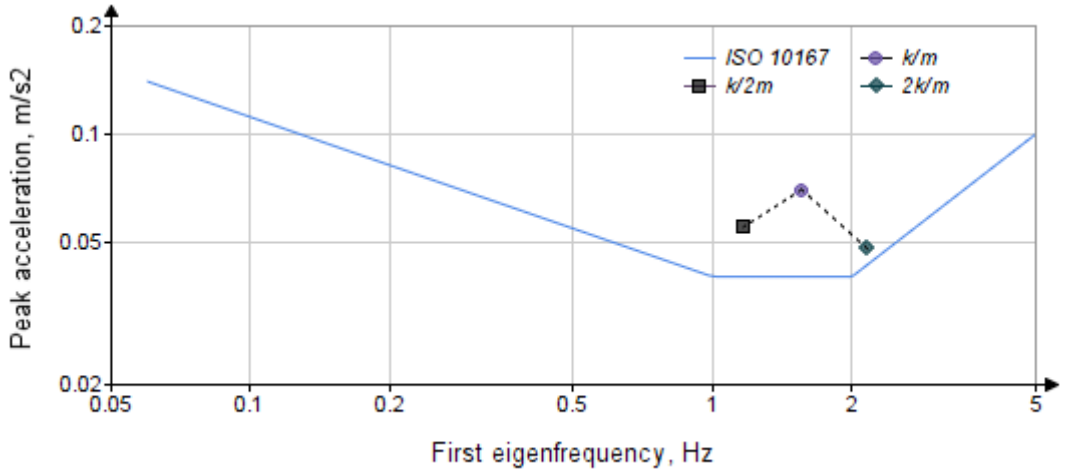

Figure 53: Parametric evaluation for residential buildings according to ISO 10137, f_0 > 1 Hz.

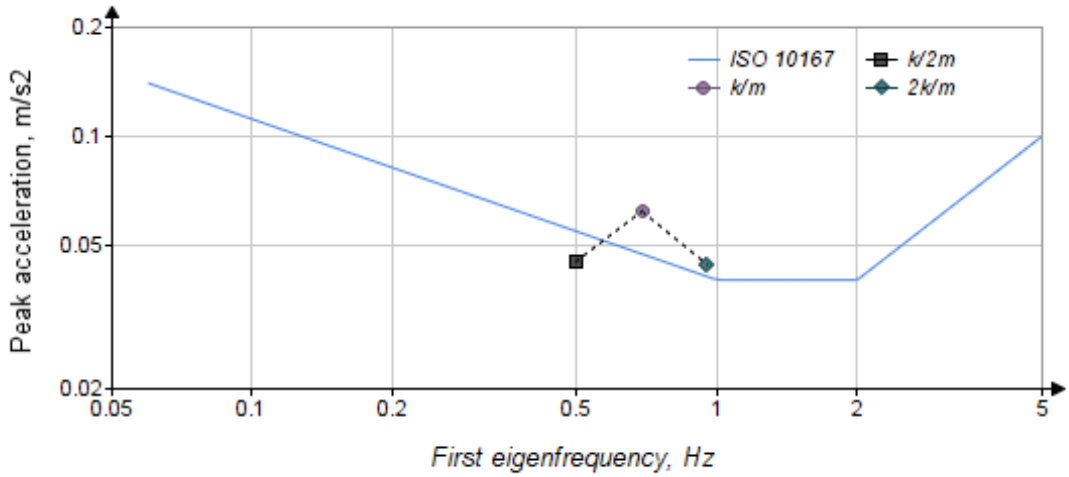

Figure 54: Parametric evaluation for residential buildings according to ISO 10137, f_0 < 1 Hz.

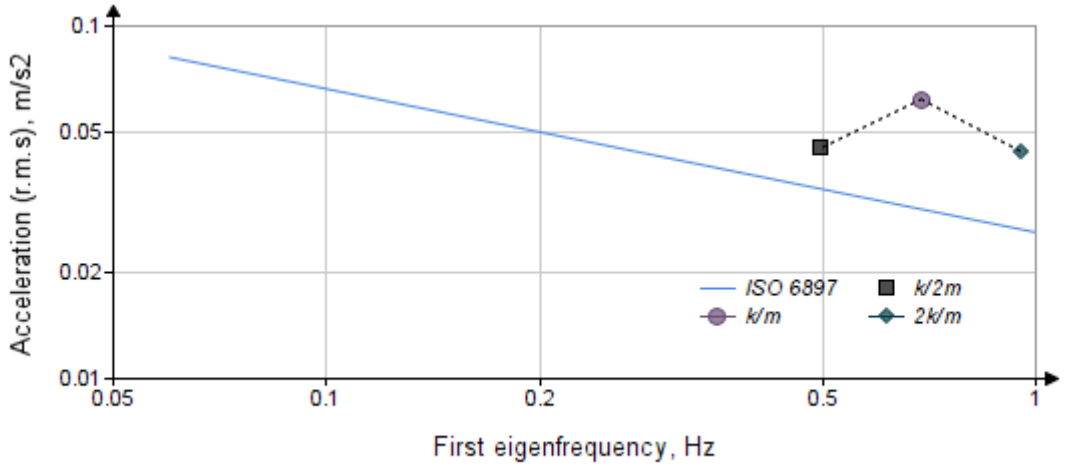

Figure 55: Parametric evaluation for general buildings according to ISO 6897, $f_0 > 1$ Hz.

The most beneficial parametric change depends what value the eigenfrequency takes. Both effects are beneficial for reducing the accelerations, but one should also consider the increased tolerance outside frequency ranges of 1 and 2 Hz. It may appear more beneficial to increase the stiffness if the fundamental eigenfrequency is over 1 Hz, while an increased mass becomes more efficient when the frequency drops under 1 Hz.

5.1.1 Evaluation of eigenfrequency in Eurocode

The fundamental eigenfrequency in Eurocode for multi-storey buildings higher than 50m is estimated by dividing 46 by the total height. It's based on compiled data of measured frequencies of buildings with varying height. The outcome is a curve created by an average of all 'frequency-samples'. The application area intends to be used as a rough look of the eigenfrequency.

A comparison between the simplified expression in Eurocode and the numerical eigenfrequency is carried out to evaluate how well the simplified expression corresponds to a complex model. Tests at different heights are carried out and plotted in Figure 56. The Eurocode expression gives an overestimation of the eigenfrequency at fewer storeys but gets closer to the numerical value as the number of storeys approaches 28-storeys.

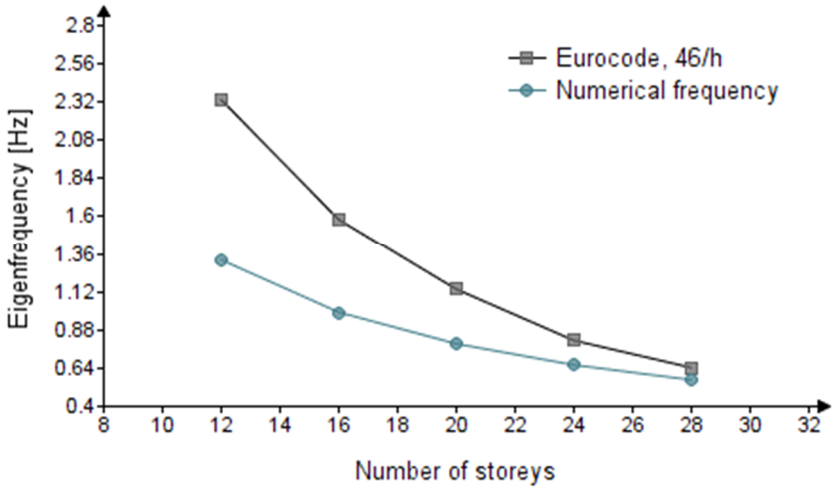

Figure 56: Graphical comparison of eigenfrequency at various number of storeys.

5.1.2 Cross-sectional study

A study of cross-sectional sizes is carried out to find an efficient and realistic size of beams, columns and diagonals. The purpose of these elements is to transfer axial forces, whereas the cross-sectional area is essential to increase the axial stiffness. The influence on the eigenfrequency can be seen in Figure 57, showing how an increased cross-section influences the eigenfrequency for diagonals and columns.

A decreasing trend on the frequency can be seen for columns and diagonals with increasing size. The sectional-shape are quadratic and is practical achieved by gluing of laminas to form wide sections. The influence of beams is not beneficial as they have a simply supported connection. An increased beam-section tends to decrease the eigenfrequency as extra mass is added. The size is therefore chosen to satisfy vertical loads in ultimate limit state.

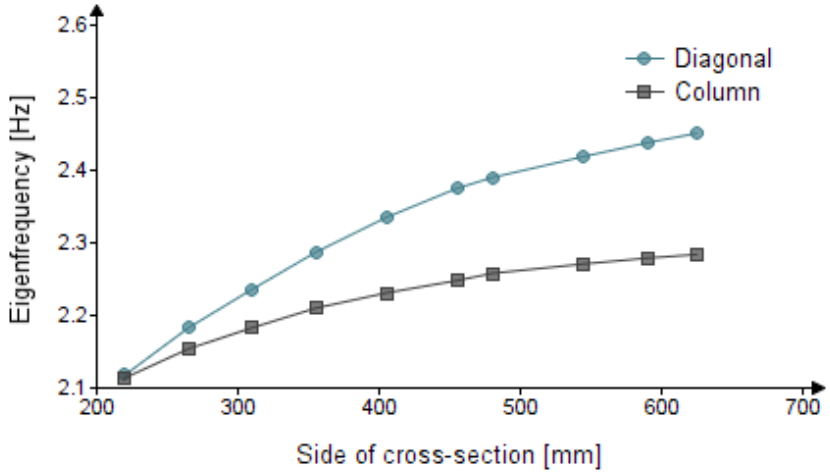

Figure 57: Influence of cross-section on the eigenfrequency of the building.

5.1.3 Comparison of bracing systems

Since the bracing of the structure provides significant stiffness, it's of interest to find the most efficient bracing system. Three options, shown in Figure 58, are evaluated by means of dynamic performance and impact on the façades.

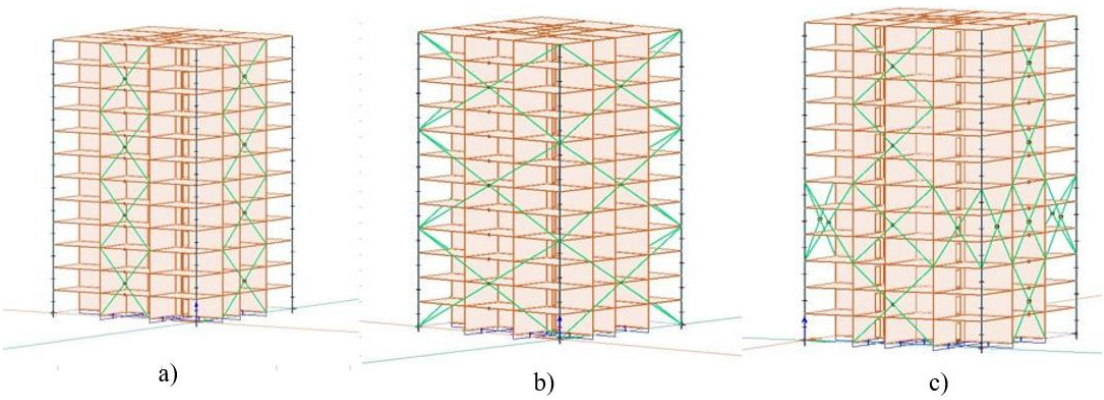

Figure 58: Investigated bracing systems. a) Centric bracing; b) Braced tube; c) Outrigger bracing.

The bracing system for case (a) is intended to be an example of material efficiency, but primarily for having low impact on windows and balcony-doors. Bracing of type (b) and (c) has proven to be very stiff and material efficient according to (Choi, Joseph, & Mathias, 2012) and qualified for the general tall building. The number of belt trusses in the outrigger system is limited to one due to its influence on the façade. Moreover, the most efficient placement of the outrigger is investigated in Table 8.

Table 8: Outrigger placement for a building of 12 storeys.

Outrigger placement

n_{storey}	f_0 [Hz]	m_e [ton/m]	$X_{max.peak}$ [m/s^2]	$X_{max}/X_{ISO\ 10137}$
1,2,3	2,377	35,55	0,042	0,876
4,5,6	2,44	35,64	0,04	0,825
7,8,9	2,305	35,92	0,043	0,928
10,11,12	2,18	36,52	0,045	1,032

The angle of the diagonals in case (a) and (c) are stretched close to 45 degrees and has proven to be structural and material efficient. Diagonals in the braced tube have an inclination of 30 degrees, which is set to limit differences in the bracing system when the number of storeys is increased. The dynamic performance for respective option is given in Table 9 and graphically presented in Figure 59.

Table 9: Dynamic performance of truss systems

Comparison of truss systems

Bracing	l_{truss} [m]	f_0 [Hz]	m_e [ton/m]	$X_{max.peak}$ [m/s^2]	$X_{max}/X_{ISO\ 10137}$
a	397	2,092	35,54	0,049	1,16
b	597	2,315	36,01	0,042	0,917
c	572	2,44	35,64	0,04	0,825

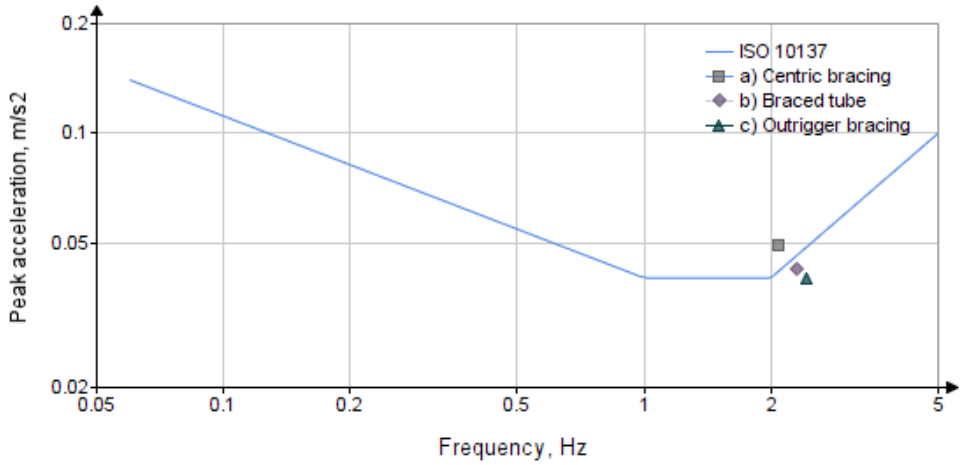

Figure 59: Evaluation according to ISO 10137

The results show that the outrigger system has the highest eigenfrequency and best dynamic performance. The outrigger provides lots of stiffness comparing with centric bracing and is more material efficient than the braced tube.

5.1.4 Modifying stiffness

The influence of stiffness on the dynamic response is studied by modifying the thickness of CLT inner-walls and cross-sections of glulam columns and trusses. A comparison between the parametric actions can be made by evaluating the peak accelerations. The influence of an increased inner-wall thickness is represented in Table 10 and graphically shown in Figure 60.

Table 10: Effect of increased wall thickness for a structure of 13-storeys.

Effect of increased wall thickness

Wall thickness	f_0 [Hz]	m_e [ton/m]	$X_{max.peak}$ [m/s^2]	X_{max} / $X_{ISO\ 10137}$
L(T)200-5S	2,179	35,77	0,047	1,071
L(T)230-5S	2,231	37,07	0,044	0,982
L(T)270-7S	2,325	38,75	0,04	0,859
L(T)300-7S	2,327	40	0,039	0,831

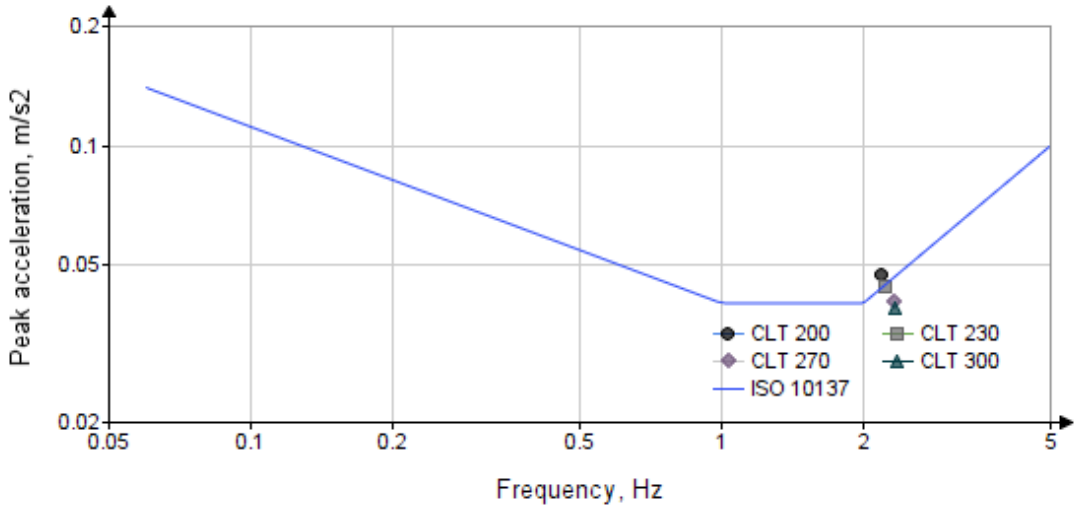

Figure 60: Graphical evaluation of increased inner wall thickness.

A trend of decreasing accelerations can be seen, as the stiffness increases with thicker walls. It should be noted that structural mass also increases up to 11% with thicker walls.

As for increasing the cross-sections, the effect is evaluated in addition to the cross-sectional study. The proportion of a section size is dependent on the chosen material and on how big the building is. Size of glulam-sections is arbitrary chosen for this specific parametric action, partly by looking at the stated glulam-sizes in Mjöstornet (Abrahamsen, 2017). Sections of 'arbitrary large' sizes are gradually assigned to columns and trusses where the dynamic response for an increased size is given in Table 11 and plotted in Figure 61.

Table 11: Effect of increasing cross sections

Effect of increased sections

Section	f_0 [Hz]	m_e [ton/m]	$X_{max.peak}$ [m/s^2]	X_{max} / $X_{ISO\ 10137}$
Trusses & Columns 405x405	2,179	35,77	0,047	1,071
Columns 620x620	2,258	36,21	0,044	0,979
Trusses & Columns 620x620	2,418	37,37	0,039	0,965
Columns 1000x1000	2,528	38,44	0,036	0,719

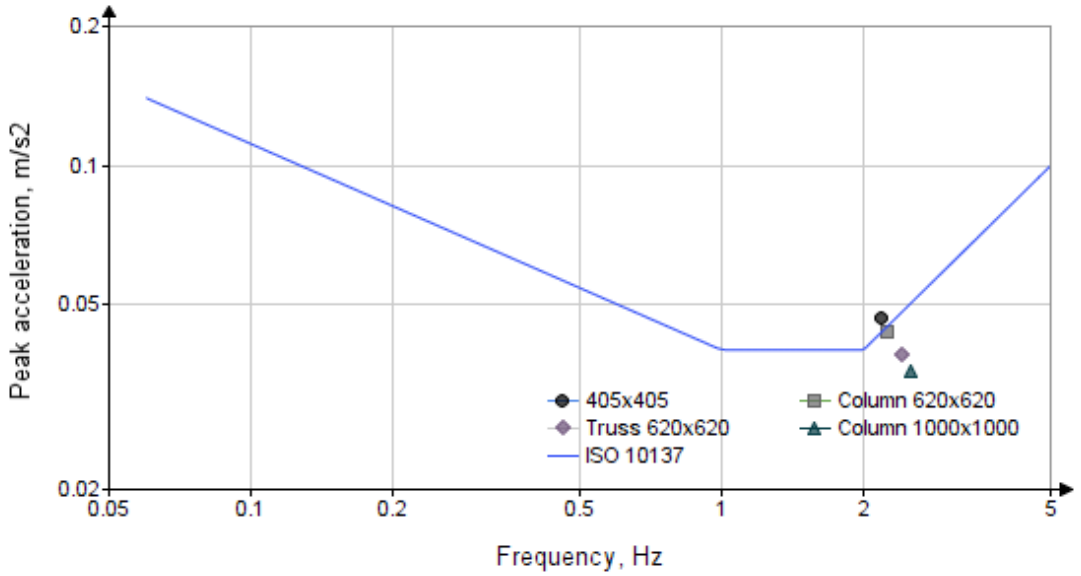

Figure 61: Graphical evaluation of increased sections.

The effect is similar to an increased wall thickness. The structural mass is slightly increased, but stiffness is found dominant and leads to a larger frequency. Comparing the results in Table 10 and Table 11, one can see that structural members in the façades has a slightly better performance. One reason to this is due to the increased stiffness by the lever arm for members in the façade.

5.1.5 *Modifying mass*

As seen from Figure 53, an increased mass decreases the eigenfrequency and acceleration. By means of computing accelerations of a building, mass is expressed in terms of equivalent mass. Equivalent mass, expressed in Equation (3.4), can be increased in two ways, either by changing the material or by concentrating the mass higher up. An advantage is taken from higher values of the mode shape, seen in Figure 62.

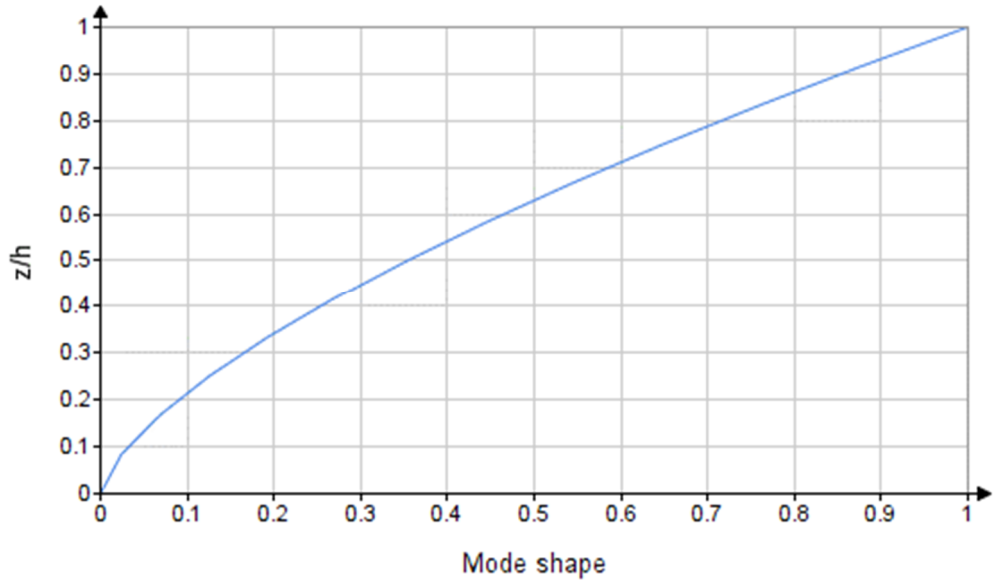

Figure 62: Mode shape depending on height.

The effect of mode shape is investigated to see where mass location is beneficial. The test is carried out on a 12-storey structure, where one floor is assigned an additional dead load of 10 kN/m^2 and placed on various levels. Results is given in Table 12 and graphically represented in Figure 63.

Table 12: Output from numerical, analytical analysis.

Effect of mass placement

n_{storey}	f_0 [Hz]	m_e [ton/m•10^2]	X_{max}/ $X_{ISO\ 10137}$
0	2,335	0,3594	0,901
1	2,33	0,363	0,897
2	2,31	0,3646	0,91
4	2,212	0,3782	0,966
5	2,156	0,393	0,985
6	2,11	0,415	0,979
9	1,881	0,5359	0,922
10	1,822	0,6016	0,855
11	1,746	0,6817	0,795
12	1,659	0,8045	0,718

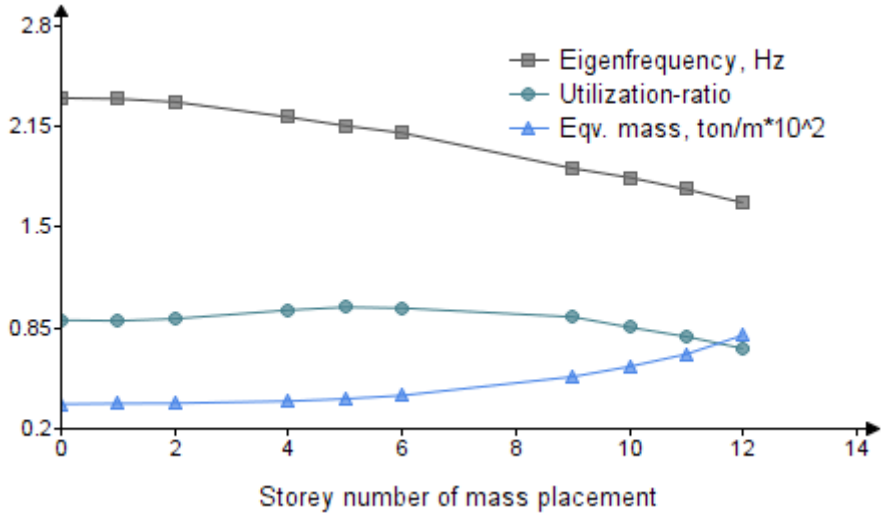

Figure 63: Effect of mass placement.

Results shows that the mass location gives a negative effect on acceleration-ratio if placed below the 10th storey which is under the top third of the building. This indicates that additional mass makes the eigenfrequency drop and the gain in equivalent mass is not sufficient. A positive effect of mass placement starts when the effect of equivalent mass prevails over a decreased frequency.

An increased mass can in practice be achieved by replacing timber floors by concrete i.e. changing material. Concrete slabs of 300 mm are used which makes the flooring 8 times heavier than the initial CLT floor. The concept of equivalent mass is used where the concrete floors are placed where they have the most impact on equivalent mass. The benefit of gradually replacing timber floors with concrete, one at the time and starting from the top, is studied in Figure 64. The effect on equivalent mass and sway accelerations decreases for more concrete floors as lower values of the mode shape is used. A converging trend on can be seen when the final (8th) concrete slab is added.

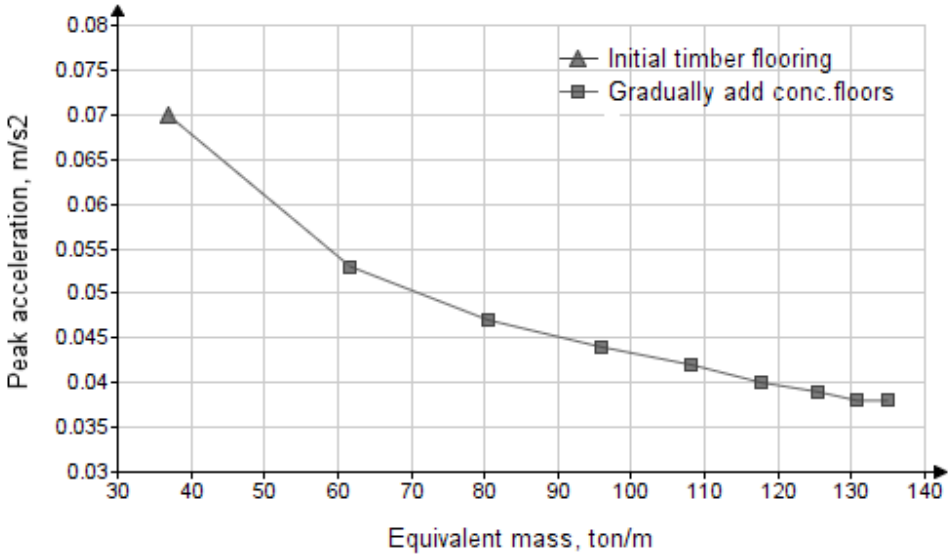

Figure 64: Effect of equivalent mass on acceleration.

5.2 Structural response

Results from structural analysis are presented with increasing number of the stabilized members. The structural performance starts with analyzing a beam-column structure with a central core in which structural elements are gradually added and leading up to the final concept.

5.2.1 Core structure

A core structure with no load-bearing elements in the façade is studied with the purpose of investigating the effect of inner stabilizing walls and to see what limits the number of storeys. On the basis of the cross-sectional study from Figure 57, beams are assigned a section of 215x315mm and columns are assigned 405x405mm section. The structural model, seen in Figure 65, will gradually be assigned inner CLT walls of 200 mm. The most effective placements of these walls are studied and documented for increasing the number of storeys as well as preserving openness to the plans.

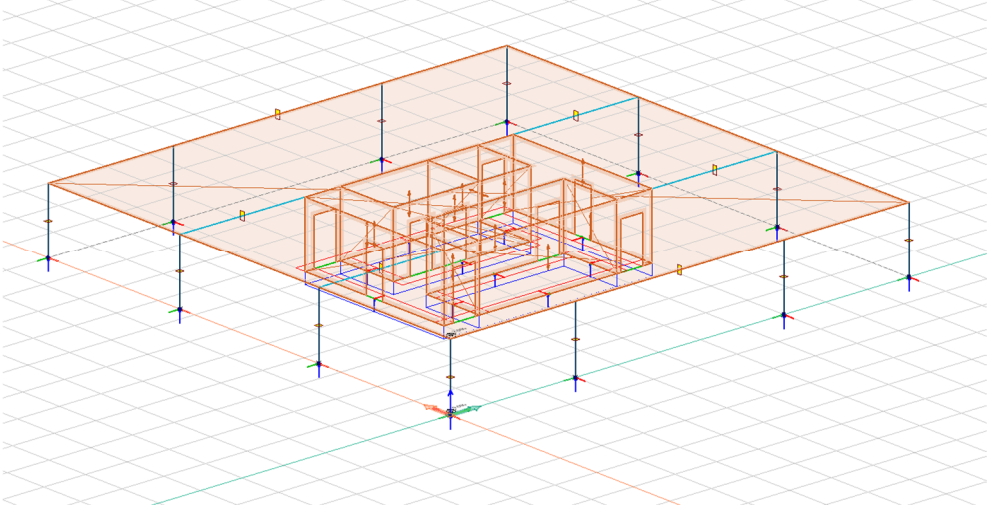

Figure 65: Principal plan of core model.

Results from analysing various number of walls is given in Table 13. The dynamic analysis shows that the fundamental mode is torsional. Torsional vibrations are outside the scope of the used wind standards and therefore treated by an assumption, saying that if $f_0 > 3\ Hz$, the accelerations are accepted without any further process. A motivation for this is that eigenfrequencies over this limit considers the energy of the winds to be low. This assumption is based on experience of Thomas Hallgren, Structural Engineer at COWI.

Table 13: Results of the structural behavior

Core structure

n_{storey}	Fig.	f_0 [Hz]	m_e [ton/m]	X_{max}/X_{ISO_10137}
4	a	3,324	-	-
5		2,63	-	-
	b	3,085	-	-
6		2,532	-	-
	c	2,815	-	-
	d	2,944	-	-
	e	2,913	-	-

The number of storeys is increased from 4 to 5 by adding inner walls and the most beneficial location, in terms of increasing the eigenfrequency, is compiled in Figure 66. The torsional mode is fundamental throughout the process of adding walls even though the building is close to symmetric, having very small eccentricities between the rotational centre and gravity centre.

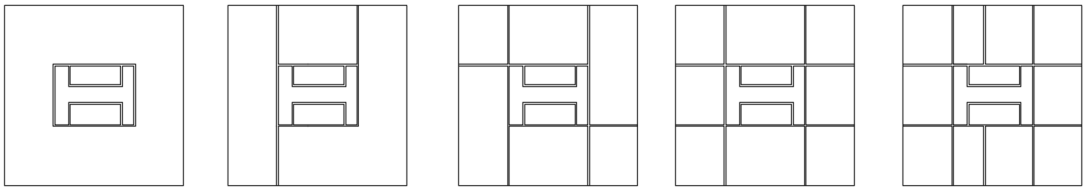

Figure 66: Best wall configuration with respect to dynamic response.

5.2.2 Braced system

Bracing is gradually added to the structure, where a structurally efficient bracing system with minor impact on the façade is of interest. The process of adding bracing and documenting the gain in number of storeys leads up to the final concept, an optimized bracing system with a realistic impact on the façade. The impact of adding bracing members i.e. diagonals with dimensions of 405x405mm is given in Table 14. Indication of figures in this table refers to Figure 67 where bracing of type 'double diagonals' is used and placed in the center-layer of respective side of the building.

Table 14: Effect of bracing the facades.

Add bracing in façade

n_{storey}	Fig.	f_0 [Hz]	m_e [ton/m]	$X_{max}/X_{ISO\ 10137}$
6	a	4,686	-	-
7		3,876	-	-
8		3,299	-	-
9		2,85		
9	b	3,043	34,09	0,493
10		2,65	34,84	0,674
11		2,351	35,3	0,887
12		2,093	35,52	1,16
12	c	2,441	35,6	0,825
13		2,179	35,77	1,071

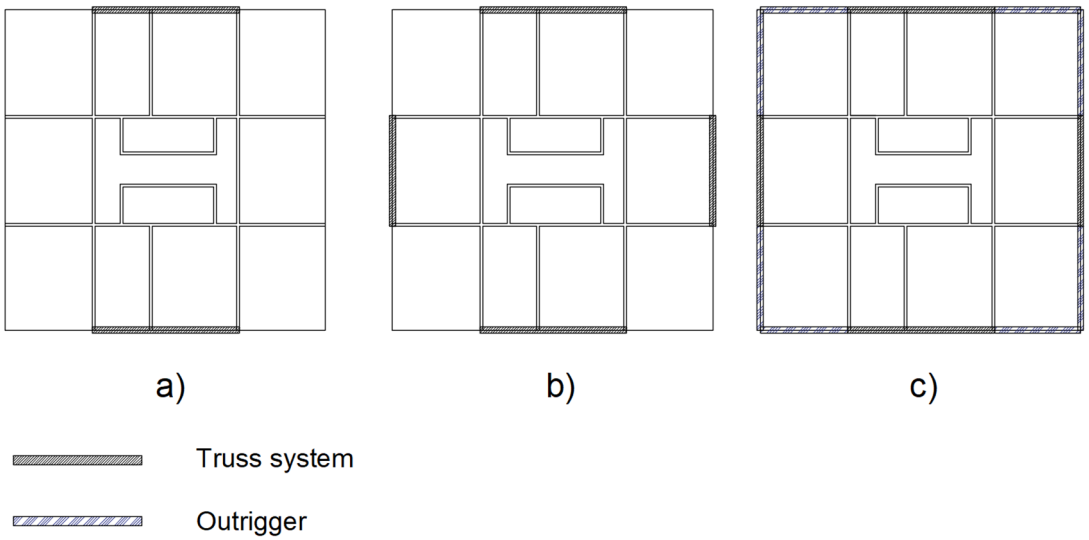

Figure 67: External bracing systems. a) Centric bracing in x-direction; b) Centric bracing in x and y-direction; c) Outrigger system.

The fundamental eigenfrequency is based on a torsional mode to the point where diagonals are implemented in both directions. According to the previously mentioned 'torsional assumption', the structure could take 8 storeys if centric bracing is placed in x-direction as for case a) and 11 storeys for case b). According to the comparison of different bracing systems in Table 9, the stiffest is the outrigger system which indicates case c). The final structural model to be analyzed further used is shown in Figure 68.

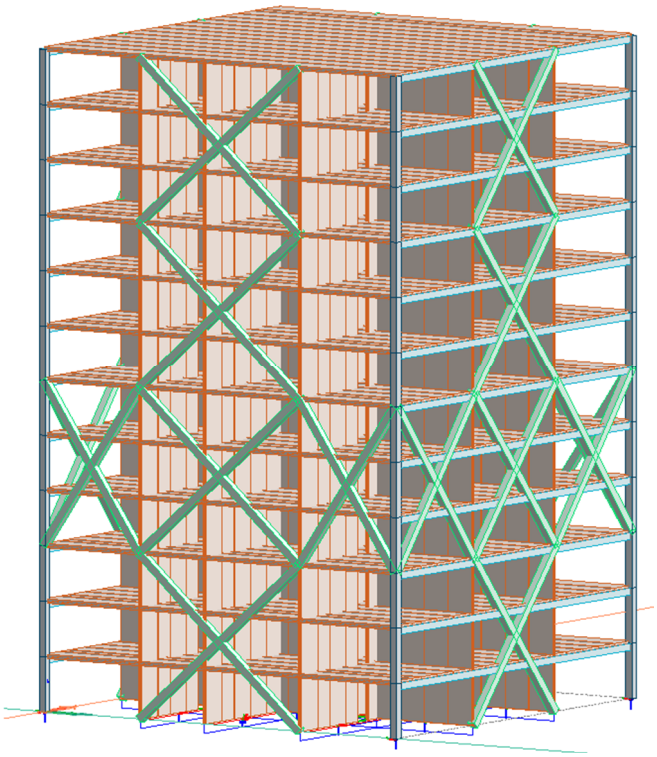

Figure 68: 3D-view of the braced system

5.2.3 Parametric study

Mass and stiffness are edited to find maximum number of storeys for the braced structure. Actions that is found practically possible to increase the height of the building is investigated and presented. Two options can be chosen as the first parametric action, depending on what demands the client has.

Table 15 indicates a timber structure with an increased mass by gradually adding concrete slabs on top storeys, known as *Option A*. The second option i.e *Option B* is shown in Table 17, intends to define maximum allowed number of storeys for a 'pure timber structure' where all structural elements are in CLT/Glulam.

When the max number of storeys is defined for respective option, next parametric action is to increase the size of cross-sections for *Option A*, meanwhile mass is increased for *Option B*.

Table 15: Effect of increase mass

Option A: Add concrete floors

n_{storey}	$n_{c.slabs}$	f_0 [Hz]	m_e [ton/m]	$X_{max.peak}$ [m/s^2]	X_{max}/ $X_{ISO\ 10137}$	X_{max}/ $X_{ISO\ 6897}$
13	1	1,708	65,6	0,034	0,862	
14		1,553	64,13	0,04	0,999	
15		1,414	62,57	0,046	1,154	
	2	1,243	82,27	0,041	1,023	
	3	1,141	98,04	0,038	0,948	
16		1,045	95,5	0,043	1,084	
	4	0,984	107,8	0,042	1,021	
	5	0,947	117,4	0,039	0,962	0,599
17		0,87	115,1	0,043	1,046	0,654
	6	0,846	122,7	0,043	0,999	0,625
18		0,779	120,4	0,48	1,08	0,679
	7	0,764	126,5	0,046	1,041	0,655
	8	0,749	131,2	0,046	1,016	0,64

The effect of using concrete floors on top storeys indicates an increase of 5-storeys, from 13 up to 17, as the 18th isn't accepted with respect to ISO 10137. The structure falls in this stage within a low-frequency range and is in addition evaluated to ISO 6897 by means of root mean square (r.m.s) acceleration for a 5-year return wind.

The change in equivalent mass decreases gradually and become more insufficient by means of limiting the peak acceleration. Comparing the max allowed acceleration with the calculated magnitude for the two standards, peak acceleration is found to be governing the number of storeys. Furthermore, more stiffness is assigned the structure by increasing the cross-sections as shown in Table 16.

Table 16: Effect of increasing the cross-sections

Option A: Increase size of sections

n_{storey}	Size of section [mm]	f_0 [Hz]	m_e [ton/m]	$X_{max.peak}$ [m/s^2]	X_{max}/ $X_{ISO\ 10137}$	X_{max}/ $X_{ISO\ 6897}$
18	Columns 620x630	0,798	131,6	0,043	0,976	
19		0,741	129,8	0,048	1,043	0,657
	Diagonal 620x630	0,776	131	0,045	1,007	0,633
	Column 1000x1000	0,84	132,1	0,041	0,952	0,596
20		0,768	130,6	0,046	1,024	0,644
	L(T)300-7S	0,85	135	0,04	0,932	0,584
21		0,797	133,3	0,044	0,99	0,622

The number of storeys can increase up to 21 storeys if size of cross sections and inner walls are increased. This parametric action is now investigated for *'Option B'* which intends to define the max number of storeys for a full timber building.

Table 17: Effect of increasing cross-sections.

Option B: Increase size of sections

n_{storey}	Size of section [mm]	f_0 [Hz]	m_e [ton/m]	$X_{max.peak}$ [m/s^2]	X_{max}/ $X_{ISO\ 10137}$
13	Columns 620x630	2,259	36,2	0,044	0,978
14		2,025	36,59	0,051	1,247
14	Trusses 620x630	2,153	37,93	0,045	1,053
	Columns 1000x1000	2,244	39,02	0,042	0,935
15		2,01	41,68	0,045	1,117
15	L(T)300-7S	2,144	43,24	0,037	0,946
16		1,933	43,52		1,152

For the case of a full timber building, the number of storeys can increase up to 15-storeys if inner wall thickness and size of cross sections are increased. The combined effect of the two parameters stiffness and mass for '*Option B'* is given in Table 17.

Table 18: Effect of changing top floors to concrete.

Option B: Add concrete floors

n_{storey}	$n_{c.slabs}$	f_0 [Hz]	m_e [ton/m]	$X_{max.peak}$ [m/s^2]	X_{max}/ $X_{ISO\ 10137}$	X_{max}/ $X_{ISO\ 6897}$
16	1	1,628	68,37	0,036	0,909	
17		1,499	67,55	0,041	1,022	
	2	1,347	85,62	0,037	0,917	
18		1,247	83,67	0,041	1,033	
	3	1,157	98,15	0,038	0,962	
19		1,072	95,98	0,045	1,079	
	4	1,016	107,7	0,039	0,964	
20		0,945	106	0,045	1,105	0,689
	5	0,908	115,6	0,044	1,042	0,65
	6	0,89	123,7	0,042	0,987	0,617
21		0,829	121,4	0,046	1,058	0,664
	7	0,814	128		1,016	0,638
	8	0,797	133,3		0,99	0,622
22		0,749	131,4	0,048	1,049	0,661

Results shows that the building can take 21 storeys with acceptable dynamic performance. The concept is at this stage identical as the one for *'Option A'* and is visualized in Figure 69.

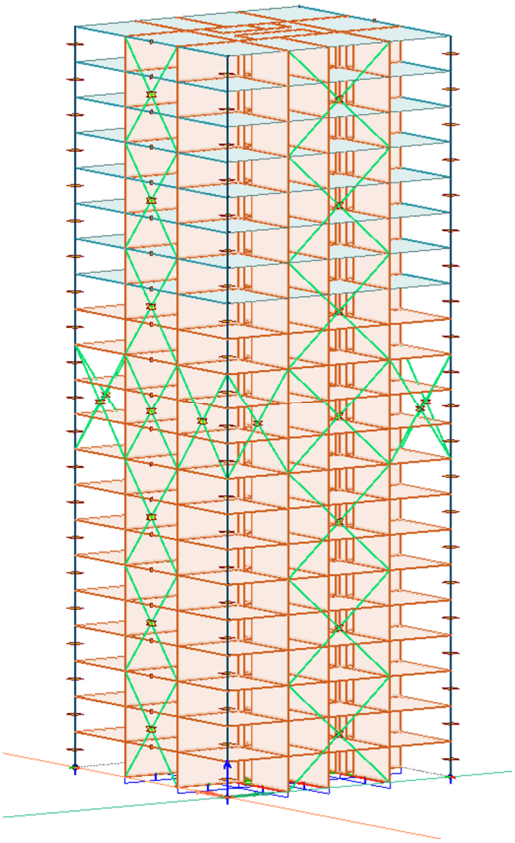

Figure 69: Structural model of the 21-storey building.

In addition to increased sections and integrating concrete floors, other parametric actions is looked upon which may not be so realistic to carry out in practice. More stiffness can be achieved by incorporating another outrigger truss in the facade. The best location of placing the outrigger is investigated to ensure a structurally efficient bracing system. Various combinations of outrigger locations are looked upon and presented in Table 19.

Table 19: Tested outrigger placement

Placement of 2nd outrigger					
Outrigger placement	f_0 [Hz]	m_e [ton/m]	$X_{max.peak}$ [m/s^2]	X_{max}/X_{ISO_10137}	$X_{max}/X_{ISO.6897}$
4,5,6 & 7,8,9	0,794				
4,5,6 & 10,11,12	0,841	131,4	0,042	0,978	0,613
4,5,6 & 13,14,15	0,823				
7,8,9 & 10,11,12	0,814				
7,8,9 & 13,14,15	0,83	131,7	0,043	0,984	0,617
10,11,12 & 13,14,15	0,796				
7,8,9 & 16,17,18	0,796				
10,11,12 & 16,17,18	0,787				

The best location of the two outriggers is where the eigenfrequency is greatest because this indicates the most increase in stiffness. The configuration of the outriggers according to Table 19 is seen in Figure 70.

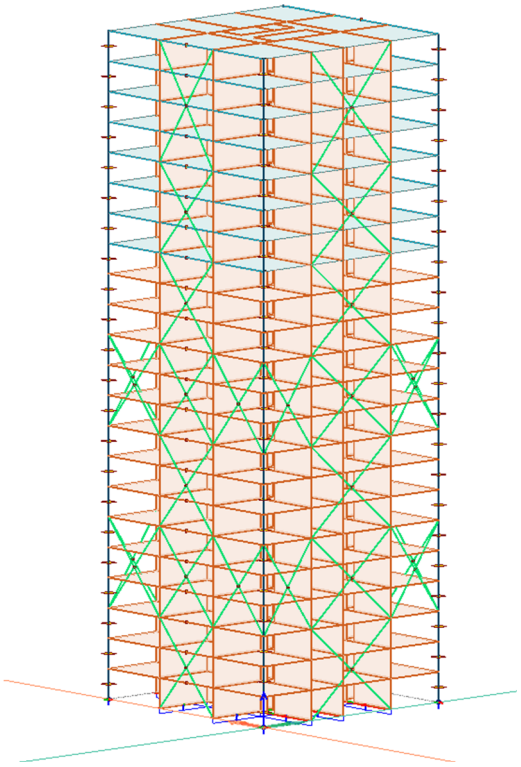

Figure 70: Configuration of the outrigger system for a structure of 22-storeys.

The structural response can at this point be studied to define the benefit of the 2nd outrigger truss. Analyzation gives following results, expressed in Table 20.

Table 20: Structural response of the building with double outrigger trusses.

Add 2nd outrigger belt

n_{storey}	f_0 [Hz]	m_e [ton/m]	$X_{max.peak}$ [m/s^2]	X_{max}/ $X_{ISO\ 10137}$	X_{max}/ $X_{ISO.6897}$
22	0,83	131,7	0,043	0,984	0,617
23	0,776	130,1	0,047	1,044	0,657

The influence on the number of storeys tells that the additional trusswork did not improve the stiffness efficiently. The prize for one additional storey comes with a cost of outrigger interference with doors and windows at facades for three more storeys.

The parametric action intends to optimize the bracing system. This action can be somewhat extended by replacing the material of diagonals from glulam to steel. The purpose is to increase the axial stiffness of the structural elements and consequently raise the eigenfrequency so that a higher building can reach acceptable acceleration-limits.

The trusses are assigned solid steel bars with a diameter of 300mm in two steps. The effect is firstly tested on the belt trusses i.e. which intends to take advantage of the stiffest truss-work in the whole structural system. Lastly the all trusses are replaced to steel increase the stiffness to the maximum. The effect on the dynamic performance is shown in Table 21.

Table 21: Structural response of modifying glulam trusses to steel trusses

Modify trusses to steel

n_{storey}	f_0 [Hz]	m_e [ton/m]	$X_{max.peak}$ [m/s^2]	X_{max}/ $X_{ISO\ 10137}$	X_{max}/ $X_{ISO.6897}$	Comment
23	0,801	130,4	0,045	1,022	0,642	Belt trusses
23	0,817	133,7	0,044	0,997	0,617	All trusses

Just as for the previous action, the impact of using steel diagonals is not sufficient. Even though the increase of axial stiffness is nearly five times higher, the eigenfrequency is just slightly increased. The section also provides additional mass but is not big enough to limit the peak acceleration.

5.2.4 Summary of results

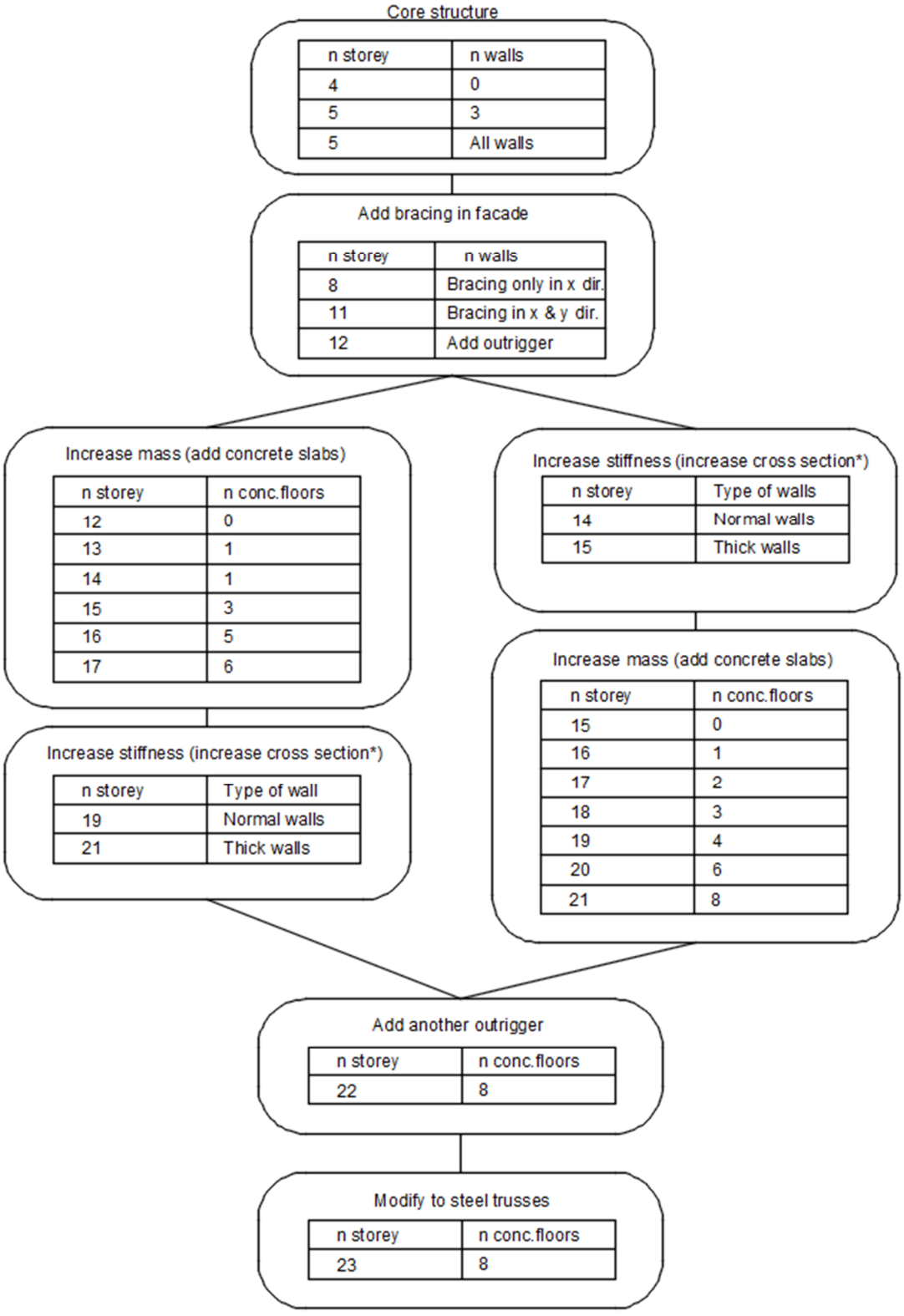

Figure 71: Summary of results from the parametric study.

**Increase cross section means using 1000x1000mm columns and 620x630mm diagonals instead of the original sections which are 405x405mm for columns and diagonals.*

6 Discussion

A discussion of the parametric effects and structural response of the building is given along with a conclusion from respective subpart. In addition, the discussion is followed by some general remarks on the study and lastly with some suggestions of further research.

6.1 Parametric effects

One of the most efficient types of bracing according to (Coull & Stafford Smith, 1991) is the braced tube. The results shows however the outrigger bracing system to have slightly better dynamic performance, indicated in Table 9. The placement of one outrigger was not as expected since the literature expresses the optimum location at the top third for a single outrigger according to (Choi, Joseph, & Mathias, 2012).

One reason for the contradiction between the literature and results may be due to the material. Outrigger bracing is mainly associated with steel and concrete structures which can be built far higher than timber. The material behaviour also plays a role here where timber is more likely to work in shear instead of bending which is the way that steel tends to work in. As timber trusses are relatively new in the industry, it could be interesting to investigate an outrigger system in timber on a deeper level.

An additional factor that isn't adopted to timber buildings is the computation of eigenfrequency according to *SS-EN-1991-1-4*. The purpose of using it as a rough check gives large differences with respect to the max heights the timber buildings are at today. In addition, there are few timber buildings and most likely none considered in the expression. The conclusion is that the expression is not applicable in the design.

Modifying either mass or stiffness in the most beneficial way depends on the frequency as seen from Figure 53. It's also shown that a doubled stiffness reduces the acceleration more than mass. Stiffness is difficult to double, as the size of cross-sections are limited in practice. Mass is however more tangible and practical to increase by the concept of equivalent mass. The allowance of other construction materials for defining of a single material building according to (Foster, Ramage, & Reynolds, 2017) makes the action relatively easy to carry out without compromising with internal planning.

6.2 Structural response

The analysis of the 'core structure' with no exterior bracing is limited due to torsional response. Previously mentioned in *SS-EN-1991-1-4*, torsion-induced vibrations are not covered which lead to the assumption where the first eigenfrequency in torsion should not be less than 3 Hertz. The basis of this isn't established in the theoretically framework but is relied on experience of the supervisor, Thomas Hallgren. Deeper insight of torque-effects is required to assess the exact number of storeys when openness at the facades is a requirement in design.

Furthermore, the result in Table 13 shows an increase from 4-storeys to 5-storeys when inner walls are added. These appear to not influence the torsional oscillations so efficiently as the eigenfrequency slightly increases with more activated inner walls. The torsional stiffness of the whole structure is limited as this stage. A reflection of the structural system is to visualize the plan-view as an open-cross section and compare the torsional stiffness to a closed cross-section. When bracing is added into the facades, see Table 14, the increase in torsional stiffness is significant as the first eigenfrequency in torsion firstly increase and later change into a transversal when diagonals is put on both directions.

Concludingly, a fully braced structure with one outrigger can be utilized for 12-storeys. The structure is based on having 'fairly large' cross sections of 405x405 for glulam columns and diagonals. By an increase of the cross-sections, an advantage can be taken with regards to the increased tolerance of peak acceleration for $f_0 > 2\ Hz$ as seen in Figure 34. This threshold is used for *'Option B'* and is used until the criteria is no longer met at 16-storeys where the eigenfrequency dropped to, $f_0 = 1.944\ Hz$. These results are represented in Table 17. Moreover, the effect of increased sections does however not influence the equivalent mass much and the timber-structure can still be considered 'lightweight'. A risk with large, stocky sections is that it's not very realistic in practice due to the impact on the aesthetics and internal planning.

The lightness of the structure can be worked against as for *'Option A'* where concrete floors are added on the top storeys. Whenever the structure falls into a low-frequency range, $f_0 < 1\ Hz$, an advantage can be taken with regards to the increased tolerance, similar to previous parametric action. As seen from Table 15, that happens when the 4th concrete slab is added on 16-storey building. The process of adding concrete stops when the effect appears to small and when there's a risk that the building cannot be categorized as a timber building. This may be the case when the 8th slab is inserted the structure of 18-storeys. Note that the actual efficiency of this parametric action can change whenever additional number of storeys have become acceptable.

No matter what order the parametric actions is carried out, a structure of 21-storeys can reach acceptable dynamic performance when assigning larger cross-sections and increasing the mass via concrete floors. Other parametric actions, such as adding a 2nd outrigger or assigning steel to the diagonals has appeared to be costly for reaching higher structure. Summing up the impact of the two actions, two additional floors can be gained and gives a total of 23-storeys. The gain in stiffness was unexpectedly low for the significant increase of axial stiffness for the diagonals. As both parametric actions are carried out late in the study and go beyond what's practically applicable, they are not investigated further.

6.3 General remarks

6.3.1 Computational model

The results are based on a flexural mode in which the mode shape factor, ζ is set to 1.5. The actual behaviour/mode is a combination of shear and bending, but shear is found dominant when the deformed shape is analysed in detail. Thus, it would have been more consistent to use the value 1.0 for the mode shape factor when evaluating against acceleration-criteria.

Comparison between the two values does however not show a significant difference on the accelerating motion, as dependant variables such as equivalent mass and standard deviation of acceleration contradicts in Equation (3.13). Some sample tests have shown a difference from 4% down to 0.5% in utilization of peak accelerations at heights between 13 and 18 storeys. The higher the structure, the smaller the margin.

An additional factor that should be noted is the structural damping of timber. According to Eurocode, the structural damping is not covered as for cases where aerodynamic effects are found to be significant in the design. Advice from specialists is therefore essential when defining structural damping. Comparing the used value of 1.5% with 1.9% as used in the design of Treet and Mjöstornet from the Norwegian code. The lower value is more conservative and leads to an acceleration-difference over 10 %. A gain of one additional storey is possible to the minimum when using the upper value from the Norwegian code.

It should be noted that the human perception limits in ISO 10137 are recommended values and it is not a regulation to be met. Furthermore, it's up to the designer and developer to inform the residents about the sway accelerations over the perception limit. This has been the case in design of Treet, where peak accelerations at the 14th storey is over the threshold for one side of the building as seen in Figure 72.

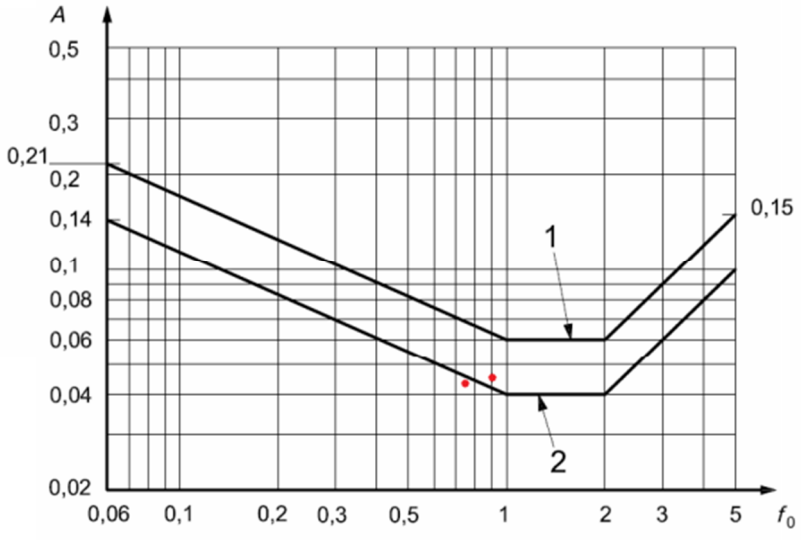

Figure 72: Evaluated peak accelerations on both sides of Treet (Bjertnaes & Malo, 2014).

As stated by (Taranath, 2011), people are more tolerant at public spaces and one could consider a mixed-use building by adding office storeys at the top to gain a few more storeys. By defining the threshold for an office building and evaluating peak accelerations to these, the building could be 28-storeys instead of 21-storeys when cross-sections are increased, and concrete slabs is inserted at the top storeys.

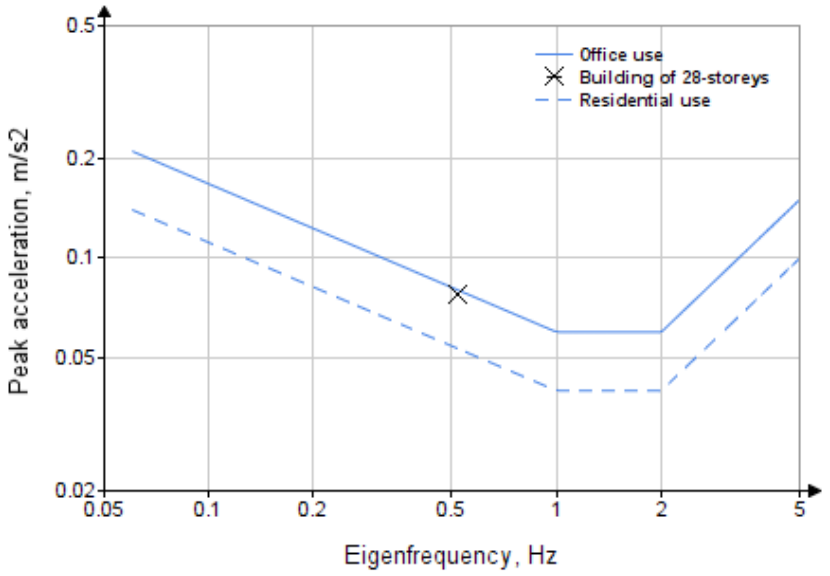

Figure 73: Evaluation of a 28-storey structure to an office building in ISO 10137

6.3.2 Further research suggestions

Throughout the work-set of the parametric study, following research suggestions have come to mind in which more generalized conclusions can be drawn about tall timber structures.

- The influence of damping on the dynamic performance could be studied to achieve a higher timber building. The cost aspect of using artificial damping could be covered in addition to judge the practical feasibility.

- The behaviour of bracing members i.e. trusses and shear walls can be investigated explicitly at various heights to judge if its governed by shear and/or bending. Thus, the mode shape factor, ζ could be chosen to represent accurate results.

- The outrigger bracing system could be further studied as the outrigger configuration contradicts with the literature. It's of interest to facilitate the choosing of optimum placement and reflect upon the reason behind that on the material level. Moreover, there's lack of resources regarding this issue.

- An assumption based on the supervisor recommendation is used to evaluate the torsional vibration since these vibrations are out of the scope of Eurocode. An alternative way could be used to evaluate the acceleration. By further investigating this aspect, a structural concept with open-plan could be improved to possibly reach greater heights than the presented results.

7 References

Abrahamsen, R. (2017). Mjøstårnet - Construction of an 81 m tall timber building. *Internationales Holzbau-Forum 2017.* Garmisch: Internationales Holzbau-Forum.

Avén, S. (1983). *Handboken bygg - Allmänna grunder.* Stockholm: LiberFörlag.

Bjertnaes, M., & Malo, K. A. (2014). Wind-Induced motions of "Treet" - A 14-storey Timber Residential Building in Norway. *World Conference on Timber Engineering 2014.* Quebec City: World Conference on Timber Engineering.

Bohne, R. A., Lohne, J., & Skullestad, J. L. (2016, November 21). *High-rise Timber Buildings as a Climate Change Mitigation Measure – A Comparative LCA of Structural System Alternatives.* Trondheim: ScienceDirect.

Boverket. (2015). *Boverket mandatory provisions amending the board's mandatory provisions and general recommendations (2011:10) on the application of European design standards (Eurocodes), EKS.* Stockholm: Boverket.

Choi, H. S., Joseph, L., & Mathias, N. (2012). *Outrigger Design for High-Rise Buildings.* New York: Routledge.

Coull, A., & Stafford Smith, B. (1991). *Tall building structures: Analysis and design.* New York, USA: Wiley & Sons.

Craig, R. R., & Kurdila, A. J. (2006). *Fundamentals of structural dynamics* (Vol. 2). New York: John Wiley & Sons.

Engström, B. (2017). Distribution of horizontal load on bracing elements. Gothenburg: Chalmers University of Technology.

Foster, R. M., Ramage, M. H., & Reynolds, T. (2017). Rethinking CTBUH Height Criteria In the Context of Tall Timber. *CTBUH Journal, 2017 Issue IV*, 28-33.

Harte, A. (2009). Introduction to timber as an engineering material. In M. Forde, *ICE Manual of Construction materials.* Galway: ICE.

ISO 10137. (2007). *Bases for design of structures- Serviceablity of buildings and walkways against vibration (ISO 10137:2007,IDT)* (Vol. 1). Stockholm: SIS Förlag AB.

ISO 6897. (1984). *Guidelines for the evaluation of the response of occupants of fixed structures, especially buildings and off-shore structures, to low-frequency horizontal motion (0,063 to 1 Hz).* Geneva: International Organization for Standardization.

Mendis, P., Ngo, T., Hira, A., Samali, B., & Cheung, J. (2007). Wind Loading on Tall Buildings. *Electronic Journal of Structural Engineering*, 41-54.

Mokeretla, M. S. (2011). *Self-damping characterisctics of transmission line conductors subjected to free and forced vibration.* Bloemfontein: Central University of Technology.

NPTEL. (2019). *Theory & Practice of Rotor Dynamics*.

Reynolds, T., Jarnerö, K., Johansson, M., Bolmsvik, Å., Olsson, J., & Linderholt, A. (2015). Building higher with light-weight timber structures - the effect of wind induced vibrations. *inter.noise 2015.* San Francisco: International Congress and Exhibition on Noise Control Engineering.

SS-EN 1991-1-4. (2005). *Eurocode 1: Actions on structures - Part 1-4: General actions - Wind actions.* Stockholm: SIS Förlag AB.

Swedish Wood. (2015). *Design of timber structures* (Vol. 1). Stockholm: Swedish wood.

Swedish Wood. (2017). *CLT handbook.* Stockholm: Swedish wood.

Taranath, B. S. (2011). *Structural Analysis and Design of Tall Buildings.* Boca ration: CRC Press .
WGBC. (2017). *Global Status Report 2017*. Retrieved from worldgbc.org: https://www.worldgbc.org/news-media/global-status-report-2017

8 Appendices

The given appendices are the analytical worksheets for the parametric study, where the software Mathcad Prime 5.0 is used in calculation. The content of Appendix A is the calculation sheet for wind-induced accelerations while Appendix B contains the numerical verification.

Appendix A: Analytical calculation sheet

Building Geometry:

$b := 22\ m$ $\quad d := 22\ m$ — Base of the building (22x22m)

$n := 18$ $\quad h_s := 2.9\ m$ — Number of storeys and height of one storey

$h := n \cdot h_s = 52.2\ m$ — Total height of the building

Building location:

$\rho_{air} := 1.25\ \frac{kg}{m^3}$ — Air density, SS-EN 1991-1-4 (4.5 NOTE 2)

$v_b := 25\ \frac{m}{s}$ — Reference wind speed in Gothenburg, EKS 10 (Fig. C-4)

$c_0(z) := 1.0$ — Topography factor, SS-EN 1991-1-4 (4.3.1)

$TC := 3$ — Terrain category III, SS-EN 1991-1-4 (Table 4.1)

$$z_0 := \begin{cases} 0.3\ m & \text{if } TC = 0 \\ 0.003\ m & \text{else if } TC = 1 \\ 0.01\ m & \text{else if } TC = 2 \\ 0.05\ m & \text{else if } TC = 3 \\ 0.3\ m & \text{else if } TC = 4 \\ 1\ m & \end{cases}$$

Roughness length, SS-EN 1991-1-4 (Table 4.1)

Output from FE-analysis:

$n_{1.x} := 0.85\ Hz$ $\quad n_{1.y} := 0.863\ Hz$ — First eigenfrequency in x-y direction

Equivalent mass:

$\zeta := 1.5$ Mode shape factor, SS-EN 1991-1-4 (F.13)

Storey height | Mode shape, SS-EN 1991-1-4 (F.3) | Mass per storey

$i := 1 .. n$

$$z_i := i \cdot h_s = \begin{bmatrix} 2.9 \\ 5.8 \\ 8.7 \\ 11.6 \\ 14.5 \\ 17.4 \\ 20.3 \\ 23.2 \\ 26.1 \\ 29 \\ 31.9 \\ 34.8 \\ \vdots \end{bmatrix} \boldsymbol{m} \qquad \phi_i := \left(\frac{z_i}{h}\right)^{\zeta} = \begin{bmatrix} 0.013 \\ 0.037 \\ 0.068 \\ 0.105 \\ 0.146 \\ 0.192 \\ 0.243 \\ 0.296 \\ 0.354 \\ 0.414 \\ 0.478 \\ 0.544 \\ \vdots \end{bmatrix} \qquad m.storey := \begin{bmatrix} 111418 \\ 111710 \\ 119054 \\ 111730 \\ 112190 \\ 124889 \\ 111852 \\ 111557 \\ 126488 \\ 111214 \\ 411000 \\ 419053 \\ 411253 \\ 411011 \\ 419626 \\ 411490 \\ 409878 \\ 403732 \end{bmatrix} \boldsymbol{kg}$$

$$m_e := \frac{\sum_{i=1}^{n} m.storey_{i-1} \cdot \phi_i^{\,2}}{h_s \cdot \sum \phi^2} = \left(1.312 \cdot 10^5\right) \frac{\boldsymbol{kg}}{\boldsymbol{m}}$$

Equivalent mass per unit length, SS-EN 1991-1-4 (F.14)

Wind-load and dynamic properties:

$k_l := 1$ — Turbulence factor, SS-EN 1991-1-4 (4.7)

$$I_v(z) := \frac{k_l}{c_0(z) \cdot \ln\left(\frac{z}{z_0}\right)}$$ — Turbulence intensity, SS-EN 1991-1-4 (4.7)

$I_v(h) = 0.194$

$z_{011} := 0.05\ m$ — Roughness length for terrain category II, SS-EN 1991-1-4 (Table 4.1)

$$k_r := 0.19 \cdot \left(\frac{z_0}{z_{011}}\right)^{0.07} = 0.215$$ — Terrain factor, SS-EN 1991-1-4 (4.5)

$T_a := 5$ — Time and wind speed with a return period of 5 years, EKS 10 Paragraph 6.3.2(1)

$$v_{b.Ta} := 0.75 \cdot v_b \cdot \sqrt{1 - 0.2 \cdot \ln\left(-\ln\left(1 - \frac{1}{T_a}\right)\right)}$$

$$c_r(z) := k_r \cdot \ln\left(\frac{z}{z_0}\right)$$ — Roughness factor, SS-EN 1991-1-4 (4.4)

$v_m(z) := c_r(z) \cdot c_0(z) \cdot v_{b.Ta}$ — Mean wind velocity, SS-EN 1991-1-4 (4.3)

$v_m := v_m(h) = 23.756\ \frac{m}{s}$

$q_m := \frac{1}{2} \cdot \rho_{air} \cdot {v_m}^2 = 352.704\ Pa$ — Mean wind pressure, SS-EN 1991-1-4 (4.10)

Logarithmic decrement of damping, SS-EN-1991-1-4 (F.1):

$$\delta = \delta_a + \delta_s + \delta_d$$

Interpolate external pressure coefficients with combined effect of zone D and E, SS-EN 1991-1-4 (Table 7.1)

$$c_{pe.10} := \begin{cases} \left\| 0.8 + 0.5 + \dfrac{\dfrac{h}{d} - 1}{5 - 1} \cdot (0.7 - 0.5) \right. & \text{if } 1 \le \dfrac{h}{d} \le 5 \\ \left\| 1.5 \right. & \text{else if } \dfrac{h}{d} > 5 \\ \left\| 0.7 + 0.3 + \dfrac{\dfrac{h}{d} - 0.25}{1 - 0.25} \cdot (0.5 - 0.3) \right. & \text{else if } 1 \ge \dfrac{h}{d} \ge 0.25 \\ \left\| 0.7 + 0.3 \right. & \text{else} \end{cases} = 1.369$$

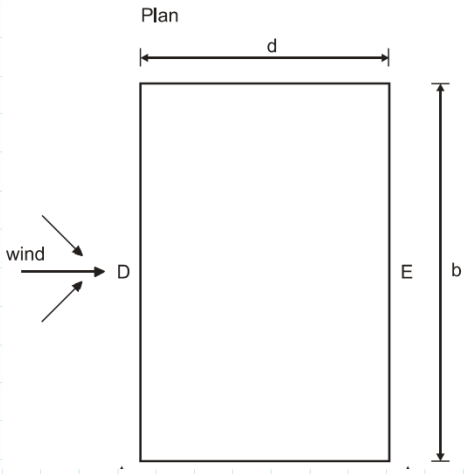

$c_f := c_{pe.10}$

Force coefficient in the wind direction, SS-EN 1991-1-4 (F.18)

$$\delta_a := \frac{c_f \cdot \rho_{air} \cdot b \cdot v_m}{2 \cdot n_{1.x} \cdot m_e} = 0.004$$

Logarithmic decrement of the aerodynamic damping for the fundamental mode, SS-EN 1991-1-4 (F.18)

$\delta_s := 1.5\% \cdot 2\ \pi = 0.094$

Logarithmic decrement of structural damping. Recommended value for timber buildings with fasteners, BSV 97 (Table 3.22a)

$\delta_d := 0 \cdot 2 \cdot \pi = 0$

Logarithmic decrement of damping due to special devices

Peak acceleration, defined from EKS 10 Paragraph 6.3.1(1)

$$y_C := \frac{150 \cdot n_{1.x}}{v_m} \cdot m$$ Non-dimensional wind energy spectrum

$$F := \frac{4 \cdot y_C}{\left(1 + 70.8 \cdot {y_C}^2\right)^{\frac{5}{6}}}$$ Non-dimensional frequency

$$h_{ref} := 10\ m$$ Recommended value of ref height

$$B := \sqrt{\exp\left(-0.05 \cdot \frac{h}{h_{ref}} + \left(1 - \frac{b}{h}\right) \cdot \left(0.04 + 0.01 \cdot \frac{h}{h_{ref}}\right)\right)}$$ Background response factor

$$\phi_b := \frac{1}{1 + \frac{3.2 \cdot n_{1.x} \cdot b}{v_m}}$$ Size factor with respect to width

$$\phi_h := \frac{1}{1 + \frac{2 \cdot n_{1.x} \cdot h}{v_m}}$$ Size factor with respect to height

$$R := \sqrt{\frac{2 \cdot \pi \cdot F \cdot \phi_h \cdot \phi_b}{\delta_s + \delta_a + \delta_d}}$$ Resonance response factor

$$v := n_{1.x} \cdot \frac{R}{\sqrt{R^2 + B^2}}$$ Up-crossing frequency

$$\phi_{1.x}(z) := \left(\frac{z}{h}\right)^{\zeta}$$ Fundamental flexural mode

Standard deviation of acceleration:

$h_d := (n-1) \cdot h_s = 49.3\ m$ Height of last inhabitant floor

$\sigma_X(z) := \frac{3 \cdot I_v(h) \cdot R \cdot q_m \cdot b \cdot c_f \cdot \phi_{1.x}(h_d)}{m_e} = 0.016\ \frac{m}{s^2}$

Comment: The acceleration is evaluated at the highest residential storey.

Peak factor:

$T_{600} := 600\ s$ Time for 10 minutes

$k_p := \max\left(\sqrt{2 \cdot \ln(v \cdot T_{600})} + \frac{0.6}{\sqrt{2 \cdot \ln(v \cdot T_{600})}}, 3\right) = 3.436$

Peak and r.m.s acceleration:

$X_{max.peak}(z) := 0.72 \cdot k_p \cdot \sigma_X(h)$ Suggested acceleration magnitude for a wind with a one-year return period, ISO 6897 (NOTES nr.3)

$X_{max.rms}(z) := \text{if } 0.063\ Hz \le n_{1.x} \le 1\ Hz$ Acceleration magnitude for a wind with a five-year return period

$\quad\quad \sigma_X(h)$

$\quad \text{else}$

$\quad\quad \text{“Not in the scope of ISO 6897”}$

ISO 10137 evaluation criteria:

log-log interpolation for curve 2:

$$A := \begin{bmatrix} 0.14 \\ 0.04 \\ 0.04 \\ 0.1 \end{bmatrix} \qquad f_0 := \begin{bmatrix} 0.06 \\ 1 \\ 2 \\ 5 \end{bmatrix}$$

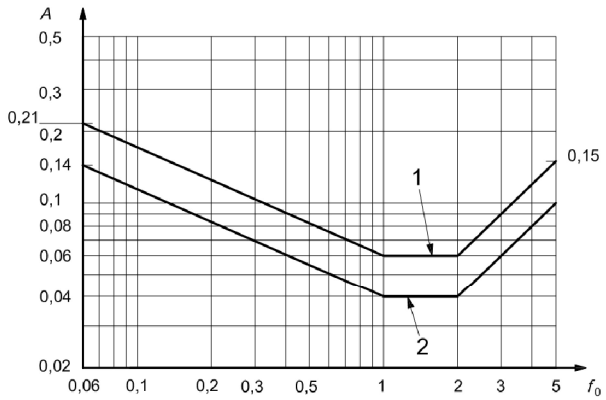

$$k := 0 .. 2$$

$$\Delta f_{0_k} := \text{for } i \in 0 .. 2 \left\| \log\left(f_{0_{k+1}}\right) - \log\left(f_{0_k}\right) \right| = \begin{bmatrix} 1.222 \\ 0.301 \\ 0.398 \end{bmatrix}$$

$$\Delta A_k := \text{for } i \in 0 .. 2 \left\| \log\left(A_{k+1}\right) - \log\left(A_k\right) \right| = \begin{bmatrix} -0.544 \\ 0 \\ 0.398 \end{bmatrix}$$

$$m_k := \left\| \frac{\Delta A_k}{\Delta f_{0_k}} \right| = \begin{bmatrix} -0.445 \\ 0 \\ 1 \end{bmatrix}$$

$$k_{xy_k} := \text{for } i \in 0 .. 2 \left\| \frac{A_k}{\left(f_{0_k}\right)^{m_k}} \right| = \begin{bmatrix} 0.04 \\ 0.04 \\ 0.02 \end{bmatrix}$$

$$n_{1.x} := n_{1.x} \cdot s = 0.85$$

$$X_{max.ISO\_10137} := \begin{array}{|l} \text{if } n_{1.x} < 1 \\ \quad \| \; k_{xy_0} \cdot n_{1.x}^{\;m_0} \\ \text{else if } 1 \le n_{1.x} \le 2 \\ \quad \| \; k_{xy_1} \cdot n_{1.x}^{\;m_1} \\ \text{else if } n_{1.x} > 2 \\ \quad \| \; k_{xy_2} \cdot n_{1.x}^{\;m_2} \\ \text{else} \\ \quad \| \; \text{“Not in the scope of ISO 10137”} \end{array} = 0.043$$

$$X_{max.peak} := X_{max.peak}(h) \cdot \frac{s^2}{m} = 0.041$$

Dimensionless accelerations are used for graphical representation

Indata for acceleration plot according to ISO 10137:

$i := 0 .. 123$ Index with 0.04 per step

$$x := 0.06, 0.1 .. 5 = \begin{bmatrix} 0.06 \\ 0.1 \\ 0.14 \\ 0.18 \\ 0.22 \\ 0.26 \\ 0.3 \\ 0.34 \\ 0.38 \\ 0.42 \\ 0.46 \\ 0.5 \\ \vdots \end{bmatrix}$$

$$y_i := \begin{array}{|l} \text{for } j \in 0 .. 123 \\ \quad \| \; \text{if } x_i < 1 \\ \quad \quad \| \; k_{xy_0} \cdot x_i^{\;m_0} \\ \quad \| \; \text{else if } 1 \le x_i \le 2 \\ \quad \quad \| \; k_{xy_1} \cdot x_i^{\;m_1} \\ \quad \| \; \text{else if } x_i > 2 \\ \quad \quad \| \; k_{xy_2} \cdot x_i^{\;m_2} \end{array} = \begin{bmatrix} 0.14 \\ 0.112 \\ 0.096 \\ 0.086 \\ 0.078 \\ 0.073 \\ 0.068 \\ 0.065 \\ 0.062 \\ 0.059 \\ 0.057 \\ 0.054 \\ \vdots \end{bmatrix}$$

Graphical evaluation:

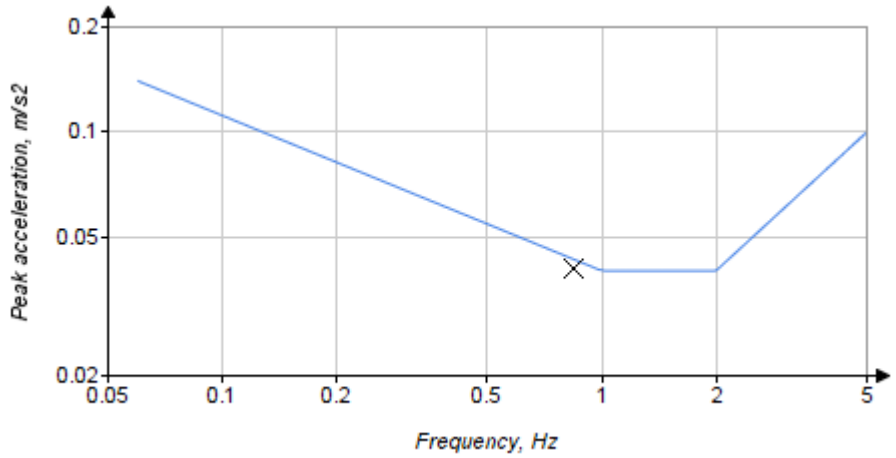

$$\frac{X_{max.peak}}{X_{max.ISO\_10137}} = 0.943$$

ISO 6897 evaluation criteria:

log-log interpolation for curve 1:

$$A := \begin{bmatrix} 0.08 \\ 0.026 \end{bmatrix} \qquad f_0 := \begin{bmatrix} 0.063 \\ 1 \end{bmatrix}$$

$$\Delta A := \log\left(A_1\right) - \log\left(A_0\right) = -0.488$$

$$\Delta f_0 := \log\left(f_{0_1}\right) - \log\left(f_{0_0}\right) = 1.201$$

$$m := \left\| \frac{\Delta A}{\Delta f_0} \right| = -0.407$$

$$k_{xy} := \frac{A}{\left(f_0\right)^m} = \begin{bmatrix} 0.026 \\ 0.026 \end{bmatrix}$$

$$X_{max.ISO\_6897} := \text{if } n_{1.x} \le 1 \left\| k_{xy_0} \cdot n_{1.x}{}^m \right| = 0.028$$
$$\text{else} \left\| \text{“Not in the scope of ISO 6897”} \right.$$

$$X_{max.rms}(h) = 0.016 \ \frac{m}{s^2}$$

$$X_{max.rms} := X_{max.rms}(h) \cdot \frac{s^2}{m} = 0.016$$

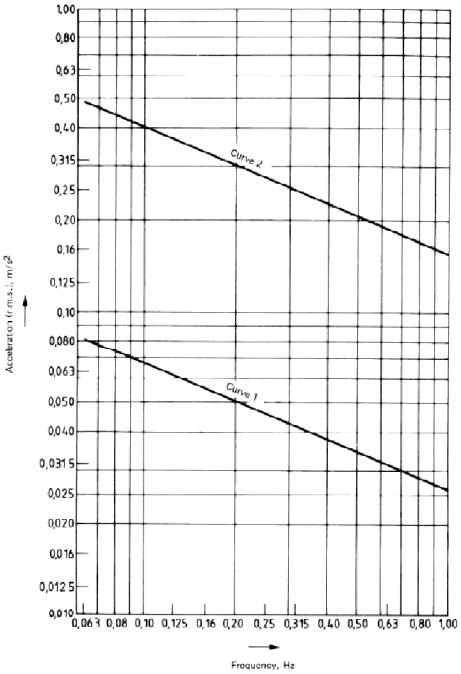

Dimensionless accelerations are used for graphical representation

Indata for acceleration plot according to ISO 6897:

$i := 0 .. 47$ Index with 0.02 per step

$$x_5 := 0.06, 0.08 .. 1 = \begin{bmatrix} 0.06 \\ 0.08 \\ 0.1 \\ 0.12 \\ 0.14 \\ 0.16 \\ 0.18 \\ 0.2 \\ 0.22 \\ 0.24 \\ 0.26 \\ 0.28 \\ \vdots \end{bmatrix} \qquad y_{5_i} := \text{for } j \in 0 .. 47 \left| \left\| k_{xy_0} \cdot x_{5_i}{}^{m} \right| \right| = \begin{bmatrix} 0.082 \\ 0.073 \\ 0.066 \\ 0.062 \\ 0.058 \\ 0.055 \\ 0.052 \\ 0.05 \\ 0.048 \\ 0.046 \\ 0.045 \\ 0.044 \\ \vdots \end{bmatrix}$$

Graphical evaluation:

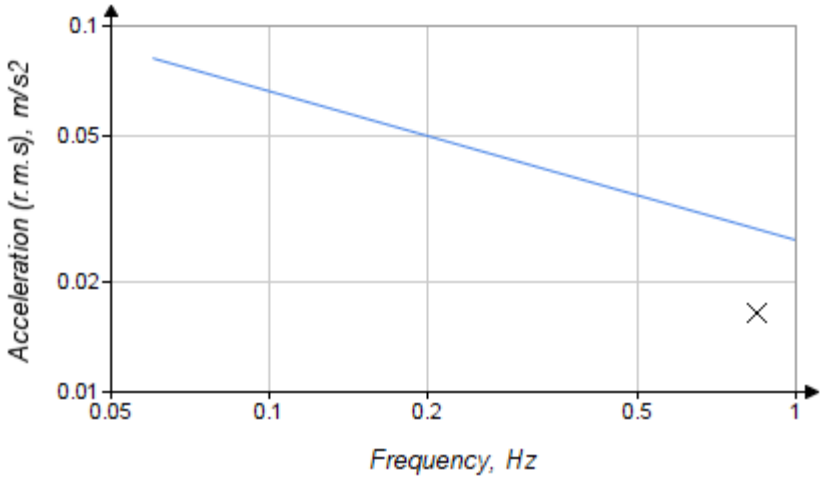

$$\frac{X_{max.rms}}{X_{max.ISO\_6897}} = 0.59$$

Risk of vortex shedding:

$St := 0.12$ — Strouhal number, SS-EN 1991-1-4 (Fig: E.1)

$v_{crit.i} := \frac{b \cdot n_{1.y}}{St} = 158.217 \ \frac{m}{s}$ — Critical wind velocity, SS-EN 1991-1-4 (E.2)

$v_m := c_r(h) \cdot c_0(h) \cdot v_b = 27.78 \ \frac{m}{s}$ — Mean wind velocity, SS-EN 1991-1-4 (4.3)

$Vortex\_shedding := \text{if } v_{crit.i} > 1.25 \cdot v_m \ \| \ \text{“No risk”} \ \text{else} \ \| \ \text{“Risk”} = \text{“No risk”}$

$\frac{v_{crit.i}}{1.25 \cdot v_m} = 4.556$ — Criteria for vortex shedding, SS-EN 1991-1-4 (E.1)

Risk of galloping:

$Sc := \frac{2 \cdot \delta_s \cdot m_e}{\rho_{air} \cdot b^2}$ — Scruton number, SS-EN 1991-1-4 (E.4)

$a_G := 1.2$ — Factor of galloping instability, SS-EN 1991-1-4 (Table: E.7)

$v_{CG} := \frac{2 \cdot Sc}{a_G} \cdot n_{1.y} \cdot b = \left(1.293 \cdot 10^3\right) \ \frac{m}{s}$ — Onset wind velocity of galloping, SS-EN 1991-1-4 (E.18)

$Galloping := \text{if } v_{CG} > 1.25 \cdot v_m \ \| \ \text{“No risk”} \ \text{else} \ \| \ \text{“Risk”} = \text{“No risk”}$

$\frac{v_{CG}}{1.25 \cdot v_m} = 37.243$ — Criteria for galloping, SS-EN 1991-1-4 (E.22)

Summary of results

$h = 52.2\ m$ $n = 18$ Total building height and no. of floors

$n_{1.x} = 0.85$ $m_e = \left(1.312 \cdot 10^5\right)\ \frac{kg}{m}$ Fundamental eigenfrequency & equivalent mass

$X_{max.rms} = 0.016$

$X_{max.ISO\_6897} = 0.028$ Acceleration (r.m.s) & max allowed acceleration according to ISO 6897

$X_{max.peak} = 0.041$

$X_{max.ISO\_10137} = 0.043$ Peak & max allowed acceleration according to ISO 10137 (Fig: D.1)

ISO 10137 graphical evaluation:

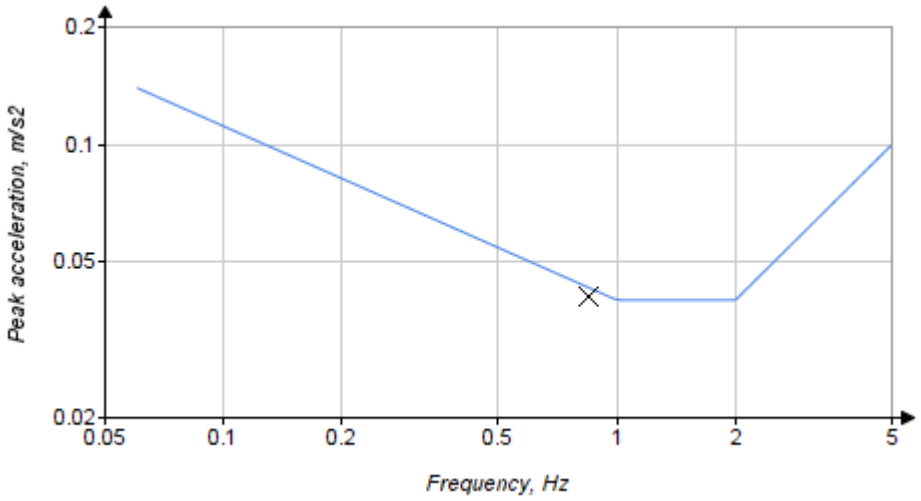

$$\frac{X_{max.peak}}{X_{max.ISO\_10137}} = 0.943$$

$$\frac{X_{max.rms}}{X_{max.ISO\_6897}} = 0.59$$

Appendix B: Verification of FE-model

Content

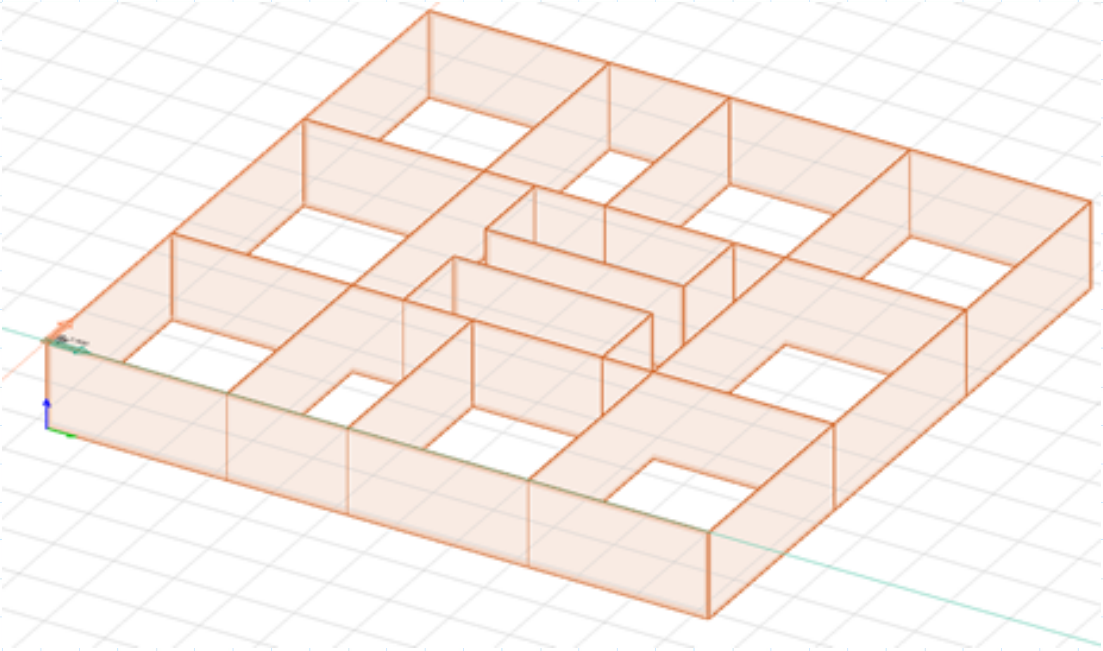

1. Wind load according to SS-EN 1991-1-4:

Building geometry:

$b := 22\ m$ $\quad d := 22\ m$ — Base of the building (22x22m)

$n := 10$ $\quad h_s := 2.9\ m$ — Number of storeys and height of one storey

$h := n \cdot h_s = 29\ m$ — Total height of the building

$t := 0.2\ m$ — Thickness of walls

Building location:

$\rho_{air} := 1.25\ \frac{kg}{m^3}$ — Air density, SS-EN 1991-1-4 (4.5 NOTE 2)

$v_b := 25\ \frac{m}{s}$ — Reference wind speed in Gothenburg, EKS 10 (Fig. C-4)

$c_0(h) := 1$ — Topography factor, SS-EN 1991-1-4 (4.3.1)

$TC := 3$ — Terrain category III and roughness length, SS-EN 1991-1-4 (Table 4.1)

$$z_0 := \begin{cases} 0.3\ m & \text{if } TC = 0 \\ 0.003\ m & \text{else if } TC = 1 \\ 0.01\ m & \text{else if } TC = 2 \\ 0.05\ m & \text{else if } TC = 3 \\ 0.3\ m & \text{else if } TC = 4 \\ 1\ m & \end{cases} = 0.3\ m$$

$z_{011} := 0.05\ m$ — Roughness length for terrain category II, SS-EN 1991-1-4 (Table 4.1)

$k_r := 0.19 \cdot \left(\frac{z_0}{z_{011}}\right)^{0.07} = 0.215$ — Terrain factor, SS-EN 1991-1-4 (Eq 4.5)

Wind-load:

$i := 0 .. n-1$

$$level := 1 .. n = \begin{bmatrix} 1 \\ 2 \\ 3 \\ 4 \\ 5 \\ 6 \\ 7 \\ 8 \\ 9 \\ 10 \end{bmatrix} \qquad h_{st_i} := level_i \cdot h_s = \begin{bmatrix} 2.9 \\ 5.8 \\ 8.7 \\ 11.6 \\ 14.5 \\ 17.4 \\ 20.3 \\ 23.2 \\ 26.1 \\ 29 \end{bmatrix} m$$

$$z_{e_i} := \begin{vmatrix} \text{if } h_{st_i} \le d \\ \quad \| \; d \\ \text{else if } d < h_{st_i} < (h-d) \\ \quad \| \; h_{st_i} \\ \text{else} \\ \quad \| \; h \end{vmatrix} = \begin{bmatrix} 22 \\ 22 \\ 22 \\ 22 \\ 22 \\ 22 \\ 22 \\ 29 \\ 29 \\ 29 \end{bmatrix} m$$

Reference height per storey, SS-EN 1991-1-4 (Paragraph 7.2.2)

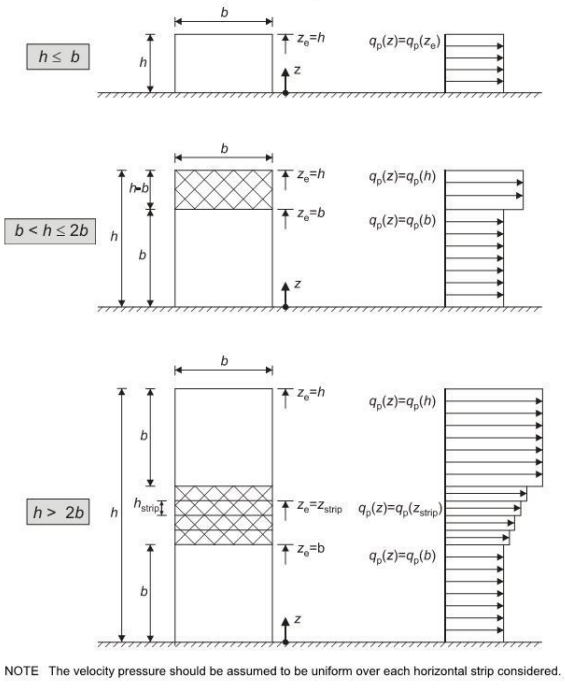

NOTE The velocity pressure should be assumed to be uniform over each horizontal strip considered.

Shape of profile of velocity pressure, SS-EN 1991-1-4 (Fig 7.4)

$k_l := 1$ Turbulence factor, SS-EN 1991-1-4 (4.7)

$$I_{v_i} := \frac{k_l}{c_0(h) \cdot \ln\left(\frac{z_{e_i}}{z_0}\right)} = \begin{bmatrix} 0.233 \\ 0.233 \\ 0.233 \\ 0.233 \\ 0.233 \\ 0.233 \\ 0.233 \\ 0.219 \\ 0.219 \\ 0.219 \end{bmatrix}$$

Turbulence intensity, SS-EN-1991-1-4 (4.7)

$$c_{e_i} := \left(1 + 6 \cdot I_{v_i}\right) \cdot \left(k_r \cdot \ln\left(\frac{z_{e_i}}{z_0}\right)\right)^2 = \begin{bmatrix} 2.051 \\ 2.051 \\ 2.051 \\ 2.051 \\ 2.051 \\ 2.051 \\ 2.051 \\ 2.242 \\ 2.242 \\ 2.242 \end{bmatrix}$$

Exposure factor, EKS (10) Paragraph 4.5(1)

Wind pressure on walls: Interpolate external pressure coefficients with combined effect of zone D and E, SS-EN 1991-1-4 (Table 7.1)

$$c_{pe.10} := \begin{cases} \text{if } 1 \le \frac{h}{d} \le 5 \\ \quad \left\| 0.8 + 0.5 + \frac{\frac{h}{d} - 1}{5 - 1} \cdot (0.7 - 0.5) \right. \\ \text{else if } \frac{h}{d} > 5 \\ \quad \left\| 1.5 \right. \\ \text{else if } 1 \ge \frac{h}{d} \ge 0.25 \\ \quad \left\| 0.7 + 0.3 + \frac{\frac{h}{d} - 0.25}{1 - 0.25} \cdot (0.5 - 0.3) \right. \\ \text{else} \\ \quad \left\| 0.7 + 0.3 \right. \end{cases} = 1.316$$

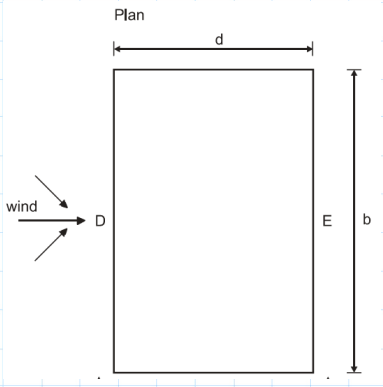

$$q_b := \frac{\rho_{air} \cdot {v_b}^2}{2} = 390.625\ \boldsymbol{Pa}$$ Mean wind pressure, SS-EN 1991-1-4 (4.10)

$$q_{p.z_i} := c_{e_i} \cdot q_b = \begin{bmatrix} 0.801 \\ 0.801 \\ 0.801 \\ 0.801 \\ 0.801 \\ 0.801 \\ 0.801 \\ 0.876 \\ 0.876 \\ 0.876 \end{bmatrix} \boldsymbol{kPa} \qquad w_{e.z_i} := q_{p.z_i} \cdot c_{pe.10} = \begin{bmatrix} 1.054 \\ 1.054 \\ 1.054 \\ 1.054 \\ 1.054 \\ 1.054 \\ 1.054 \\ 1.152 \\ 1.152 \\ 1.152 \end{bmatrix} \boldsymbol{kPa}$$

Peak velocity pressure and wind pressure, SS-EN-1991-1-4 (5.2)

Wind load acting on each floor:

$$Q_{w.z_i} := \begin{vmatrix} \text{if } i = n-1 \\ \quad \| \ w_{e.z_i} \cdot \frac{h_s}{2} \\ \text{else} \\ \quad \| \ w_{e.z_i} \cdot h_s \end{vmatrix} = \begin{bmatrix} 3.058 \\ 3.058 \\ 3.058 \\ 3.058 \\ 3.058 \\ 3.058 \\ 3.058 \\ 3.342 \\ 3.342 \\ 1.671 \end{bmatrix} \frac{kN}{\boldsymbol{m}}$$

Wind load from FEM-Design:

$$Q_{w.z.FEM} := \begin{bmatrix} 3.06 \\ 3.06 \\ 3.06 \\ 3.06 \\ 3.06 \\ 3.06 \\ 3.06 \\ 3.34 \\ 3.34 \\ 1.67 \end{bmatrix} \frac{\boldsymbol{kN}}{\boldsymbol{m}}$$

Analytical and numerical comparison:

$$Q_{w.comp_i} := \frac{Q_{w.z_i} - Q_{w.z.FEM_i}}{Q_{w.z.FEM_i}} = \begin{bmatrix} -6.846 \cdot 10^{-4} \\ -6.846 \cdot 10^{-4} \\ -6.846 \cdot 10^{-4} \\ -6.846 \cdot 10^{-4} \\ -6.846 \cdot 10^{-4} \\ -6.846 \cdot 10^{-4} \\ -6.846 \cdot 10^{-4} \\ 5.751 \cdot 10^{-4} \\ 5.751 \cdot 10^{-4} \\ 5.751 \cdot 10^{-4} \end{bmatrix}$$

2. Total moment at the supports

$H_i := Q_{w.z_i} \cdot d$ Horizontal force on each storey, $Q_{w.z}$ defined in Ch.1

$M_i := H_i \cdot h_{st_i}$ Moment due to wind load on each storey

$M_{tot} := \sum M = \left(1.015 \cdot 10^4\right)\ \boldsymbol{kN \cdot m}$ Total moment acting on the building in either direction

$$M_{totx.fem} := \left(259.94 + 274.41\right)\ \boldsymbol{kN} \cdot 11\ \boldsymbol{m} + \left(59.23 + 55.31\right)\ \boldsymbol{kN} \cdot 5\ \boldsymbol{m} \hookleftarrow$$
$$+ 25.86\ \boldsymbol{kN} \cdot 6.6\ \boldsymbol{m} \cdot 2 + 1013.11\ \boldsymbol{kN \cdot m} \cdot 2 \hookleftarrow$$
$$+ 845.995\ \boldsymbol{kN \cdot m} \cdot 2 + 37.313\ \boldsymbol{kN \cdot m} \cdot 2$$

Reaction due to wind load in the basement level

Analytical and numerical comparison:

$$\frac{M_{tot} - M_{totx.fem}}{M_{totx.fem}} = -0.041$$

3. Vertical loads

Indata:

$\rho_{CLT} := 400 \ \frac{kg}{m^3}$ Density of cross-laminated timber

$t_{floor} := 0.23 \ m$ $t_{walls} := 0.2 \ m$ Thickness of CLT elements

$l_{walls} := 8 \cdot 22 \ m + 7.2 \cdot 2 \ m + 2.9 \cdot 4 \ m + 6.6 \cdot 2 \ m$ Total wall length

$A_{walls} := l_{walls} \cdot h_s - 25 \cdot {t_{walls}}^2 = 623.08 \ m^2$

$A_{shaft} := (6.6 \cdot m \cdot 2.9 \cdot m) \cdot 2 = 38.28 \ m^2$ Area of walls, shafts and floor

$A_{floor} := d^2 - A_{shaft} = 445.72 \ m^2$

Self-weight and imposed load:

$G_k := \rho_{CLT} \cdot g \cdot (A_{walls} \cdot t_{walls} + A_{floor} \cdot t_{floor}) = 890.96 \ kN$

$q_k := 2 \ \frac{kN}{m^2}$ $Q_k := q_k \cdot A_{floor}$ Imposed load, EKS 10 (Table C-1)

$\Psi_2 := 0.3$ Load factor, EKS 10 (Table B-1)

$G_{storey} := G_k + \Psi_2 \cdot Q_k = (1.158 \cdot 10^3) \ kN$ Dynamic mass conversion

Mass of each storey:

$$G_{z_i} := \frac{(G_k + \Psi_2 \cdot Q_k)}{g} = \begin{bmatrix} 1.181 \cdot 10^5 \\ 1.181 \cdot 10^5 \\ 1.181 \cdot 10^5 \\ 1.181 \cdot 10^5 \\ 1.181 \cdot 10^5 \\ 1.181 \cdot 10^5 \\ 1.181 \cdot 10^5 \\ 1.181 \cdot 10^5 \\ 1.181 \cdot 10^5 \\ 1.181 \cdot 10^5 \end{bmatrix} kg \qquad G_{z.FEM} := \begin{bmatrix} 116974 \\ 118577 \\ 116197 \\ 118198 \\ 118817 \\ 118046 \\ 118884 \\ 117552 \\ 119647 \\ 94217 \end{bmatrix} kg$$

Analytical and numerical comparison:

$$G_{comp_i} := \frac{G_{z_i} - G_{z.FEM_i}}{G_{z.FEM_i}} = \begin{bmatrix} 0.01 \\ -0.004 \\ 0.017 \\ -6.336 \cdot 10^{-4} \\ -0.006 \\ 6.533 \cdot 10^{-4} \\ -0.006 \\ 0.005 \\ -0.013 \\ 0.254 \end{bmatrix}$$

Total mass:

$$m_{tot} := \sum G_z = \left(1.181 \cdot 10^6\right)\ \boldsymbol{kg}$$

$$m_{tot.fem} := \sum G_{z.FEM} + 21691\ \boldsymbol{kg} = \left(1.179 \cdot 10^6\right)\ \boldsymbol{kg}$$

$$\frac{m_{tot.fem} - m_{tot}}{m_{tot}} = -0.002$$ Difference in total mass

Comment: The total masses is nearly identical. Half the mass of walls at the roof and the base is considered in FEM Design, meanwhile the analytical mass is kept konstant. The mass at the base is therefore added at the end to reflect the full structural mass

4. Horizontal force distribution on shear walls

$G_C := \left[\frac{d}{2} \ \frac{d}{2}\right] = [11 \ \ 11] \ m$ Gravity centre of structural system

$n_w := 16$ Total number of walls

$n_{w.x} := 6$ Number of walls in x-direction

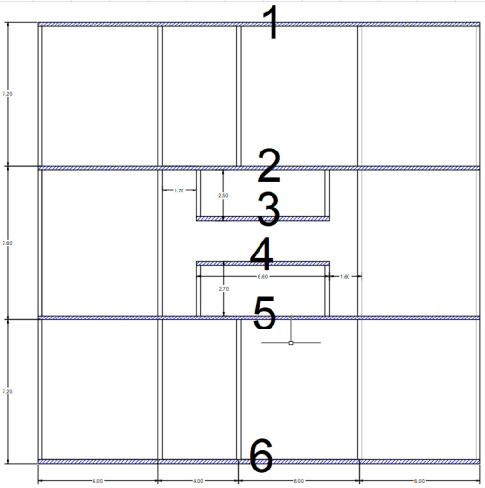

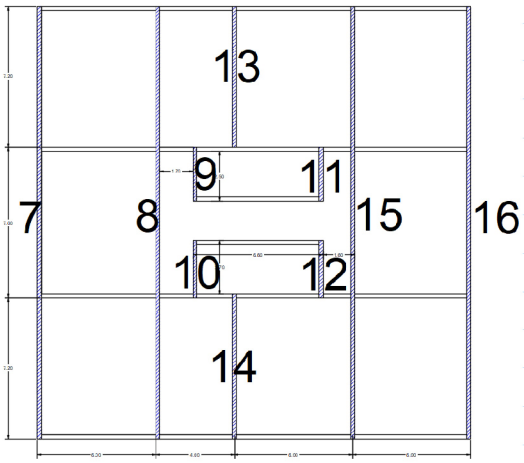

Wall ID:

$W_n := 1 .. n_w = \begin{bmatrix} 1 \\ 2 \\ 3 \\ 4 \\ 5 \\ 6 \\ 7 \\ 8 \\ 9 \\ 10 \\ 11 \\ 12 \\ 13 \\ 14 \\ 15 \\ 16 \end{bmatrix}$

Global coordinates:

$coord := \begin{array}{c} \begin{matrix} x & y \end{matrix} \\ \begin{bmatrix} 11 & 21.9 \\ 11 & 14.7 \\ 11 & 11.9 \\ 11 & 10.2 \\ 11 & 7.3 \\ 11 & 0.1 \\ 0.1 & 11 \\ 6.1 & 11 \\ 7.7 & 13.1 \\ 7.7 & 8.6 \\ 14.3 & 13.1 \\ 14.3 & 8.6 \\ 10 & 3.6 \\ 10 & 18.4 \\ 16.1 & 11 \\ 21.9 & 11 \end{bmatrix} \end{array} m$

Length of each wall:

$length := \begin{array}{c} \begin{matrix} x & y \end{matrix} \\ \begin{bmatrix} 22 & 0.2 \\ 22 & 0.2 \\ 6.6 & 0.2 \\ 6.6 & 0.2 \\ 22 & 0.2 \\ 22 & 0.2 \\ 0.2 & 22 \\ 0.2 & 22 \\ 0.2 & 2.9 \\ 0.2 & 2.9 \\ 0.2 & 2.9 \\ 0.2 & 2.9 \\ 0.2 & 7.2 \\ 0.2 & 7.2 \\ 0.2 & 22 \\ 0.2 & 22 \end{bmatrix} \end{array} m$

Comment: The global coordinates is based on origo location in bottom-left edge

Shear stiffness:

Timber plates stiffness usually governed by the shear stiffness. For simplicity, it's assumed that all walls work only in shear, meaning that bending stiffness of the braced member is neglected. Shear stiffness S_s can be represented by the depth of wall since all members have same modulus of elasticity, height and thickness.

$$S_s := \frac{E \cdot t \cdot b}{l}$$

where:

E is the modulus of elasticity

b is the depth of the wall

l is the height of the wall

t is the thickness of the wall

$$j := 0 .. n_w - 1$$

$$S_{x_j} := length_{j,0} \qquad S_{y_j} := length_{j,1}$$

$$b_i S_{xi_j} := coord_{j,1} \cdot S_{x_j} \qquad a_i S_{yi_j} := coord_{j,0} \cdot S_{y_j}$$

Rotational center:

$$R_{C_{0,0}} := \frac{\sum a_i S_{yi}}{\sum S_y} \quad , \quad R_{C_{0,1}} := \frac{\sum b_i S_{xi}}{\sum S_x}$$

$$R_C = \begin{bmatrix} 10.913 & 11.005 \end{bmatrix} \ m$$

$$coord_{new_{j,0}} := coord_{j,0} - R_{C_{0,0}} \qquad coord_{new_{j,1}} := coord_{j,1} - R_{C_{0,1}}$$

$$coord_{new} = \begin{bmatrix} 0.087 & 10.895 \\ 0.087 & 3.695 \\ 0.087 & 0.895 \\ 0.087 & -0.805 \\ 0.087 & -3.705 \\ 0.087 & -10.905 \\ -10.813 & -0.005 \\ -4.813 & -0.005 \\ -3.213 & 2.095 \\ -3.213 & -2.405 \\ 3.387 & 2.095 \\ 3.387 & -2.405 \\ -0.913 & -7.405 \\ -0.913 & 7.395 \\ 5.187 & -0.005 \\ 10.987 & -0.005 \end{bmatrix} \ m$$

Radial distance from rotation centre

Global torsional stiffness:

$$S_T := \sum_{j=0}^{n_w - 1} \left(S_{x_j} \cdot coord_{new_{j,1}}{}^2 \right) + \sum_{j=0}^{n_w - 1} \left(S_{y_j} \cdot coord_{new_{j,0}}{}^2 \right) = \left(1.233 \cdot 10^4 \right) \ m^3$$

Horizontal force in walls working in x-direction:

$H_{tot} := \sum H = 654.723 \ kN$

Total horizontal force acting in x, y-dir.
Horizontal force on each storey, $Q_{w.z}$ defined in 'Wind load according to SS-EN-1991-1-4'

$e_y := R_{C_{0,1}} - G_{C_{0,0}} = 0.005 \ m$

Eccentricity in y-direction

$T := H_{tot} \cdot e_y = 3.426 \ kN \cdot m$

Global torsional moment

$$H_{x_j} := H_{tot} \cdot \frac{S_{x_j}}{\sum S_x} + T \cdot \frac{S_{x_j} \cdot coord_{new_{j,1}}}{S_T}$$

Horizontal force in the walls

$$x := \text{submatrix}\left(H_x, 0, 5, 0, 0\right) = \begin{bmatrix} 139.639 \\ 139.595 \\ 41.873 \\ 41.87 \\ 139.55 \\ 139.506 \end{bmatrix} \ kN \qquad H_{x.fem} := \begin{bmatrix} 145.170 \\ 151.825 \\ 34 \\ 34 \\ 151.825 \\ 145.172 \end{bmatrix} \ kN$$

Analytical and numerical comparison:

$$\frac{x - H_{x.fem}}{x} = \begin{bmatrix} -0.04 \\ -0.088 \\ 0.188 \\ 0.188 \\ -0.088 \\ -0.041 \end{bmatrix}$$

$SUM_x := \sum H_x = 654.723 \ kN$ Control of the result in x-direction

Horizontal forces in walls working in y-direction:

$e_x := R_{C_{0,0}} - G_{C_{0,1}} = -0.087 \ m$ Eccentricity in x-direction

$T := H_{tot} \cdot e_x = -56.834 \ kN \cdot m$ Global torsional moment

H_{y_j} := if $j \geq n_{w.x}$

$$H_{tot} \cdot \frac{S_{y_j}}{\sum S_y} + T \cdot \frac{S_{y_j} \cdot coord_{new_{j,0}}}{S_T}$$

else

$$H_{tot} \cdot \frac{S_{y_j}}{\sum S_y} + T \cdot \frac{S_{x_j} \cdot coord_{new_{j,1}}}{S_T}$$

Horizontal forces in the walls

$$y := \text{submatrix}\left(H_y, 6, 15, 0, 0\right) = \begin{bmatrix} 126.13 \\ 125.522 \\ 16.525 \\ 16.525 \\ 16.436 \\ 16.436 \\ 40.95 \\ 40.95 \\ 124.508 \\ 123.92 \end{bmatrix} \ kN \qquad H_{y.fem} := \begin{bmatrix} 123.81 \\ 128.86 \\ 12.37 \\ 13.10 \\ 12.455 \\ 13.24 \\ 36.15 \\ 44.96 \\ 131.99 \\ 127.31 \end{bmatrix} \ kN$$

Analytical and numerical comparison:

$$\frac{y - H_{y.fem}}{y} = \begin{bmatrix} 0.018 \\ -0.027 \\ 0.251 \\ 0.207 \\ 0.242 \\ 0.194 \\ 0.117 \\ -0.098 \\ -0.06 \\ -0.027 \end{bmatrix}$$

$SUM_y := \sum H_y = 654.723 \ kN$ Control of the result in y-direction

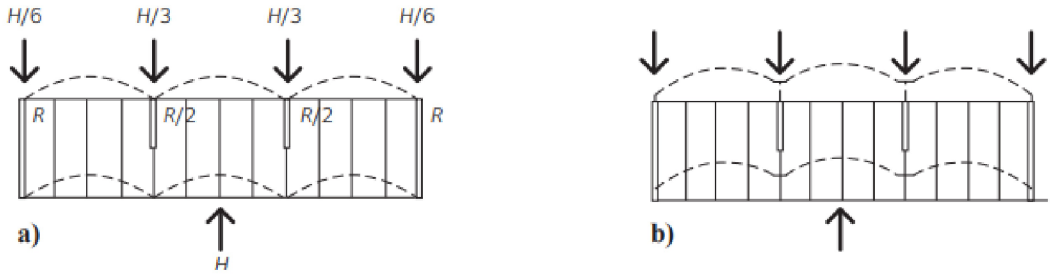

a) Flexible roof diaphragm, b) semi-rigid roof diaphragm.

Comment: The differences between the two methods can be explained by the rigidity of the floor-diaphragm and the neglected bending stiffness in the analytical approach. Moreover, the analytical results are based upon a rigid diaphragm which appears to not reflect the numerical model where the force distribution is more complex.

5. Deflection check

A simplified version of the building is used for describing bending and shear deformations. Hence, exterior walls are used while inner walls are not. Numerical results are compared to a Timoshenko beam for two load cases.

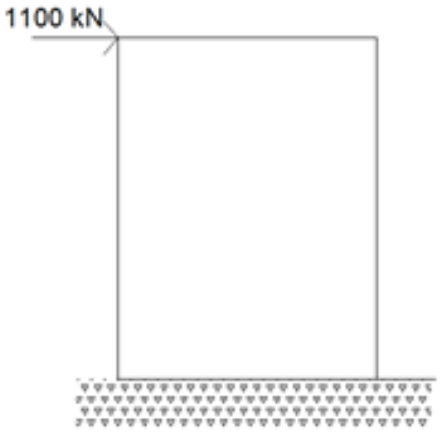

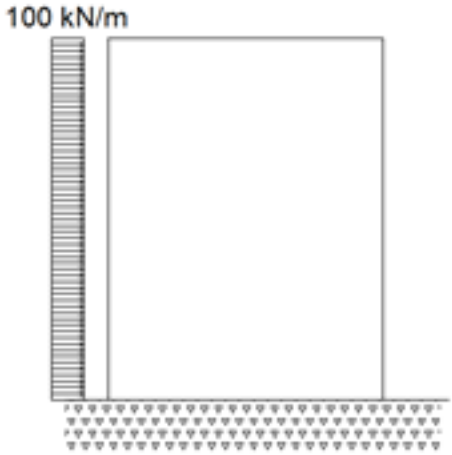

Load case 1

$L := h = 29\ m$

$A_w := d \cdot t \cdot 2 = 8.8\ m^2$

Load case 2

Span of the cantilever beam

Area of walls exterior walls in x,y -direction

Material properties:

$k_{def} := 0.6$

Deformation factor for cross-laminated timber

$E_{mean} := 5.861\ GPa$

$G_{mean} := 0.59\ GPa$

Mean modulus of elasticity & shear modulus

$E_{mean.fin} := \frac{5861}{(1 + k_{def})}\ MPa$

$G_{mean.fin} := \frac{590}{(1 + k_{def})}\ MPa$

Final mean shear modulus, modulus of elasticity is used in service state.

Load case 1: Concentrated horizontal force on top of the building

$P := 1100\ kN$ Horizontal force on top of the building

$I_s := \left(\frac{d^4}{12} - \frac{(d - 2 \cdot t)^4}{12}\right) = (1.381 \cdot 10^3)\ m^4$ Moment of intertia of building

$k_t := \frac{5}{6}$ Timoshenko shear coefficient

$x_p := 0\ m$ Length, acoounting for max deflection

Deflection in service state:

$$w_{sls} := \frac{P \cdot (L - x_p)}{k_t \cdot A_w \cdot G_{mean.fin}} - \frac{P \cdot x_p}{2 \cdot E_{mean.fin} \cdot I_s} \cdot \left(L^2 - \frac{x_p^2}{3}\right) + \frac{P \cdot L^3}{3\ E_{mean.fin} \cdot I_s} = 13.564\ mm$$

$w_{sls.b} := \frac{P \cdot L^3}{3\ E_{mean.fin} \cdot I_s} = 0.002\ m$ Deflection due to bending

$w_{sls.s} := \frac{P \cdot (L - x_p)}{k_t \cdot A_w \cdot G_{mean.fin}} = 0.012\ m$ Deflection due to shear

$w_{sls.FEM} := 13.9\ mm$

Analytical and numerical comparison:

$$\frac{w_{sls} - w_{sls.FEM}}{w_{sls.FEM}} = -0.024$$

Load case 2: Distributed horizontal load over the height

$q_w := 100 \ \frac{kN}{m}$ — Distributed wind load

$\beta_z := 1.2$ — Shear coefficient, accounting for shape of cross-section

Deflection in service state:

$w_{sls.b} := \frac{q_w \cdot h^2}{2 \cdot E_{mean.fin} \cdot A_w} = 1.304 \ mm$ — Deflection due to bending

$w_{sls.s} := \frac{q_w \cdot h^2 \cdot \beta_z}{2 \cdot G_{mean.fin} \cdot A_w} = 15.55 \ mm$ — Deflection due to shear

$w_{sls} := w_{sls.b} + w_{sls.s} = 16.855 \ mm$

$w_{sls.FEM} := 16.99 \ mm$

Analytical and numerical comparison:

$\frac{w_{sls.FEM} - w_{sls}}{w_{sls.FEM}} = 0.008$